The Dissertation Committee for Adam Philip Pacsi certifies that this is the approved version of the following dissertation:

Spatially Resolved Life Cycle Models for the Environmental Footprint of Electricity Generation

Committee:

David T. Allen, Supervisor

Elena C. McDonald-Buller

Lea Hildebrandt Ruiz

Thomas F. Edgar

Michael F. Blackhurst

Spatially Resolved Life Cycle Models for the Environmental Footprint of Electricity Generation

by

Adam Philip Pacsi, B.S.

Dissertation

Presented to the Faculty of the Graduate School of

The University of Texas at Austin

in Partial Fulfillment

of the Requirements

for the Degree of

Doctor of Philosophy

The University of Texas at Austin

August 2014

Dedication

To Frances and my family for always being there to support me, through my doctoral studies and in life.

Acknowledgements

I would like to thank Dr. David Allen for his support and guidance for my doctoral research. I would also like to acknowledge all of the co-authors on my publications for their guidance and help. I would like to acknowledge all of my colleagues at the Center for Energy and Environmental Resources (CEER) for their help with the completion of this work, especially Yosuke Kimura, Gary McGaughey, Dave Sullivan, and Elena McDonald-Buller. Finally, I would like to thank the other graduate students in the Allen research group including Daniel Zavala-Araiza, Cameron Faxon, and Nawaf Alhajeri.

Spatially Resolved Life Cycle Models for the Environmental Footprint of Electricity Generation

Adam Philip Pacsi, Ph.D.

The University of Texas at Austin, 2014

Supervisor: David T. Allen

Electricity generation has significant environmental impacts, including on regional air quality, greenhouse gas emissions, and water availability. Modeling the overall environmental impact of electricity generation requires linked simulations of power generation, air pollution physics and chemistry, greenhouse gas emissions, and water use. Tools for performing these analyses in an integrated manner are just beginning to emerge. This work expands on the development of linked models for electricity generation, air quality, and water use that have provided single-day snapshots of these environmental impacts. The original model used a non-linear optimization model for power generation, a regional photochemical model for air quality impacts, and self-contained modules for greenhouse gas emissions and water usage at power plants in Texas.

The new model includes life cycle scenarios for the power sector (including changes in both the fuel production and electricity generation stages) and expands the temporal scale of the modeling framework to include impacts on monthly, seasonal, and annual time scales instead of on single days. In addition, the air quality framework has been expanded to include atmospheric particulate matter as an air quality impact. This modeling framework will be used to assess the air quality impacts of new natural gas

developments in the Barnett and Eagle Ford shale regions in Texas, the consumptive water impact of new natural gas development in Texas, the impact of seasonal versus ozone forecast-based pricing for power plant NO_x emissions in the state of Texas, and the potential cost and air quality impacts of drought-based operation of the power grid in Texas.

Table of Contents

List of Tables

List of Figures

Chapter 1: Introduction

1.1 Background and Motivation

Electricity generating units (EGUs), commonly referred to as power plants, are important contributors to many regional environmental concerns. EGUs emit substantial fractions of the sulfur dioxide (SO_2), nitrogen oxides (NO_x), and carbon dioxide (CO_2) released in the United States (Alhajeri et al. 2011a); electricity generation is also the largest category of water use in the United States, measured as withdrawals (Kenny et al. 2009). As a result, changes to the electricity generation system have the ability to influence many regional environmental parameters, including air quality, water availability, and greenhouse gas emissions.

Power plant emissions control has been widely recognized as an important tool for meeting National Ambient Air Quality Standards (NAAQS) for air pollutants, especially ozone and fine particulate matter (PM). Ozone is a secondary pollutant formed by a series of photochemical reactions involving volatile organic compounds (VOCs) and NO_x, both of which are emitted by power plants. Fine PM refers broadly to liquid and solid species (aerosols) in the air with an aerodynamic diameter of less than 2.5 microns, which are small enough to pass through barriers in the lungs (Dockery et al. 1994); Power plants both directly emit fine PM and emit SO_2 and other species that can subsequently react to form PM. In Texas, sulfate (SO_4), which results from the oxidation of SO_2, is the largest single mass component of fine PM (Russell et al. 2004).

In recent years, many efforts, such as the Clean Air Interstate Rule (CAIR) and the Acid Rain Program (ARP), have targeted reductions in the emissions of NO_x and SO_2 from EGUs to reduce regional ozone and PM levels. Previous emission reduction programs have often involved cap and trade systems in which a cap on emissions for a particular species is set within a trading region, but the mechanisms for compliance for

individual EGUs (i.e. buying emissions trading credits versus installing new control technologies) are based on market decisions. Generally, these cap and trade programs have been focused on single pollutants, such as SO_2 or NO_x; however, due to the interconnectedness of EGU environmental impacts, changes in electricity generation based on targets for NO_x and SO_2 emissions reductions can, in some cases, also change CO_2 emissions and water use (Alhajeri et al. 2011a). In addition, emissions control programs focus on precursor emission reductions (NO_x and SO_2) as a proxy for reductions in ozone and PM, respectively, rather than the predicted changes in the secondary species. Previous research on the Electricity Reliability Council of Texas (ERCOT), the electrical grid that serves much of Texas, has demonstrated that the same reductions in NO_x emissions from different EGUs can have a markedly different impact on ozone formation based on different meteorological conditions and ambient air quality factors, such as the presence of high levels of biogenic VOCs (Nobel et al. 2001). It has been suggested that PM sulfate (PSO_4) formation from SO_2 emissions would also have spatial and temporal variations (Brock et al 2002).

The work described in this dissertation examines the response of the environmental footprint (NO_x, SO_2 and CO_2 emissions, ozone formation, PM formation, water use) of an electrical grid to market forces (fuel prices, emission pricing) and to other external drivers. An Integrated Model developed for ERCOT by researchers at the University of Texas at Austin (UT) and the Massachusetts Institute of Technology (MIT) is used as an analysis tool and is extended in this work.

The UT/MIT Integrated model combines models for electricity generation, regional air quality, and water use related to EGUs in ERCOT. Under the current modeling framework, price signals for NO_x emissions have been used to drive changes in electricity dispatch within ERCOT under summer-time electricity demand levels in

Texas. The analyses indicate that emission pricing drives a shift from the use of coal as a fuel to the use of natural gas as a fuel, with associated reductions in SO_2, NO_x, CO_2, and water usage (Alhajeri et al. 2011a). Trade-offs between the prices of NO_x and CO_2 have also been investigated (Alhajeri 2012). In addition, the impacts of NO_x emissions pricing on ozone formation in Texas on a few representative days have been examined using the CAMx regional photochemical model (Alhajeri 2012); however, the effects on particulate sulfate (PSO_4) formation were not included.

The worked described in this dissertation will add several features to the modeling capabilities of the UT/MIT Integrated Model. Recognizing that EGU emissions can have a significant impact on PM concentrations in Texas, the Integrated Model has been expanded to include the effects of EGU SO_2 emissions reductions on PSO_4, the main secondary PM species associated with electricity generation in Texas. Furthermore, the current model had used daily resolution in emission pricing and had used very limited time periods for air quality modeling, typically considering just a few representative days for analysis. This work both expands and further resolves the time periods for the model. Air quality modeling has been performed on a monthly time scale and responses to price signals on time scales from hourly to seasonal has been considered. Finally, the scope of the model has been expanded to include impacts of changes in fuel supplies. Revolutionary changes in natural gas production (including the use of hydraulic fracturing) have dramatically affected the pricing and availability of natural gas. Inexpensive natural gas causes changes in the fuels used in electricity generation, causing changes in environmental footprints (deGouw et al. 2014). This work considers the response of the UT/MIT Integrated model to fuel price changes and also couples the Integrated Model to modules that assess the environmental footprints of natural gas

production in the ERCOT supply region, to arrive at more comprehensive assessments of the environmental footprints of new natural gas production than is currently possible.

1.2 RESEARCH OBJECTIVES

Previous research (Alhajeri et al. 2011a) has indicated that environmental dispatching based on NO_x emissions prices for the ERCOT grid causes a reduction in SO_2 emissions from EGUs as generation is shifted from coal-fired power plants to natural gas powered facilities. Since PM sulfate, which is formed from the oxidation of SO_2, is the largest component of fine PM in eastern Texas (Russell et al. 2004), NO_x trading in ERCOT has the potential to decrease PM concentrations in eastern Texas. **Objective 1 was to develop the framework for modeling changes in secondary PM formation from EGU emissions in the UT/MIT Integrated Model using representative high ozone days.**

To date, the UT/MIT Integrated Model has been applied for hourly emissions on single representative high ozone days for eastern Texas. The results for ozone (Alhajeri 2012) have been similar to across the board emissions reductions over time, but have included significantly larger localized maximum reductions. Daily meteorological conditions can significantly affect the ozone and PM impacts of environmental dispatching. In addition, emission reductions may influence the ozone formation on subsequent days, leading to the need for models that are temporally linked. Furthermore, daily consumer demand levels (for example, high demand on a very hot summer day from increased air-conditioning use) can affect the flexibility of the grid to dispatch electricity to lower emission EGUs. Over longer periods, the spatial variability in impacts may or may not converge on an average behavior. **Objective 2 was to extend the UT/MIT Integrated Model framework from single day snap-shots to linked**

episodes on a monthly time scale in order to examine the air quality impacts over more policy relevant time scales.

The extended UT/MIT Integrated Model framework that includes fine particulate matter chemistry (Objective 1) and multiple, linked days (Objective 2) was used to examine a wide variety of environmental issues related to power generation. The robustness of the UT/MIT Integrated Model framework is such that changes to power plant emissions could be driven by many different factors. Previous research (Alhajeri 2012) has shown that ERCOT has sufficient installed capacity to shift the spatial location of electricity generation on representative days based on drought. **Objective 3 was to examine whether ERCOT could be used over a monthly time scale as a virtual water pipeline to shift the spatial location of electricity generation based on drought to increase water availability in the most drought stricken areas.**

New natural gas development in Texas due to hydraulic fracturing and horizontal drilling has caused a significant increase in domestic supply (EIA 2012), which has caused natural gas prices to stabilize at approximately $3-4 per MMBTU (EIA 2014d). Indirectly, decreases in natural gas prices can affect the fuel usage decisions in the ERCOT grid, leading to changes in emissions from EGUs related to increased usage of natural gas facilities in lieu of coal-fired power plants. **Objective 4 was to simulate the regional air quality impacts (ozone and PM concentrations) of a variety of ratios of natural gas prices to coal prices in ERCOT over a monthly period.**

In addition to affecting fuel costs in ERCOT, new natural gas development in Texas will impact water usage, greenhouse gas emissions, and regional air quality parameters. Direct effects of hydraulic fracturing would include the emissions and water usage due to natural gas production activities. Indirectly, the increased availability of natural gas will influence electricity generation, as will be explored in Objective 4. If the

direct and indirect water usage, air quality, and greenhouse gas effects of new natural gas production in Texas are determined, the net environmental impacts (water usage, regional ozone/PM concentrations, and greenhouse gas emissions) of new natural gas development can be examined. **Objective 5 was to incorporate VOC, NO_x, and fuel cost data related to natural gas production into the UT/MIT Integrated Model to develop a more comprehensive environmental assessment of the air quality impacts of new natural gas production activities in the Barnett Shale in Texas.**

Objectives 4 and 5 show the combined impact of natural gas production emissions from the Barnett Shale and changes in the electricity generation sector in Texas for the ERCOT grid. The Barnett Shale has some unique characteristics (isolated grid, production emissions downwind of major metropolitan areas) that may cause different air quality results than if the integrated model would be applied to other regions. **Objective 6 was to perform a similar analysis on the Eagle Ford Shale in Texas to compare trends in regional ozone formation to results from the Barnett Shale.**

Objectives 4-6 focus on the air quality impacts of new natural gas production in Texas. Since water is consumed both as a fluid for hydraulic fracturing (the natural gas production stage) and as a cooling fluid at power plants (the use phase of the life cycle), changes to the power sector and to the natural gas production sector have the potential to change the magnitude and spatial location of water consumption in Texas since power plants and their fuel supplies are not always co-located. **Objective 7 was to apply the framework developed for the combined air quality impacts of natural gas development and use to examine the changes in consumptive water use in Texas.**

1.3 DISSERTATION OVERVIEW

The remainder of the dissertation documents how the objectives were implemented, using specific case studies. Chapter 2 is a literature review and develops the necessary framework for the dissertation. Chapter 3 compares the ozone impacts of a seasonal emissions price for NO_x to a system that only institutes emissions pricing on predicted high ozone days and includes photochemical modeling over month-long episode. Chapter 4 examines the combined air quality and water use impacts of a theoretical scenario in which ERCOT operations were based on the spatial location of drought in Texas, such that changes in the dispatch of electricity generation could increase water availability in targeted regions. Chapter 5 examines the ozone and fine particulate matter impacts associated with the combined changes in emissions from increased natural gas production in the Barnett Shale in Texas and from price-based changes in the power sector. Chapter 6 extends the analysis from Chapter 5 for the Barnett Shale to the Eagle Ford Shale, to determine the extent to which ozone results in Texas are sensitive to location of production emissions and shale-specific emission practices. Chapter 7 examines the combined consumptive water impacts of changes in natural gas production and use in Texas in a spatially-resolved manner. Chapter 8 discusses the major conclusions of the dissertation and provides recommendations for future research.

Chapter 2: Literature Review

2.1 Power Plant- Related Region Environmental Parameters

In the United States, electricity generating units (EGUs), which are commonly known as power plants, are major emitters of nitrogen oxides (NO_x), sulfur dioxide (SO_2), and greenhouse gases (including carbon dioxide) as well as a major driver of regional water withdrawals (and to a lesser extent, water consumption). This chapter discusses the scientific basis of the regional environmental effects of electricity generation and focuses primarily on Texas, which is the main region analyzed in this work.

2.1.1 Electricity Generation in Texas

The electricity generation infrastructure in the United States consists broadly of EGUs (power plants) which generate electricity and the distribution network that brings the electricity from the EGUs to the end users. In the continental United States, there are three regions for electricity generation and distribution that are highly-interconnected within each region, but have limited connectivity crossing regions. The regions (shown in Figure 2-1) are: the eastern United States, the western United States, and the Electricity Reliability Council of Texas (ERCOT).

Due to the relatively low degree of interconnection to other grids and the small geographic area, the ERCOT grid will serve as the test bed for changes to electricity generation throughout this work. ERCOT serves 85% of the area of Texas and 23 million customers using 550 EGUs with 74,000 MW of installed capacity for peak demand (ERCOT 2014b). In 2011, the installed capacity was 57% natural gas, 23% coal, 7% nuclear, and 13% wind power. While the installed capacity for natural gas was larger than for coal, the actual generation in 2011 was roughly equal for the two fuels, 39% coal

and 40% natural gas (ERCOT 2012). While the installed has remained relatively similar between 2011 and 2013, the utilization of natural gas increased to 41% of the generation in 2013, while coal usage decreased to 37% (ERCOT 2014b).

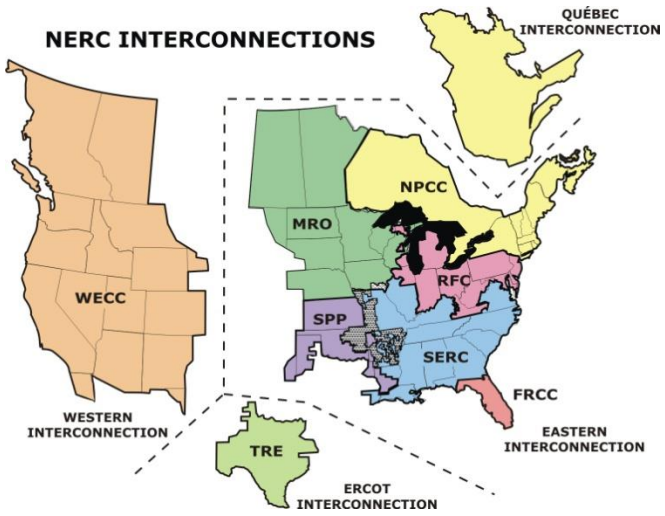

Figure 2-1. Map of main NERC interconnections in the continental United States (ERCOT 2009).

2.1.2 Ground Level Ozone Formation

Ozone (O_3) is listed as a criteria air pollutant by the Environmental Protection Agency (EPA), which has set a 75 ppb attainment standard for the annual 4th highest daily maximum eight hour average (CASCA 2012). In the lungs, ozone is thought to be a source of highly reactive free-radicals that can cause damage to lung tissue, and the extent of the damage is related to the duration and magnitude of elevated exposure as well as the activity level of individuals during episodes of high ozone (Devlin et al. 1997). Elevated ozone concentrations have been linked to increased respiratory mortality and hospital visits (Bell et al. 2004; Gryparis et al. 2004; Ito et al. 2005; Anenberg et al. 2010). The health effects of ozone are particularly pronounced during the warmer summer months (Gryparis et al. 2004) and disproportionately affect children and groups

with low socio-economic status (Lin et al. 2006). Some debate exists in the literature over the relative importance of extremely elevated one-hour maximum ozone concentrations (Burnett et al. 2004; Gryparis et al. 2004) versus sustained elevated ozone concentrations (Bell et al. 2004).

At ground level, ozone is formed by a series of photochemical reactions of volatile organic compounds (VOC) and nitrogen oxides (NO_x). The most basic reaction scheme for ozone formation (Seinfeld et al. 2006) is as follows:

$$NO_2 + h\nu \rightarrow NO + O \qquad \text{(Reaction 2-1)}$$

$$O + O_2 + M \rightarrow O_3 + M \qquad \text{(Reaction 2-2)}$$

$$O_3 + NO \rightarrow NO_2 \qquad \text{(Reaction 2-3)}$$

Reactions 2-1 to 2-3 result in a dynamic equilibrium in which the concentration of ozone is proportional to the concentration ratio of NO_2 to NO ($[O_3]$ is proportional to $[NO_2]/[NO]$). The oxidation of various anthropogenic and biogenic hydrocarbons can increase the amount of NO_x that is present as NO_2, causing a shift towards the production of more ozone. The ratio of NO_x to VOC is an important factor in ozone chemistry, as the limiting factor in the reactions can differ based on localized concentrations of the ozone precursors (Sillman 1999).

Electricity generation can have a significant impact on regional ozone concentrations since EGUs account for roughly 20% of NO_x emissions in the United States (EPA 2012b), with a typical split factor of 90% NO and 10% NO_2 (Mauzerall et al. 2005). NO_x is formed in high temperature combustion process from the oxidation of nitrogen, which is present in the reaction both from the fuel and from the atmosphere (Seinfeld et al. 2006). In general, ozone formation in urban areas tends to be initially limited by the availability of VOCs, while downwind ozone formation in rural areas is generally limited by the amount of NO_x that is available for reaction (Sillman 1999). A

noted reversal in this trend is the Houston Ship Channel, in which industrial emissions of highly-reactive VOCs (HRVOC) have led to spikes in urban ozone concentrations in a NO_x-limited ozone formation regime (Daum et al. 2003; Nam et al. 2006; Xiao et al. 2010). Within plumes from large power plants, the ozone chemistry tends to be more controlled by the availability of VOCs than surrounding ambient conditions (Sillman 1999) until the plume becomes fully mixed with the ambient atmosphere (Frost et al. 2006).

2.1.3 Ground Level Fine Particulate Sulfate

Fine particulate matter (PM) is currently regulated by the EPA with an annual average standard of 12 $\mu g/m^3$ averaged over 3 years (EPA 2014c), which is a decrease from the previous annual average standard of 15 $\mu g/m^3$ (CASAC 2009). While PM can be composed of a variety of organic and inorganic precursors, the largest single mass component of PM in Texas is particulate sulfate [PSO_4] (Russell et al. 2004), which is formed from the oxidation of gaseous sulfur dioxide (SO_2). PM is regulated due to its small aerodynamic diameter (less than 2.5 microns), which allows for deposition in the smaller portions of the lungs where gas exchange occurs (Dockery et al. 1994). Long term exposure to elevated levels of PM is correlated with increased overall mortality in adults, especially from cardiopulmonary issues and lung cancer (Pope et al. 2002; Anenberg et al. 2010) while short term spikes in PM concentrations have been correlated with decreased lung function, especially for individuals with asthma (Dockery et al. 1994).

SO_2 emissions in the United States are dominated by EGUs, which account for approximately 70% of US emissions (EPA 2014b). SO_2 is formed from the oxidation of trace sulfur components in the fuel and is a byproduct of combustion (particularly from

coal). The conversion of SO_2 to PSO_4 occurs both in the gas phase and aqueous phase (Seinfeld et al. 2006) with the aqueous phase reactions in cloud water dominating the total global sulfur cycle but the gas phase oxidation pathway being dominant in large plumes during cloudless summer days (Brock et al. 2002). Several modeling studies (Mueller et al. 2004; Bergin et al. 2007) have found regional PSO_4 concentrations to be highly sensitivity to changes in EGU emissions, particularly near large point sources.

2.1.4 Water Usage

Recent droughts throughout the United States, particularly in Texas, have brought renewed emphasis to the sustainable usage of freshwater resources. Considering projected population growth in Texas, water scarcity issues are expected to continue in the future (Stillwell et al. 2011a). Nationally, thermoelectric power generation accounts for 39% of freshwater withdrawals and 3% of freshwater consumption (DOE 2008). Consumption is defined as the amount of water taken from a reservoir but not returned to it due to forces such as evaporative loss while withdrawals are defined as the total amount of water taken from the source (Macknick et al. 2012; Averyt et al. 2013).

Substantial variation occurs among the cooling water requirements (both consumptive and non-consumptive) at different EGUs due to factors such as climate, location, fuel type, and cooling system configuration (Stillwell et al. 2011a). In power generation, the largest demand for freshwater is for use as cooling water to condense steam (DOE 2008), and nationally, 99% of cooling water comes from surface water withdrawal (Huston et al. 2004). Water-cooling systems in power plants have traditionally been classified as either closed-loop (9% of EGU-related water withdrawals), in which cooling water is recirculated after use as a coolant, or once-through (91% of EGU-related water withdrawals), in which water is only used once as a

coolant and then returned to the body of water (Huston et al. 2004). For power plants, a once through cooling system configuration would generally require a higher rate of water withdrawals (but lower rate of water consumed) than an equivalent closed loop plant.

2.1.5 Greenhouse Gas Emissions

Concerns about global warming have led to increased emphasis on the greenhouse gas (GHG) impacts of industrial processes. Carbon dioxide (CO_2) is the primary greenhouse gas associated with fossil fuel combustion, but lesser amounts N_2O and CH_4, which are 298 and 25 times more potent greenhouse gases than CO_2 over a 100 year time horizon, respectively (Solomon et al. 2007) , are also produced as byproducts of combustion (EPA 2014a). The greenhouse gas intensity of power generation varies both by the fuel type used and the efficiency of the individual EGU, and electricity generation accounted for 40% of all CO_2 emissions in the United States in 2010 (EPA 2014b). For natural gas combined cycle power plants, the GHG emissions at the power plant (during the use phase of the life cycle) are ~50% of the emissions per megawatt hour [MWh] of a typical coal-fired power plant (Jaramillo et al. 2007; Alvarez et al. 2012). The potential GHG benefits from the use phase due to the utilization of natural gas EGUs instead of coal EGUs, however, may be eliminated if upstream methane emissions from the natural gas supply chain are more than 3.2% (Alvarez et al. 2012), especially if a short-term global warming potential is considered (Howarth et al. 2011). Substantial research efforts have been undertaken to quantify the GHG emissions associated with various aspects of the natural gas supply chain (Allen et al. 2013; Jackson et al. 2014), but large uncertainty remains in emissions estimates from this sector (Brandt et al. 2014).

2.2 METHODS FOR EMISSIONS REDUCTIONS

For electricity generation, emissions reductions can occur either through the installation of new control technologies or through the shifting of generation to EGUs with a lower emissions rate per megawatt hour (MWh). This section will describe control options for NO_x and SO_2 emissions.

2.2.1 Control Technologies

NO_x control technologies tend to focus either on combustion techniques to control the formation of thermal NO_x or on the treatment of flue gas before it is emitted to the atmosphere. Without treatment, NO_x could be emitted in the range of 100-200 ppm from natural gas burners and 300-1200 ppm from coal-fired EGUs. Combustion control techniques involve reducing the flame temperature at combustion, which must be high enough to allow for efficient combustion, or reducing the oxygen concentration (either through limiting excess air or burning with excess fuel) to reduce the formation of NO_x from atmospheric nitrogen. Low NO_x burners are an example of a combustion control technique in which fuel or air is injected to the burner in stages to reduce the amount of excess oxygen for NO_x formation and can reduce NO_x emissions by 90-140 ppm in flue gas from coal fired power plants (Schnelle et al. 2002).

NO_x control through the treatment of flue gas tends to have higher capital cost than combustion control techniques but is generally more effective. The two most common techniques, Selective Non-catalytic Reduction (SNCR) and Selective Catalytic Reduction (SCR), both involve the use of ammonia or urea to reduce NO_x to nitrogen and water. The major difference is that SCR uses lower temperatures and a catalyst to facilitate the destruction of NO_x via an ammonia injection. The catalysts tend to be expensive; thus, a SNCR unit is often placed before an SCR unit to reduce the size of the catalyst bed needed for the application. SNCR and SCR are 30-50% and 70-90%

effective at NO_x removal, respectively (Schnelle et al. 2002). Due to its higher effectiveness at NO_x reduction, SCR is often applied to large coal-fired power plants that are used in base load generation. Burtraw et al. (2001) examined various scenarios for a 70% reduction in NO_x emissions from power plants in the Northeastern United States and found that the cost of properly deployed SCR and SNCR would be between $1,119 - $2,163 per ton of NOx reduced. Decisions to install post-combustion NO_x controls at coal-fired EGUs are also related to the type of electricity market in the region with EGUs. EGUs in deregulated electricity markets (such as ERCOT) are less likely to install SNCR or SCR than similar power plants in publicly-owned or rate regulated markets due to inability to recover the investment costs (Fowlie 2010).

Most coal-fired EGUs use Flue Gas Desulfurization (FGD) for control of SO_x emissions. FGD involves the use of a calcium (such as limestone) or sodium (such as caustic ash) oxidant to oxidize SO_2 to water soluble species that can be removed from the flue gas. Peterson and Rochelle (1988) found that the extent of SO_2 oxidation and removal depended on the ratio of silica (from fly ash) to calcium (from limestone). This ratio controlled the fraction of the powder injected that was available for reaction with gas phase SO_2. With dry FGD using limestone, 25% of the SO_2 can be converted to gypsum, which has economic value. Other byproducts from the process may affect the quality of waste water by increasing sulfate and sulfite concentrations. FGD has been shown to be 95% effective in removing SO_2 from the flue gas of coal-fired power plants (Schnelle et al. 2002). FGD also has the co-benefit of removing trace organic acids as a co-precipitate with gypsum (Ruiz-Alsop et al. 1988). The costs of FGD implementation depend on the capacity of the EGU and on the FGD method chosen, but are in the range of $150-$400 per kWh (Srivastava et al. 2001).

2.2.2 Emissions Trading

When designing NO_x and SO_2 reduction programs, policy makers have multiple options for obtaining targeted emissions decreases from EGUs. Mandating specific control technologies, such as SCR or FGD, have become less popular in recent years due to the success of market-based initiatives. Many market-based emissions are based on Title IV of the 1990 Clean Air Act in which a cap and trade system for SO_2 emissions allowances was created. Under cap and trade programs, a hard emissions cap for the targeted pollutant is set for a particular geographic region, and sources within that region are given a specific allotment of emissions. Generally, these hard caps are reduced in subsequent years. Each producer is able to decide whether to meet lower emissions caps through installing new control technologies or through buying unused emissions permits from other sources that have over-complied. Chestnut et al. (2005) indicated that the SO_2 cap and trade program in the eastern United States was expected to reduce emissions of NO_x and SO_2 by 30% and 50%, respectively, by 2010. This corresponded to an annual average PM decreases of 1.0-2.5 $\mu g/m^3$ and seasonal 8-hour ozone decreases of 0-6 ppb throughout the eastern United States. In addition, the choice of a market-based approach instead of mandating specific technologies saved more than 37% in the compliance cost for the program (Burtraw et al. 1999) while having net economic benefits when health effects of emission reductions, particularly from PM reductions, are considered (Chestnut et al. 2005). Additional cap and trade programs for NO_x emissions from EGUs in the northeastern United States have also been undertaken. Burtraw et al. (2001) found that annual cap and trade approaches were more effective than ozone season approaches and that most of the NO_x trading program net benefit came from associated PM reductions.

In the short term, cap and trade programs for EGU emissions work by changing the dispatch order of power plants toward EGUs with less of the targeted pollutant per

MWh of generation. In the long term, facilities with high emissions per MWh may install new control equipment and become more competitive in the dispatch order (Newcomer et al. 2008). Several potential issues may arise in cap and trade systems. First, many facilities tend to front load emissions reductions in a cycle. Smith et al. (2007) observed that during the implementation of a CO_2 cap and trade system in the United Kingdom, firms tended to have significant reductions at the start of the two year cycle; however, excess CO_2 credits were available at the end of the cycle, allowing for more generation from carbon intensive fuel sources. Second, concern exists about the creation of pollution hotspots (areas in which locally increased emissions at facilities with increased generation under a program worsens air quality in those locations). In Texas, trading programs for highly reactive VOCs (Wang et al. 2005) and EGU NO_x emissions (Alhajeri 2012) were found to create localized ozone hotspots; however, the magnitude and expanse of these hotspots was much less than ozone reductions from the program. Chestnut et al. (2005) also reported that areas with high SO_2 emissions before the Acid Rain Program tended to be the same areas with high SO_2 emissions after the program, indicating that significant hotspot formation was unlikely. Farrell et al. (2009) found that including mechanisms in programs to prevent banking or hot spot formation tended to reduce the overall efficiency and net benefits of the programs.

2.2.3 Variation in the Effect of NO_x and SO_2 Emission Changes

While ozone and PM sulfate control programs tend to focus on precursor emissions of NO_x and SO_2, respectively, the non-linearity of ozone and sulfate chemistry can cause the same primary emission reductions to have vastly different effects on secondary pollutant formation. In Texas, Nobel et al. (2001) examined the effects of a daily ~20 ton NO_x reduction two coal-fired power plants. The maximum 1-hour ozone

concentration reductions from an urban power plant in San Antonio were substantially less in magnitude and spatial extent than reductions at a rural EGU in northeastern Texas, which was located in an area with high biogenic VOC emissions. Likely, the discrepancy in the downstream ozone formation impacts had to do with the ozone chemistry being NO_x-limited in the rural area and VOC-limited in the urban area (Sillman 1999). Mauzerall et al. (2005) found that the health effects of the same increase in EGU generation for a power plant in eastern Pennsylvania could be doubled on a hot day versus a cool day in the summer. Thus, spatial variations in temperature and VOC concentrations can have a large impact on the effectiveness of NO_x emissions reductions.

While the formation of PM sulfate from SO_2 is not a linear process, several studies (Muller et al. 2004; Bergin et al. 2007) have found SO_2 emissions to be the most sensitive parameter for PSO_4 formation chemistry. For many years, SO_2 conversion in the plumes of large power plants was thought to occur at an approximately constant rate of 6% per hour in the summer months (Cass 1980). A recent plume study in the southern United States (Brock et al. 2002) concluded that conversion rates vary day to day within the same EGU plume and between different EGU plumes on the same day. At this time, the variation in the potency of SO_2 emissions from power plants to PM sulfate formation has not been thoroughly addressed in the literature.

2.3 THE UT/MIT INTEGRATED MODEL

In order to assess the combined water usage, greenhouse gas, and regional air quality effects of power generation in the ERCOT grid, the UT/MIT Integrated Model was developed. This section will discuss the development and past implementations of this model.

2.3.1 Development of the UT/MIT Integrate Model

The UT/MIT Integrated Model (Figure 2-2) has been a collaborative effort by researchers at the University of Texas at Austin (UT) and the Massachusetts Institute of Technology (MIT) for the ERCOT grid in Texas. The project combined models for electricity generation [PowerWorld] (PowerWorld Corporation 2012), water usage, greenhouse gas emissions, and regional air quality [CAMx] (ENVIRON 2011) to allow researchers to assess a broader environmental footprint for electricity generation in the ERCOT grid. The rest of this section will describe the development of the individual portions of this model.

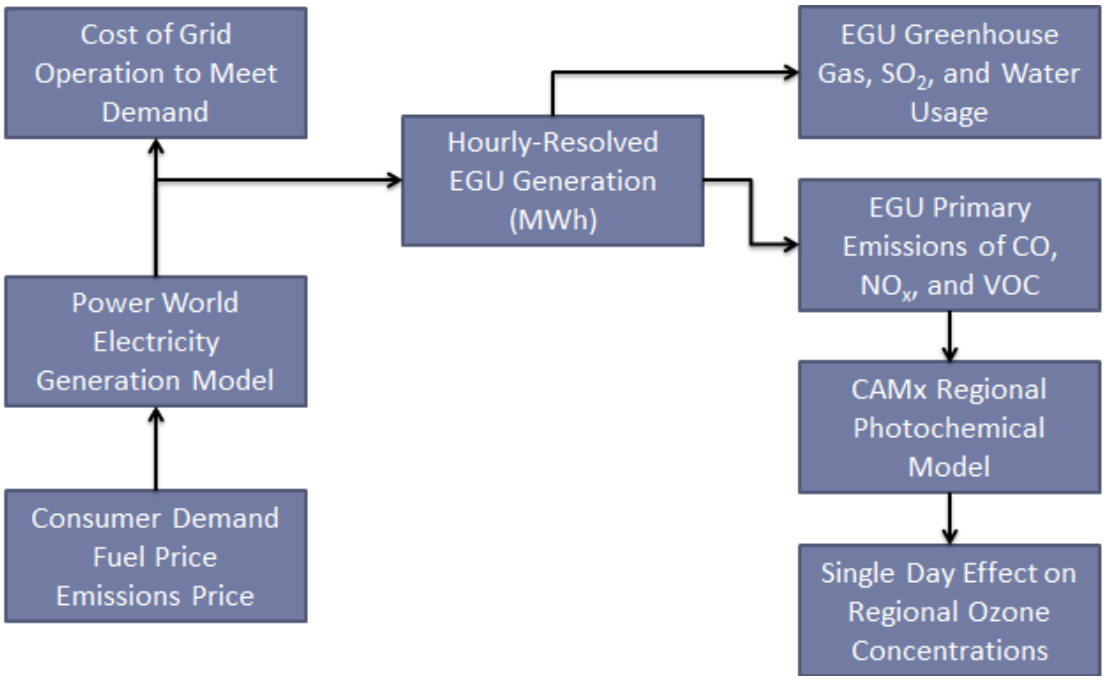

Figure 2-2. The existing UT/MIT Integrated Model framework based on descriptions from Alhajeri (2012).

The UT/MIT Integrated Model is driven by the PowerWorld model for electricity generation, which determines for each hour which EGUs would be operating within

ERCOT to meet electricity demand. The model incorporates EGU minimum and maximum capacity constraints as well as ERCOT transmission constraints. The model minimizes the total cost of generation in ERCOT using a non-linear Newton-Rhapson solution method (PowerWorld Corporation 2012). The specific implementation of the PowerWorld model for the ERCOT grid was developed at MIT in a study for the future of carbon capture technologies in Texas (Chiyangwa 2010). Currently, the cost (c_i) of operation for each *i* EGU within ERCOT is modeled as follows (Alhajeri 2012):

$$c_i\left(\frac{\$}{MWh}\right) = H_i(pf_i + pn_iN_i + ps_iS_i + pc_iC_i) + O\&M_i$$

where H_i is the heat rate (MMBTU/MWh), pf_i is the fuel cost ($/MMBTU), and $O\&M_i$ is the operations and maintenance cost ($/MWh) for each EGU. The option to model emissions pricing scenarios within ERCOT exists for CO_2 (*c)*, NO_x (*n)*, and SO_2 (*s)* using the plant specific average annual emissions rates [tons/MMBTU] (N_i, S_i, and C_i) from the eGRID database (EPA 2012a) and the emissions price (p) in $/ton. The output from the PowerWorld model is the generation (MWh) for each EGU in the ERCOT grid for each hour in the simulation. The hourly generation profile of ERCOT drives the scenario-specific calculation of water usage (consumption and withdrawals), GHG emissions, and regional air quality precursor emissions, based on specific factors for each EGU.

The GHG emissions and water usage requirements based on the generation profile for ERCOT are determined by multiplying the hourly generation at each EGU by a constant factor. The EGU-specific factor for CO_2 emissions, which is the predominant greenhouse gas from the power generation sector, is an annual average factor for emissions per MWh of generation from the year 2005 in the eGRID database (EPA

2012a). The water withdrawal factor (1000 m^3 per MWh) was developed by King et al. (2008) for the Texas Water Development Board.

Alhajeri (2012) developed the infrastructure for translating generation data from the PowerWorld model into CAMx ready point source emissions files. For his work on NO_x trading in ERCOT, Alhajeri (2012) calculated the base case generation for EGUs in the ERCOT grid based on day-specific measured NO_x emissions from the Texas Commission on Environmental Quality (TCEQ). For each EGU in each PowerWorld scenario, the ratio of generation in the scenario to the generation in the base case was multiplied by the base case emissions of NO_x, CO, and VOCs to get the new emissions from each ERCOT EGU. Other CAMx input parameters (such as vehicular emissions and meteorological data) remained unchanged from the TCEQ base case. Using underlying chemical mechanisms, CAMx is able to calculate changes in ozone formation associated with changes in EGU NO_x emissions. The model framework developed by Alhajeri (2012) allowed for the calculation of changes in SO_2 emissions based on per MWh emission factors from eGRID (EPA 2012a), but these emissions were not allocated spatially or added into the CAMx photochemical model in order to resolve the PM impacts.

2.3.2 Previous Uses for the UT/MIT Integrated Model Framework

Alhajeri (2012) tested the robustness of the entire UT/MIT Integrated Model under different scenarios. The majority of his work focused on the environmental impacts of imposing NO_x emissions prices in the range of \$0-\$50,000 per ton on the EGU emissions from the ERCOT grid. The major findings were that up to 50% reductions in NO_x emissions from ERCOT were possible without the installation of additional controls and that co-benefits included reductions in CO_2, SO_2, and Hg emissions. The cost was

comparable to state of the art NO_x control technologies when the co-benefits were included (Alhajeri 2012). Alhajeri (2012) also found that trade-offs existed between NO_x and CO_2 minimization strategies in ERCOT. Finally, Alhajeri found that water availability could be used as a driver of the PowerWorld Model through the movement of generation from extreme and exceptional drought regions in Texas to areas with more water availability. These projects focused on representative days for electricity demand rather than seasonal changes, and different simulation days were not linked.

2.4 Emissions from New Natural Gas Production Sources

This section discusses the UT/MIT Integrated Model in the context of a proposed implementation for a regional life cycle air quality impact assessment for new natural gas production in Texas. While previous applications (Alhajeri et al. 2011a; Alhajeri 2012) of the UT/MIT Integrated Model framework have focused on the impact of changes in emissions prices for the grid, the model framework could be expanded to examine the impacts of changing fuel prices (pf_i) rather than emissions prices in ERCOT.

2.4.1 Change in Fuel Price and Availability

The price of natural gas has decreased in recent years due to an influx of new supply from hydraulic fracturing in shale gas plays. Texas includes several shale gas plays that were among the first developed nationally (including the Barnett Shale in the Dallas-Fort Worth area and the Haynesville Shale on the border with Louisiana) as well as emerging shale gas plays, such as the Eagle Ford Shale in south Texas. Figure 2-3 contains a map of the major shale gas plays and ERCOT EGUs. Webber (2012) estimates that significant demand for natural gas in the power generation sector would exist with prices in the range of $1-3 per MMBTU as a replacement for coal-fired power generation. For reference, the minimum monthly-average natural gas price for Texas

power producers since the rapid development of shale gas resources in the United States began was $2.21 per MMBTU in April 2012 (EIA 2014d), and the $1 per MMBTU price referenced in Webber (2012) is substantially lower than historic natural gas prices. At low natural gas prices, the increase in the dispatch order for natural gas EGUs (particularly but not exclusively at efficient combined-cycle facilities) and the decrease in the dispatch order of coal-fired power plants offers potential benefits for regional air quality since the GHG, NO_x, and SO_2 emissions from natural gas EGUs are generally lower than equivalent coal-fired EGUs. However, the upstream impacts of shale gas production must be more fully understood in order to gain a perspective on the entire life cycle of the fuel source and to quantify potential benefits or trade-offs. By combining the impacts of spatially-resolved emissions changes from the power sector and the natural gas production sector, it is possible to understand which geographic areas would have the most potential for air quality changes due to increased natural gas development and use.

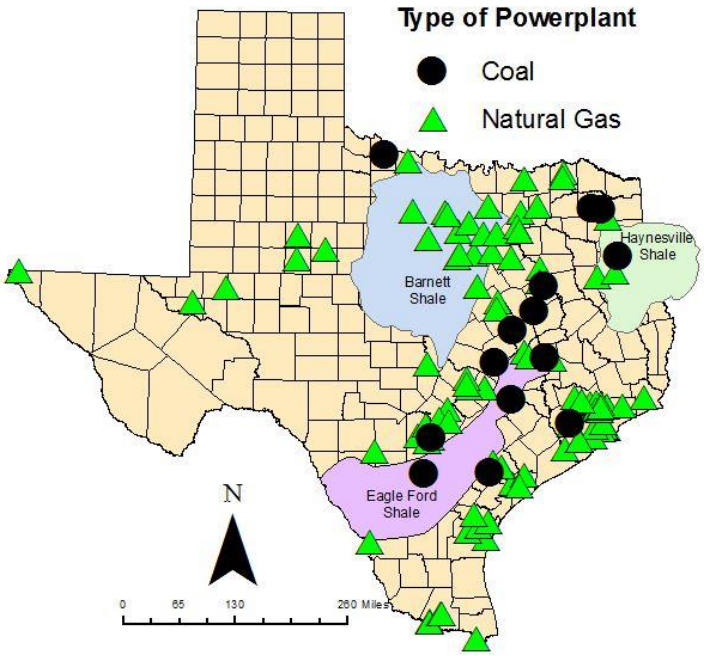

Figure 2-3. Location of ERCOT EGUs and major shale gas plays in eastern Texas.

2.4.2 Potential Air Quality Impacts

Venkatesh et al. (2012) found that reductions in total NO_x and SO_2 emissions from EGUs in ERCOT could be as high as 30% and 50%, respectively, if natural gas reached $1.50 per MMBTU. While $1.50 per MMBTU is below future estimates of natural gas prices in the United States, this study offers an upper bound of changes that would likely occur in the ERCOT grid with lower natural gas prices. Jaramillo et al. (2007) found that upstream NO_x emissions from natural gas production were small compared to emissions reductions in NO_x emissions from coal-fired power plants for the Marcellus Shale. However, when aggregated on the scale of counties or entire shale regions, the total emissions from natural gas production activities can be above the threshold for major point source consideration (Litovitz et al. 2013). Part of the challenge of air quality planning associated with these industries is that the production activities typically include a wide array of sources, spread over a large geographic region, and from many different companies, which may have inconsistent production and emission control practices. Kemball-Cook et al. (2010) estimated the ozone impacts in the Haynesville region associated with various shale gas development scenarios, but this work did not address possible changes in emissions from the power sector. Before this dissertation, no study has coupled the emissions reductions from the power generation sector associated with lower natural gas prices with emissions from natural gas production in a photochemical modeling framework in order to estimate changes in the formation of ozone and PM.

2.4.3 Greenhouse Gas Impacts

On a per MWh basis only considering combustion emissions, coal-fired EGUs in the United States have a greenhouse gas footprint that is on average 1.8 times higher than natural gas power plants (Jaramillo et al. 2007). However, the upstream GHG emissions

from natural gas production must also be examined to determine the GHG footprint over the life cycle of the fuel source. In particular, methane emissions from new shale gas production operations appear to influence the life cycle. The difference in the life cycle of shale gas compared to traditional natural gas and coal is a current debate in the literature. The GHG debate centers on the quantity of fugitive emissions that occur during production. Howarth et al. (2011) estimated that 7% of total methane produced from shale gas is lost as fugitive emissions, which caused the GHG emissions of new shale gas production to be 30-200% higher than traditional natural gas production and comparable to coal on a 20 year timeline. Using a more modest fugitive emissions rate of 2%, Jiang et al. (2011) found that Marcellus Shale gas had an 11% higher GHG footprint than traditional natural gas and was 20-50% lower than the life cycle of coal when EGU combustion was included in the calculations. Substantial research efforts have been undertaken to quantify the GHG emissions associated with various aspects of the natural gas supply chain (Allen et al. 2013; Jackson et al. 2014), but large uncertainty remains in emissions estimates from this sector (Brandt et al. 2014).

2.4.4 Water Use Impacts

Previous studies on the water impacts of new natural gas developments have tended to either quantify the total water consumed in the production stage (Nicot et al. 2012; Murray 2013) in a particular geographic region or have examined total water consumption over the fuel life cycle through use in the electricity generation sector (Grubert et al. 2012; Laurenzi et al. 2013). For Texas, Nicot et al. (2012) found that water withdrawals for shale gas development were less than 1% of the total withdrawals in the state, but that withdrawals could be a much higher percentage of local withdrawals (up to 10%) during periods with locally-intense new well developments. Life cycle

assessments (Grubert et al. 2012; Laurenzi et al. 2013) have found that the water consumption per MWh of electricity generated at an efficient natural gas combined cycle power plant is ~50% less per MWh of electricity generated at a coal-fired power plant. These life cycle assessments, however, have not examined the potential for locally increased water consumption in natural gas production regions, which are not necessarily co-located with electricity generation resources.

2.5 SUMMARY

Previous research on the environmental impacts of new natural gas development has typically focused either on inventorying the emissions or water usage in a particular geographic region (without considering the potential changes in the power sector) or on performing a life cycle assessment over a wide geographic region to compare the emissions or water use per MWh between natural gas and coal. These life cycle assessments studies have not allowed for spatial resolution of the potential changes (which would not occur in a spatially uniform manner) or accounted for the fact that all marginal natural gas production is not used for the displacement of coal-fired power generation. For example, the marginal natural gas production may be used for additional home heating in the winter. The UT/MIT Integrated Model can be used to address this knowledge gap by combining potential upstream emissions and water use changes with price-based changes in the power sector.

Chapter 3: Potential impacts of an ozone forecast-driven air quality market for NOx emissions from eastern Texas power plants

3.1 CONTEXT

Chapter 3 describes the expansion of the UT/MIT Integrated model to include fine particulate matter chemistry (Objective 1) and to allow for the examination of ozone impacts over a monthly time frame by linked simulation days (Objective 2). These objectives are completed in the context of a case study that compares the ozone impacts of a seasonal NO_x emissions price to a strategy that uses NO_x emissions prices to influence dispatch decisions only on days with forecast high ozone concentrations in eastern Texas.

3.2 ABSTRACT

For a theoretical nitrogen oxides (NO_x) emissions market for eastern Texas power plants during the 2006 ozone season, the effectiveness of a single, seasonal NO_x emissions price was compared to scenarios in which pricing occurred only on predicted high ozone days in eastern Texas. The dispatching of electricity generation based on the price of NO_x emissions was estimated using an optimal power flow model, and photochemical modeling of a month-long subset of the 2006 ozone season with an elevated number of days with forecast high ozone was undertaken to assess the impact of the emissions changes on ozone and fine particulate matter ($PM_{2.5}$). Compared to a seasonal NO_x price of $10,000 per ton, charging $20,000 per ton of NO_x on high ozone days resulted in lower costs and more effective reductions in 8 hour ozone concentrations, particularly in northeastern Texas. This result was robust when considering other factors such as emissions carry-over, exposure metrics, and macro-scale meteorology.

3.3 INTRODUCTION

The application of market-based approaches to drive changes in the electricity generation sector has the potential to influence many environmental concerns such as air quality, greenhouse gas emissions, and water availability. (Alhajeri et al. 2011a) Over the last several decades, cap and trade programs such as the Acid Rain Program for sulfur dioxide emissions (SO_2) (Burtraw et al. 1999) and the NO_x State Implementation Plan (SIP) Call Program for nitrogen oxide (NO_x) emissions (Burtraw et al. 2005) in the eastern United States have become the preferred policy method for reducing air quality precursor emissions from electricity generation units (EGUs) since individual EGUs can decide whether to achieve compliance through the addition of new pollution control technologies or through purchasing unused emissions credits from other facilities. Since 1999, power plant NO_x emissions reductions achieved through various cap and trade programs instituted in the eastern United States have led to decreased ozone concentrations, with effects generally being higher on days with elevated ozone concentrations. (Gego et al. 2008; Godowitch et al. 2008; Rieder et al. 2013) Butler et al. (2011) estimated that EGU NO_x emissions in the eastern United States decreased by 48% between 1997 and 2005 as a result of cap and trade programs, reducing mean daily maximum 8-hour average ozone concentrations by 7-8 ppb.

NO_x emissions pricing in the power generation sector has been proposed as a driver for EGU NO_x reductions. (Newell et al. 2003; Chen et al. 2005; Alhajeri et al. 2011a; Alhajeri 2012; Sun et al. 2012) In a deregulated electricity market with sufficient excess capacity, NO_x emissions pricing offers the ability to rapidly change the dispatch order of individual EGUs from higher emitting NO_x power plants to ones with lower emissions rates (Alhajeri et al. 2011a) at comparable cost to other emissions controls (Alhajeri 2012; Sun et al. 2012). Ozone responses to changes in NO_x emissions are

highly non-linear (Sillman 1999) and can differ regionally (Nobel et al. 2001; Mauzerall et al. 2005) and even within a single urban area (Daum et al. 2003; Xiao et al. 2010). In addition, Federal ozone regulations in the United States are based on the fourth highest annual daily maximum 8-hour ozone concentration (EPA 2014c). Thus, from the perspectives of regulation and ozone formation, spatial and temporal considerations for NO_x emissions reductions are important. Applying a single seasonal NO_x emissions price does not focus changes when the marginal health and ozone formation damages would be the greatest (Muller et al. 2009), which would be an important consideration for an efficient emissions reduction program (Tong et al. 2006; Mauzerall et al. 2005; Mesbah et al. 2012; Mesbah et al. 2013). In addition, NO_x trading programs should account for environmental justice and the formation of hotspots, which are areas with increased concentrations caused by shifts in regional emission profiles.

This work examines the impacts of a theoretical air quality market for NO_x emissions from the Electricity Reliability Council of Texas (ERCOT) in which emissions prices are applied based on a day-ahead ozone forecasts for eastern Texas from the Texas Commission on Environmental Quality (TCEQ). Sun et al. (2012) concluded that uncertainty in ozone forecasting would not be a cost hindrance to a NO_x pricing program targeting emissions in the PJM Classic grid in the northeastern United States. This work compares the application of a seasonal NO_x emissions price to an emissions price that is only imposed on predicted high ozone days when marginal health impacts (Gryparis et al. 2004, Mauzerall et al. 2005) and regulatory concerns would be elevated. ERCOT is an interesting test-bed for examining the potential impacts of a NO_x emissions market based on air quality forecasting since the state has a relatively self-sufficient electric grid and large in-state production of natural gas and coal, leading to a diverse portfolio of generation options that are representative of the nation as a whole (Grubert et al. 2012).

In 2006, ERCOT had an installed capacity that was 21% coal, 72% natural gas, 6% nuclear, 1% wind, and 1% other while the actual fuel mix for electricity generation was 38% coal, 46% natural gas, 14% nuclear, 2% wind, and 1% other. (ERCOT 2012) In addition, ERCOT is a competitive electricity market (Daneshi et al. 2011), in which individual EGUs may have decreased incentive to install capital-intensive emissions controls without guaranteed dispatch (Fowlie et al. 2010), increasing the potential usefulness of NO_x pricing in the grid.

3.4 Materials and Methods

3.4.1 Electricity Generation Model

This work examined the operation of the ERCOT electric grid for the entire 2006 ozone season (May through September) using PowerWorld Simulator Version 16 (PowerWorld Corporation 2012). For each hour, the PowerWorld model solved for the generation at each EGU, using a non-linear optimization algorithm that minimized the total operating cost in ERCOT while enforcing constraints to meet demand, on transmission line capacity, on generator minimum and maximum power levels, and accounting for line losses. A linear programming (LP) approach was used to allow for the inclusion of inequality constraints. More information on this PowerWorld model is available in previously published studies. (Alhajeri et al. 2011a; Pacsi et al. 2013a, Pacsi et al. 2013b)

In this study, emissions prices for EGU NO_x emissions in ERCOT were included in the cost c for each generator i:

$$c_i\,(\$/\text{MWh}) = H_i\,(pf_i + pn_i\,N_i) + O\&M_i$$

where H_i is the heat rate of the EGU (MMBTU/MWh) (EPA 2012a), pf_i is the fuel cost ($/MMBTU), pn_i is the NO_x emissions permit price ($/ton NO_x), N_i is the EGU-specific

NO_x emissions rate [ton NO_x/MMBTU] (EPA 2012a), and $O\&M_i$ is the variable operation and maintenance cost ($/MWh) from the type of EGU (EIA 2006). For this study, constant fuel prices of $1.89 per million British thermal units (MMBTU) for coal and $5.94 per MMBTU for natural gas were used in the study based on the average cost for sales to Texas electricity producers during the 2006 ozone season (EIA 2006). It is important to note that NO_x emissions prices (pn_i) are distinct from the abatement cost for an emissions reduction program. In this work, NO_x emissions pricing is used as a cost driver to change the dispatch order of facilities within ERCOT from facilities with higher NO_x emissions rates to those with lower rates. The use of NO_x emissions pricing would, thus, have both a recoverable cost in terms of the emissions price and a non-recoverable (abatement) cost from the use of facilities with higher fuel and/or operations and maintenance costs. The non-recoverable cost is estimated as the difference between the total increase in ERCOT cost from the PowerWorld model and recoverable (emissions) cost. The recoverable cost (tons NO_x * $/ton NO_x) could be used to off-set cost in a variety of ways (such as being provided to consumers to reduce the impact of higher prices being charged due to the emissions trading scheme or being distributed to generators as a way of reducing the cost passed along to consumers). Determination of the most efficient use of the recoverable (emissions) cost is beyond the scope of this work, however.

In a separate simulation for the 2005 ozone season, the PowerWorld model for ERCOT was validated against seasonal total emissions data from the Emissions & Generation Resource Integrated Database (eGRID) (EPA 2012a). Compared to the 2005 ozone season data in eGRID for ERCOT, total seasonal NO_x, SO_2, and CO_2 emissions from the PowerWorld model were within 2.2%, 1.1%, and 3.6% of the eGRID data, respectively. While no eGRID data gathering campaign was undertaken for 2006,

analysis in Alhajeri (Alhajeri 2012) indicates that the little difference exists between using eGRID emissions rates from 2005 and 2007 for ERCOT.

This study compares the structuring of an air quality market based solely on emissions reductions over the ozone season to a market which is based on targeting NO_x emissions reductions on days in which a concentration of 85 ppb ozone or greater was predicted anywhere in eastern Texas (TCEQ 2014b). For the seasonal emissions price market scenario, a NO_x emissions price of $10,000 per ton was applied to ERCOT throughout the entire ozone season. In this work, this scenario will be labeled $10k_alldays. For the forecast-based market, no emissions prices ($0/ton) were applied on days without a high ozone prediction. Scenarios in which the NO_x emissions price on forecast high ozone days in eastern Texas was equal to the seasonal price ($10k_forecast) and double the seasonal price ($20k_forecast) were examined. Ozone forecasts were chosen as the driver of the decision to charge a NO_x emissions price since they are available on the previous day, which would be compatible with the day-ahead market for most of the power production in ERCOT. For this work, an 8-hour high ozone threshold of 85 ppb ozone was used, which is consistent with the TCEQ forecasting during the 2006 ozone season. Beginning in 2008, the TCEQ changed its forecasting threshold to 75 ppb based on changes in the Air Quality Index of the U.S. EPA. Annual performance reviews of the TCEQ ozone forecast since 2005 (Figure 3-1) indicate better than 92% correct prediction of days as having elevated ozone or not for all urban areas in eastern Texas, indicating that uncertainty in ozone forecasting is not expected to have a major impact on the results of this study. The prices of $10,000 per ton and $20,000 per ton were chosen since these emissions prices are in the range where the total cost per ton of NO_x reduced is at a minimum in ERCOT (Figure 3-2). Finally, a scenario in which no NO_x emissions prices ($0k_alldays) were charged during the entire ozone season was

undertaken, in order to serve as a base case for comparison that was roughly equivalent to actual ERCOT operation in 2006.

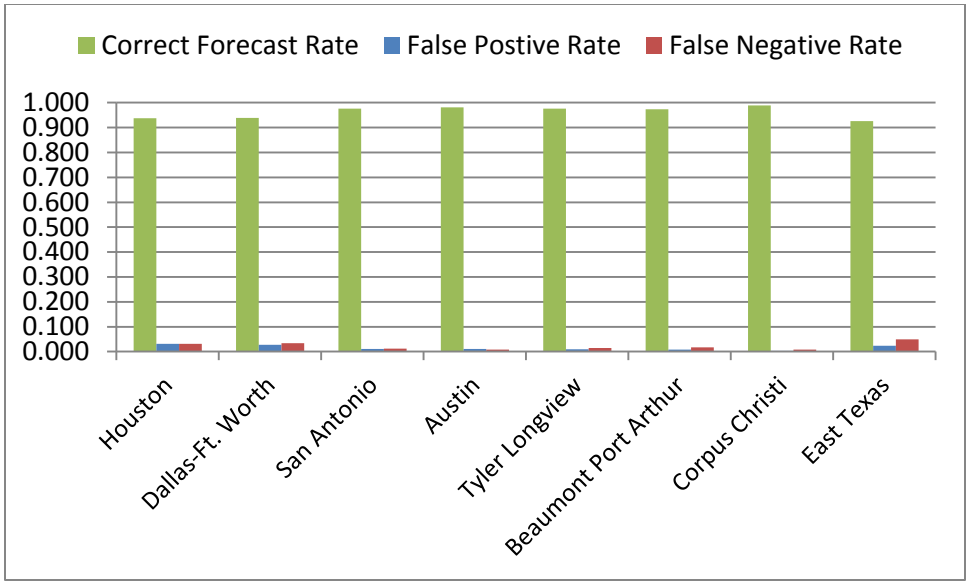

Figure 3-1. For each urban area in eastern Texas and for all of eastern Texas as used in this study, the correct prediction rates, false positive rate, and false negative rate from 2008-2012 as determined by the TCEQ.

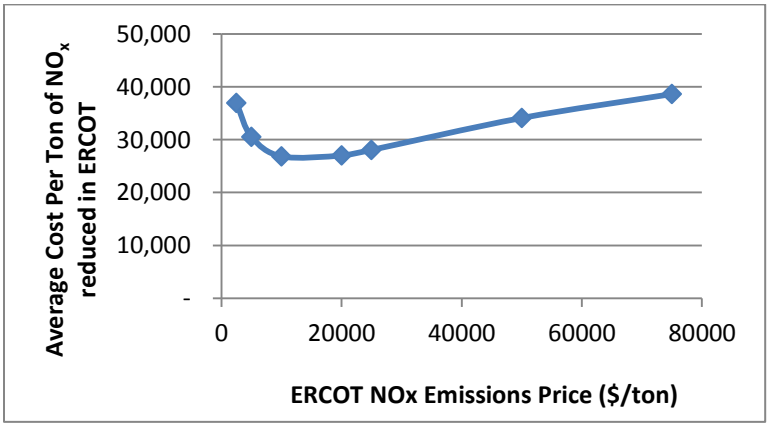

Figure 3-2. Average cost per ton of NO_x reduced associated with the application of a single NO_x emissions price in ERCOT over the entire 2006 May through September ozone season.

3.4.2 Air Quality Model

The base air quality model used in this work was developed by the TCEQ for evaluating air quality management strategies for the Dallas-Ft. Worth (DFW) region (TCEQ 2010). The episode extends from May 31-July 2, 2006, which was a period with many high ozone days throughout eastern Texas. The air quality episode was used in the State Implementation Plan (SIP), and the evaluations of the model performance compared relative to ambient observations during the period in eastern Texas are available from the TCEQ (TCEQ 2010). Changes to the air quality model, in particular to power plant emissions, are described in depth below.

While the air quality episode does not extend throughout the entire May-September 2006 ozone season, it represents a subset of the ozone season in which forecast-based NO_x emissions pricing would have been applied relatively more frequently (70% in the episode versus 37% over the entire ozone season due to the relative frequency of days with ozone forecasts above 85 ppb in eastern Texas). In addition, the air quality episode contains two periods (June 2-15 and June 26-July 1) with elevated ozone concentrations throughout eastern Texas that represent the two dominant macro-scale meteorological conditions that typically cause high ozone concentrations in eastern Texas. The high ozone period from June 2-15 is representative of conditions that most commonly occur during the first half of the ozone season and are characterized by limited transport of background ozone concentrations from geographic regions located far from Texas. In contrast, the high ozone period during June 26 – July 1 followed the passage of a cold front through Texas; these high ozone episodes are more common during late summer and are often associated with the long-range transport of background ozone concentrations into Texas from the Central Plains and/or eastern US.

Understanding the implications of performing photochemical modeling on 33-day subset of the five month ozone season in Texas requires knowledge of the relationship between electricity generation and high ozone in Texas. First, the potential NO_x emission reduction for ERCOT at a given NO_x emissions price is inversely related to the total daily generation in ERCOT (Figure 3-3). On days with higher demand for electricity, the grid has less flexibility to shift generation to lower NO_x emissions. Second, high ozone days in eastern Texas during the 2006 ozone season occurred over a wide range of electricity generation levels (Figure 3-4). During the 33-day photochemical modeling episode used in this work, the potential NO_x emission reductions at different NO_x emissions prices (Table 3-1) were, on average, similar to the overall potential reductions that would occur at the same theoretical NO_x emissions price over the entire season. While the average NO_x emissions reductions per day would be similar between the 33-day subset of the ozone season and the entire ozone season, it is possible that the ozone formation response in the atmosphere would be different during the 33-day episode, which focused on days with elevated ozone concentrations in eastern Texas. Estimating the difference in the ozone response to NO_x emissions reductions during the rest of the ozone season (compared to the 33-day photochemical modeling episode) is beyond the scope of this work. Rather, this subset of the ozone season is modeled in order to show the potential order of magnitude impacts and to examine the possible spatial extent of ozone formation changes.

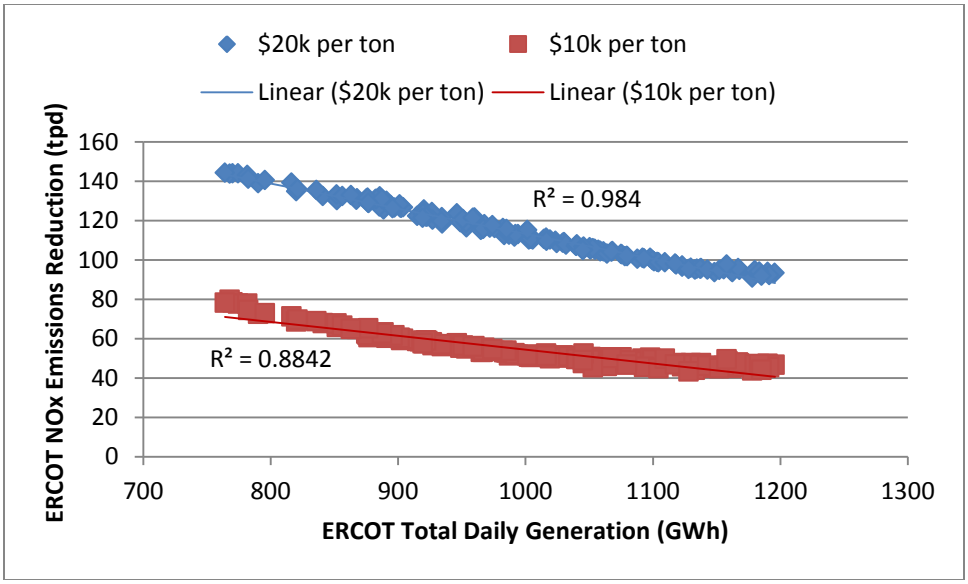

Figure 3-3. Relationship between the total daily generation within ERCOT and the NO_x emissions reduction potential in the grid for all days in the 2006 ozone season at the two NO_x emissions prices examined in this work.

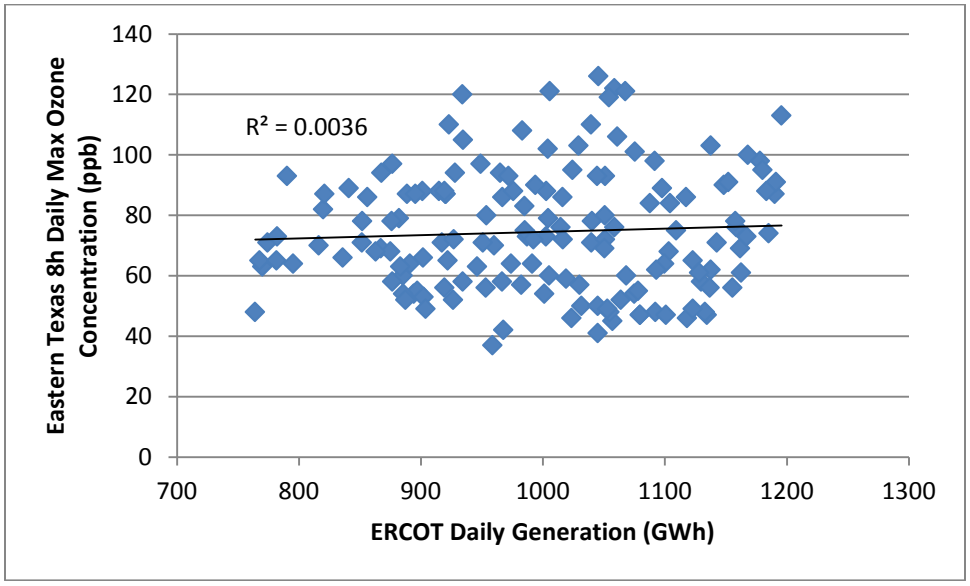

Figure 3-4. Relationship between the daily maximum 8h ozone concentration in eastern Texas and the daily generation level within ERCOT during the 2006 ozone season.

	Average NO_x Reductions (tpd)			
	2006 Ozone Season		June 2006 Episode	
NO_x Price ($/ton)	**All Days**	**Forecast High Ozone Days**	**All Days**	**Forecast High Ozone Days**
2,500	8.6	9.0	8.5	9.0
5,000	22.6	22.5	21.2	21.3
10,000	54.5	53.2	52.9	52.1
20,000	113.5	110.3	112.8	110.6
25,000	136.1	132.5	136.1	133.6
50,000	205.2	200.2	205.8	202.4
75,000	233.0	227.7	233.1	229.2

Table 3-1. Comparison of the daily average NO_x emission reduction potential (tons per day) of various NO_x emissions prices for ERCOT during the entire 2006 ozone season and the 33-day subset used in photochemical modeling. Comparisons are also made for days with high ozone forecasts from the TCEQ.

The air quality simulations were performed with the Comprehensive Air Quality Model, with extensions [CAMx] (ENVIRON 2011), which is a three dimensional Eulerian model which calculates the impacts of emissions, chemistry, advection, and dispersion on atmospheric chemical concentrations. (ENVIRON 2011) This work utilized CAMx version 4.51 with CF aerosol chemistry and plume-in-grid (PiG) treatment of large point source plumes. The CAMx domain (Figure 3-5) included the eastern United States at 36 km x 36 km resolution, eastern Texas and surrounding states at 12 km x 12 km resolution, and the DFW region at 4 km x 4 km resolution.

The TCEQ model for the Dallas-Ft. Worth SIP (TCEQ 2010) did not include estimates of primary particulate matter (PM) or SO_2 emissions for the domain since it was created with a focus on ozone. Methodology for the inclusion of primary PM emissions and non-EGU SO_2 emissions is available in previously published work. (Pacsi

et al. 2013a) It is important to note that primary PM emissions were kept constant throughout all scenarios, and primary PM emissions changes between scenarios would be expected to small compared to changes in secondary PM formation associated with changes in SO_2 emissions from power plants.

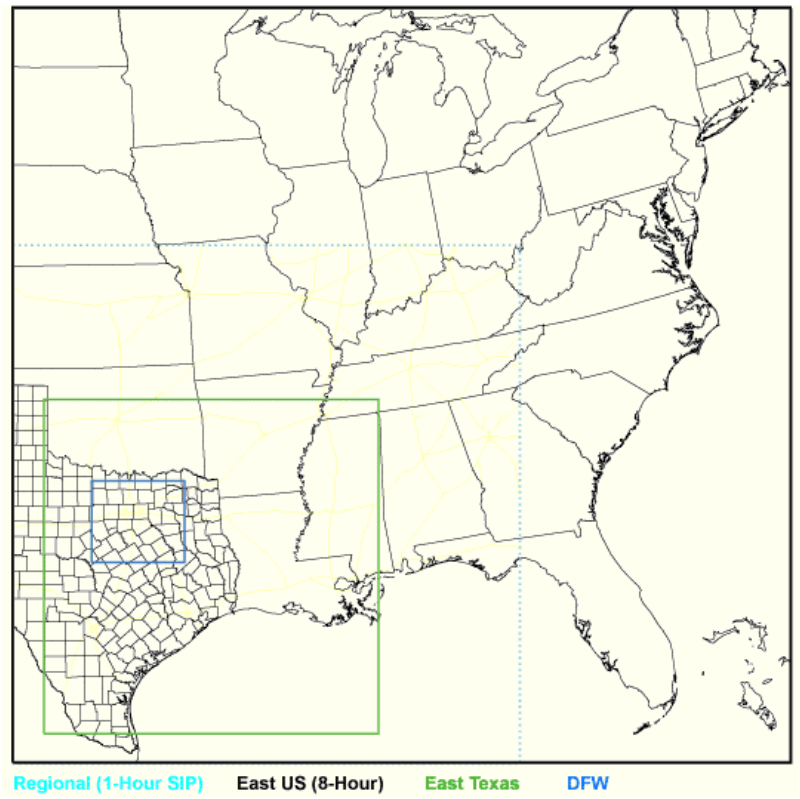

Figure 3-5. CAMx modeling domain with 36 km x 36 km resolution for the eastern United States (black box), 12 km x 12 km resolution for eastern Texas (green box), and 4km x 4 km resolution for the Dallas-Ft. Worth region (blue box).

3.4.3 Power Plant Emissions

For each hour in the episode and each NO_x pricing scenario that was examined, the PowerWorld model solved for the hourly generation (MWh) at each EGU in ERCOT. NO_x and SO_2 emissions rates (tons/hour) for each EGU were estimated based on the

hourly generation and the year 2005 average emissions factor (tons/MWh) for the same power plant (EPA 2012a). Since the eGRID database does not contain emissions rates for carbon monoxide (CO) and volatile organic compounds (VOC), a ratio of episode total VOC and CO to NO_x emissions was determined based on the original TCEQ inventory (TCEQ 2010). The NO_x emissions rates for each hour were then multiplied by this factor to estimate CO and VOC emissions for power plants in ERCOT.

3.5 Results and Discussions

3.5.1 ERCOT Response to NO_x Pricing over the Ozone Season

The seasonal NO_x emissions associated with the three NO_x pricing scenarios in this work (Table 3-2) were compared to a scenario without NO_x emissions pricing ($0k_alldays) that was roughly comparable to actual ERCOT pricing conditions in 2006. A similar breakdown of the emissions changes occurring during the 33-day photochemical modeling episode is available (Table 3-3). Applying a $10,000 per ton emissions price throughout the entire ozone season drives larger total NO_x emissions reductions over the entire season than the application of emissions pricing on the 37.3% of the days with forecast high ozone concentrations. However, in the $10k_alldays scenario, only 36.4% of NO_x emissions reductions over the entire ozone season occur on forecast high ozone days, revealing a potential inefficiency in pricing all emissions reductions equally. Based on the way that current ozone regulations are written, ozone reductions on days above the 8 hour ozone standard are more important than reductions on other days. For the 2006 ozone season, the non-recoverable cost increase of imposing a $10,000 per ton NO_x emissions price only on forecast high ozone days is 37.5% of the cost associated with a price across the entire season (Table 3-2), and this ratio is consistent at higher NO_x emissions prices than $10,000 per ton (Table 3-4). Thus, the

non-recoverable cost increase in ERCOT of implementing a NO_x pricing scheme to trigger emissions reductions is directly related to the frequency at which the price is implemented. In addition, the imposition of a $20,000 per ton NO_x emissions price only on high ozone days is less expensive than a seasonal NO_x emissions price of $10,000 per ton (Table 3-2) while driving an average of 57.1 more short tons per day (tpd) of NO_x reductions on forecast high ozone days (Table 3-1).

Scenario	*Daily Average NO_x Emissions (tpd)*	*Percent Change in NO_x Emissions on All Days*	*Percent Change in NO_x Emissions on High Ozone Days*	*Percent of Seasonal Emissions Reductions the Occur on Forecast High Ozone Days*	*Percent Increase in Non-Recoverable Cost for ERCOT*	*Average Cost Increase for ERCOT ($/MWh)*
$0k_alldays	421.6	N/A	N/A	N/A	N/A	N/A
$10k_alldays	367.1	-12.9%	-12.4%	36.4%	4.0%	1.42
$10k_forecast	401.8	-4.7%	-12.4%	100%	1.5%	0.53
$20k_forecast	380.5	-9.7%	-25.8%	100%	3.1%	1.11

Table 3-2. Comparison of ERCOT power plant NO_x emissions and cost changes over the entire 2006 ozone season based on different NO_x.

Scenario	*Daily Average NO_x Emissions (tpd)*	*Percent Change in NO_x Emissions on All Days*	*Percent Change in NO_x Emissions on High Ozone Days*	*Percent of Seasonal Emissions Reductions the Occur on Forecast High Ozone Days*	*Percent Increase in Non-Recoverable Cost for ERCOT*	*Cost Increase for ERCOT ($/MWh)*
$0k_alldays	419.1	N/A	N/A	N/A	N/A	N/A
$10k_alldays	366.2	-12.6%	-12.3%	68.7%	4.0%	1.42
$10k_forecast	382.8	-8.7%	-12.3%	100%	2.8%	0.99
$20k_forecast	342.0	-18.4%	-26.2%	100%	5.8%	2.08

Table 3-3. Comparison of ERCOT power plant NO_x emissions and cost changes over the 33 day photochemical modeling episode for June 2006.

	Daily Average NO_x Reductions from $0/ton price		Percent Increase In ERCOT Total Cost Versus No NO_x Pricing			
			2006 Ozone Season		June 2006 Episode	
NO_x Price ($/ton)	**Tons per Day**	**% Reduction**	**All Days**	**Forecast High Ozone**	**All Days**	**Forecast High Ozone**
2,500	8.8	2%	0.9%	0.3%	0.9%	0.7%
5,000	21.9	5%	1.9%	0.7%	1.9%	1.3%
10,000	53.2	13%	4.0%	1.5%	4.0%	2.8%
20,000	111.7	27%	8.3%	3.1%	8.3%	5.8%
25,000	134.5	32%	10.3%	3.9%	10.4%	7.3%
50,000	203.2	48%	18.9%	7.1%	19.0%	13.3%
75,000	230.6	55%	24.3%	9.1%	24.3%	17.0%

Table 3-4. Relationship between the daily average NO_x reduction potential (tons per day) in ERCOT at specific NO_x emissions prices in ERCOT and the non-recoverable increase in ERCOT total cost associated with the price application only on high ozone days or across all days in the period of interest.

Since the ozone formation changes associated with NO_x emissions reductions varies with the location of the emissions due to factors such as biogenic VOC concentration in the area surrounding the plume (Mauzerall et al. 2005, Nobel et al. 2001), the spatial distribution of changes to NO_x emissions is important. When compared to the scenario that was roughly equivalent to grid operation in 2006 ($0k_all days), the $10k_alldays scenario involves a 12.9% net decrease in daily average NO_x emissions from ERCOT (Table 3-2) with the largest decreases occurring at small number of power plants (Figure 3-6a). The characteristics of EGUs with decreased NO_x emissions (Table 3-5) are predominantly base-load coal plants in fuel type with reductions also coming

from natural gas peaking plants with high NO_x emissions rates. More than 99% of the plants with increased generation based on NO_x emissions prices were natural gas EGUs (Table 3-6). For the plants that increased generation under the \$10k_alldays scenarios compared to the \$0k_alldays scenarios, 10% were base-load facilities, and 78% were intermediate load facilities. When comparing the \$20k_forecast and \$10k_alldays strategies (Figure 3-6b) over the entire ozone season, the emissions reductions at the high-emitting coal-fired power plants are greater when the lower emissions price is applied on all days. The magnitude of emissions reductions from these facilities, however, is larger at the higher NO_x emissions price on forecast high ozone days (Figure 3-7).

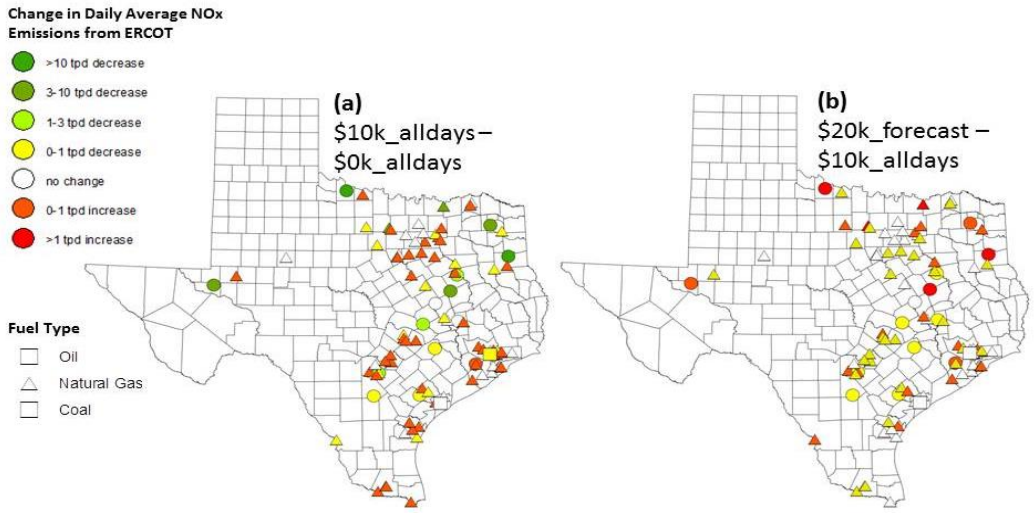

Figure 3-6. Spatial location of changes in daily average ERCOT EGU NO_x emissions (short tons per day) during the 2006 ozone season between (a) the application of a daily NO_x emissions price of \$10,000 per ton and \$0 per ton and (b) the application of a NO_x emissions price of \$20,000 per ton only on forecast high ozone days and the application of a NO_x emissions price of \$10,000 per ton over the entire ozone season.

	Percent of Decreased Generation			Percent of Decreased NOx Emissions		
Capacity Factor	**$10k_ alldays**	**$10k_ forecast**	**$20k_ forecast**	**$10k_ alldays**	**$10k_ forecast**	**$20k_ forecast**
Base Load	83%	81%	86%	78%	76%	82%
Intermediate	2%	2%	1%	1%	1%	0%
Peaking	15%	17%	13%	21%	23%	17%
Fuel Type						
Coal	87%	85%	92%	83%	80%	88%
Natural Gas	13%	15%	8%	16%	20%	12%
Other	0%	0%	0%	0%	0%	0%

Table 3-5. Capacity factor range and fuel type characteristics of power plants that have decreased generation and NO_x emissions compared to the $0k_alldays scenario.

	Percent of Increased Generation			Percent of Increased NO_x Emissions		
Capacity Factor	**$10k_ alldays**	**$10k_fo recast**	**$20k_for ecast**	**$10k_allda ys**	**$10k_fore cast**	**$20k_fo recast**
Base Load	10%	10%	11%	9%	9%	11%
Intermediate	78%	78%	75%	76%	74%	70%
Peaking	12%	12%	14%	16%	16%	20%
Fuel Type						
Coal	1%	1%	1%	1%	2%	2%
Natural Gas	99%	99%	99%	99%	98%	98%
Other	0%	0%	0%	0%	0%	0%

Table 3-6. Capacity factor range and fuel type characteristics of power plants that have increased generation and NO_x emissions compared to the $0k_alldays scenario.

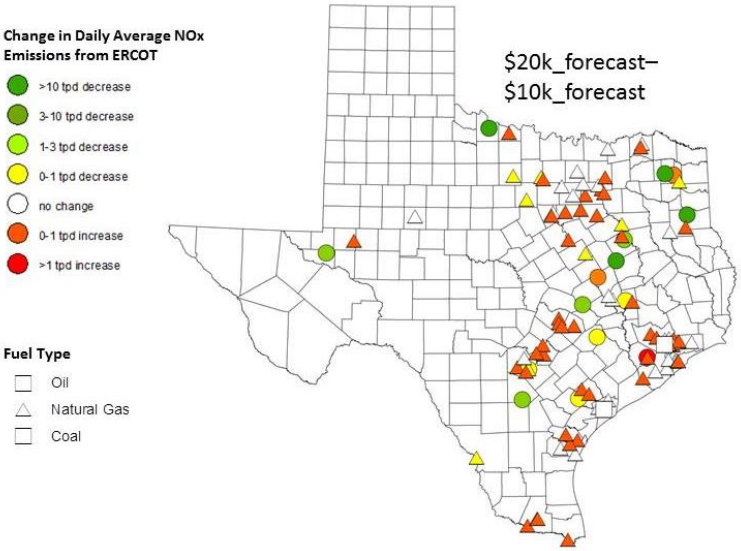

Figure 3-7. Difference in daily average NO_x emissions during the 2006 ozone season between applying a $20k per ton and a $10k per ton NO_x price on forecast high ozone days only.

3.5.2 Regional Ozone Impact

Photochemical modeling of a 33-day period of the 2006 ozone season from May 31-July 2, 2006, was undertaken to determine the impacts on ozone formation of the shifts in emissions from different pricing schemes during an episode with several days with elevated ozone concentrations. During this period, 70% of the days had a high ozone forecast for at least one urban area in eastern Texas compared to 37% of the days over the entire ozone season. The change in ERCOT non-recoverable (abatement) cost and NO_x emissions for the four scenarios examined in this work for this 33-day period are shown in Table 3-2. During this episode, it is important to note that both the NO_x emissions reductions and non-recoverable cost increase in ERCOT are larger in the $20k_forecast case than the $10k_alldays case, which is the opposite trend from the ozone season as whole and is due to the higher than average number of high ozone forecasts during this period. The ozone formation impacts of implementing a single

emissions price on all days ($10k_alldays) and a higher price on only forecast high ozone days ($20k_forecast) are shown based on changes in each grid cell to the episode average 8 hour daily maximum ozone concentration (Figure 3-8) and to the episode maximum 8 hour ozone concentration (Figure 3-9). For reference, the ozone concentrations associated with the $0k_alldays scenario (which was roughly equivalent to ERCOT base-case operation, which was not driven by NO_x emissions pricing) are given in Figure 3-10.

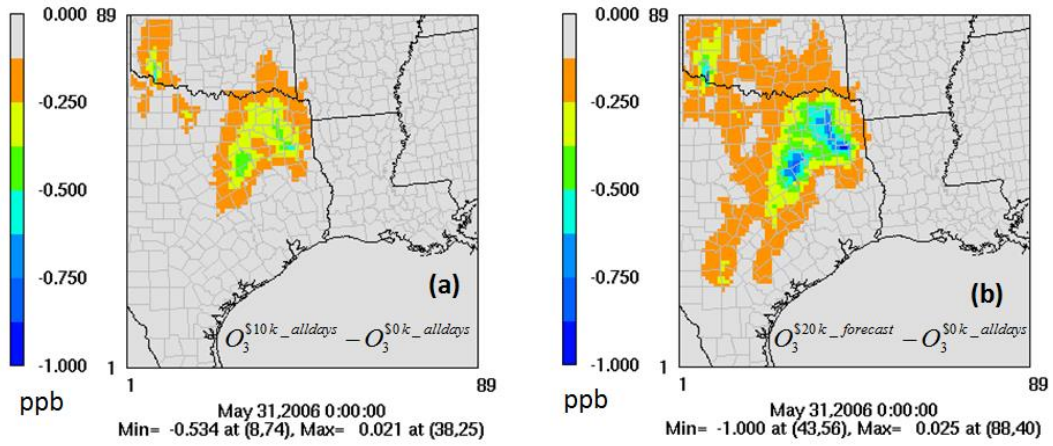

Figure 3-8. Changes to the average daily maximum 8h ozone concentration for each grid cell in the eastern Texas domain over 33 day photochemical modeling episode between the $0k_alldays scenario and (a) $10k_alldays and (b) $20k_forecast. Negative values (shown as colors in the Figure) indicate a decrease in the ozone concentration metric compared to a scenario without emissions prices.

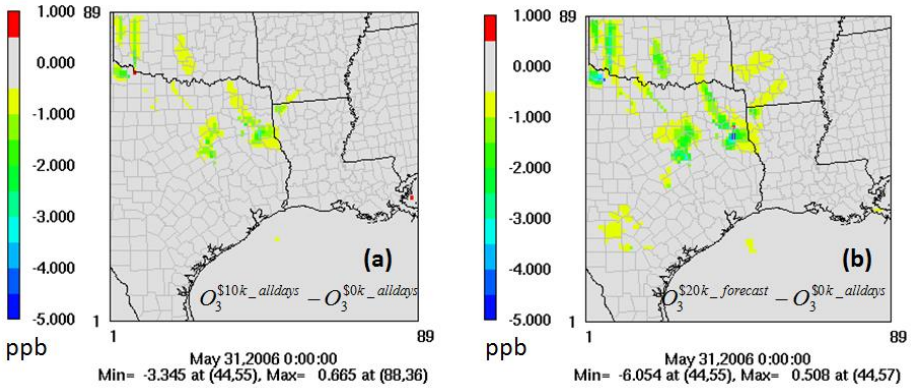

Figure 3-9. Change in the episode maximum 8-hour ozone concentration for (a) $10k_alldays and (b) $20k_alldays compared to the $0k_alldays scenario. Negative values (shown as yellow to blue colors in the Figure) indicate a decrease in episode maximum ozone concentration compared to a scenario without NO_x emissions prices. Episode maximum ozone concentrations are paired in space between scenarios but not necessarily in time.

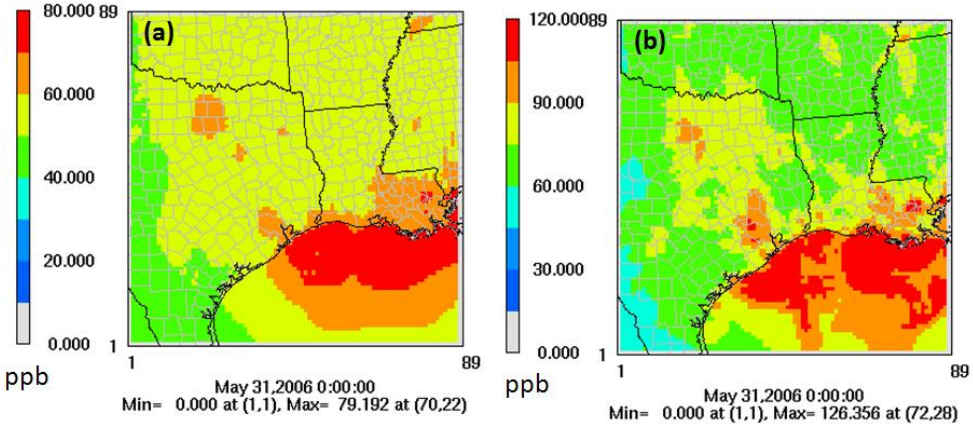

Figure 3-10. Episode (a) average daily maximum 8h ozone concentration and (b) maximum 8h ozone concentration for the $0k_alldays scenario, which was roughly equivalent to actual grid cost conditions in 2006.

Comparing the episode average changes to the daily maximum 8 hour ozone concentration and the change to the episode maximum 8 hour ozone concentration (paired in space but not in time between scenarios) for each grid cell, the application of a $20,000 per ton emissions price on high ozone days yields larger decreases in both

magnitude and spatial extent than the application of a $10,000 per ton emissions price on all days during the episode. Ozone decreases tend to be highest in northeastern Texas, where significant emissions reductions occur from dispatching electricity generation away from several coal-fired power plants with high NO_x emissions rates (Figure 3-6). Since the Federal 8 hour ozone standard is written as being the average of the annual 4th highest daily maximum 8h ozone concentrations from the previous three years (EPA 2014c), the episode maximum 8 hour ozone concentration can be an important metric from a regulatory perspective. Large reductions in this metric (Figure 3-9) occurred in the plumes of coal-fired power plants in northeastern Texas and were a maximum of 6 ppb. Reductions to the episode average daily maximum 8 hour ozone concentration (Figure 3-8) were generally lower in magnitude (< 1 ppb). In the $20k_forecast case (Figure 3-8b), small ozone decreases (<0.3 ppb) were modeled in several urban areas of Texas, including Dallas-Ft. Worth and San Antonio. Ozone concentrations in the Houston area, however, remained largely unaffected by changes in power plant NO_x emissions. Finally, the formation of ozone hotspots, or areas with increases in ozone concentrations near facilities with increased generation and NO_x emissions did not appear to be a major concern with NO_x pricing schemes in Texas during the 2006 ozone season. Hotspot formation, however, has been a shown to be a concern with NO_x trading schemes with a different geographic location and time (Mesbah et al. 2012, Mesbah et al. 2013) than this study.

3.5.3 Additional Ozone Formation Considerations

While the application of a higher NO_x emissions price ($20,000 per ton) has a larger impact on the 8h ozone metric associated with the determination of compliance with the National Ambient Air Quality Standards (NAAQS) over the 33 day episode in

this work, the impact of emissions carry-over, macro-scale meteorological influences, and exposure metrics were also considered in this work. Carry-over impacts occur when NO_x emissions reductions on a previous day lead to lower ozone concentrations on the next day due to decreased initial ozone and NO_x concentrations. In this work, carry-over was characterized in two ways through comparisons of the \$10k_alldays to the \$10k_forecast and the \$20k_forecast scenarios (Figures 3-11 and 3-12). The first type of carry-over (Figure 3-11) occurs on the first day in a series with a high ozone forecast. For two days prior to June 2, high ozone had not been forecast in eastern Texas, and as a result, emissions prices had been imposed in the \$10k_alldays case but not in the forecast-based scenarios. In Figure 3-11, yellow to red colors indicate areas where NO_x emissions reductions on previous days in the \$10k_alldays case continued to have impacts on the 8h daily maximum ozone concentration on June 2. Blue areas (Figure 3-11b) indicate regions in which the higher NO_x emissions price (\$20,000 per ton) drives decreased ozone concentration compared to the \$10,000 per ton price. The second type of carry-over occurs on the first day without a high ozone forecast after several days with one. The higher NO_x reductions in the \$20k_forecast scenario on forecast high ozone days compared to the \$10k_alldays case continues to impact ozone concentrations even with NO_x pricing on that day (Figure 3-12). For both types of carry-over, the magnitude of carry-over impacts on daily maximum 8h ozone is 0.2 to 0.5 ppb and is, thus, smaller in both magnitude and spatial extent than changes in ozone formation caused by charging a higher emissions price on that day. This finding is consistent with previous work (Frost et al. 2006) that the ozone formation impacts of NO_x emissions reductions tend to dissipate on subsequent days as the plume fully mixes with the surrounding atmosphere.

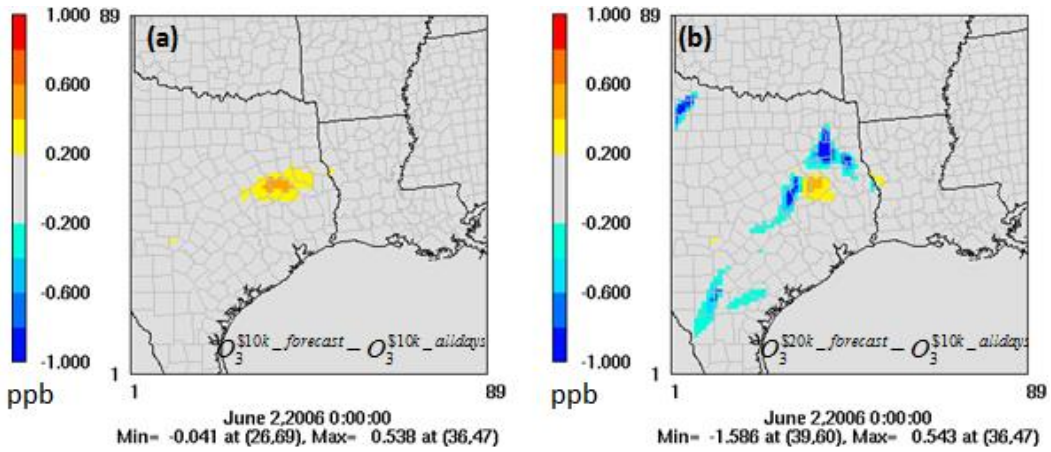

Figure 3-11. Magnitude of next day carry-over impacts on daily maximum 8h ozone concentration on June 2, 2006, in which forecast-based NO_x emissions pricing had not been applied for two previous days. Comparisons to the $10k_alldays scenario are made to (a) the $10k_forecast scenario, in which the only difference is the application of NO_x emissions pricing over the preceding three days and (b) the $20k_forecast, which allows for the comparison of the magnitude of carry-over impacts compared to the impacts of charging higher emissions prices on June 2, 2006. Yellow to red colors indicate areas in which ozone concentrations are elevated in the forecast scenarios compared to the scenario with emissions prices on all days while blue colors indicate decreased ozone concentrations.

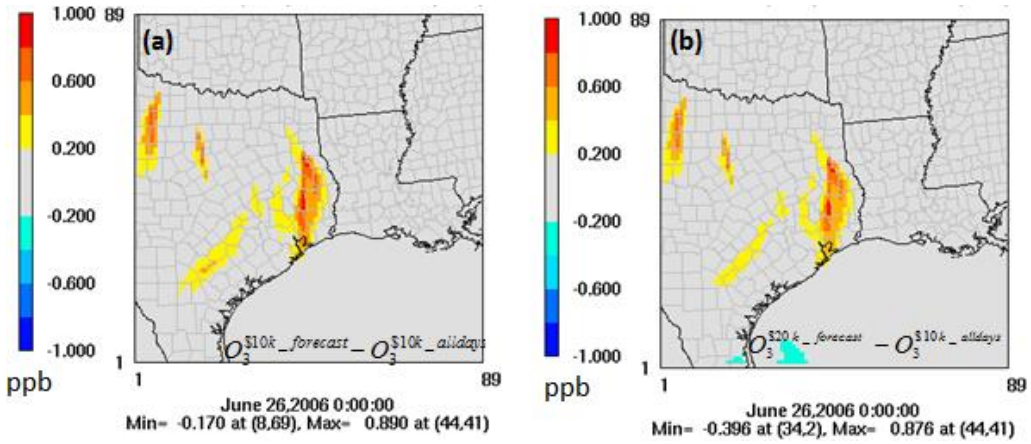

Figure 3-12. Magnitude of next day carry-over impacts on daily maximum 8h ozone concentration on June 26, 2006, in which forecast-based NO_x emissions pricing had been applied for the three previous days. Comparisons to the \$10k_alldays scenario are made to (a) the \$10k_forecast scenario, in which the only difference is the application of NO_x emissions pricing on June 26 and (b) the \$20k_forecast, which allows for the comparison of the magnitude of carry-over impacts from higher emissions reductions on previous days compared to the deployment of emissions prices on June 26, 2006. Yellow to red colors indicate areas in which ozone concentrations are elevated in the forecast scenarios compared to the scenario with emissions prices on all days while blue colors indicate decreased ozone concentrations.

As mentioned previously in this work, eastern Texas has two types of macro-scale meteorological conditions that typically cause high ozone concentrations which will be referred to as early season meteorology and late season meteorology. In the photochemical modeling episode, the early season meteorology was prevalent from June 2-15 while the late season meteorology was prevalent from June 26 – July 1. Comparison of two forecast-based emissions trading levels (\$10,000 per ton and \$20,000 per ton) are shown in Figure 3-13. At the same NO_x emissions price, the average changes to the daily maximum 8h ozone concentration are similar during the periods with early season ozone and late season ozone meteorology.

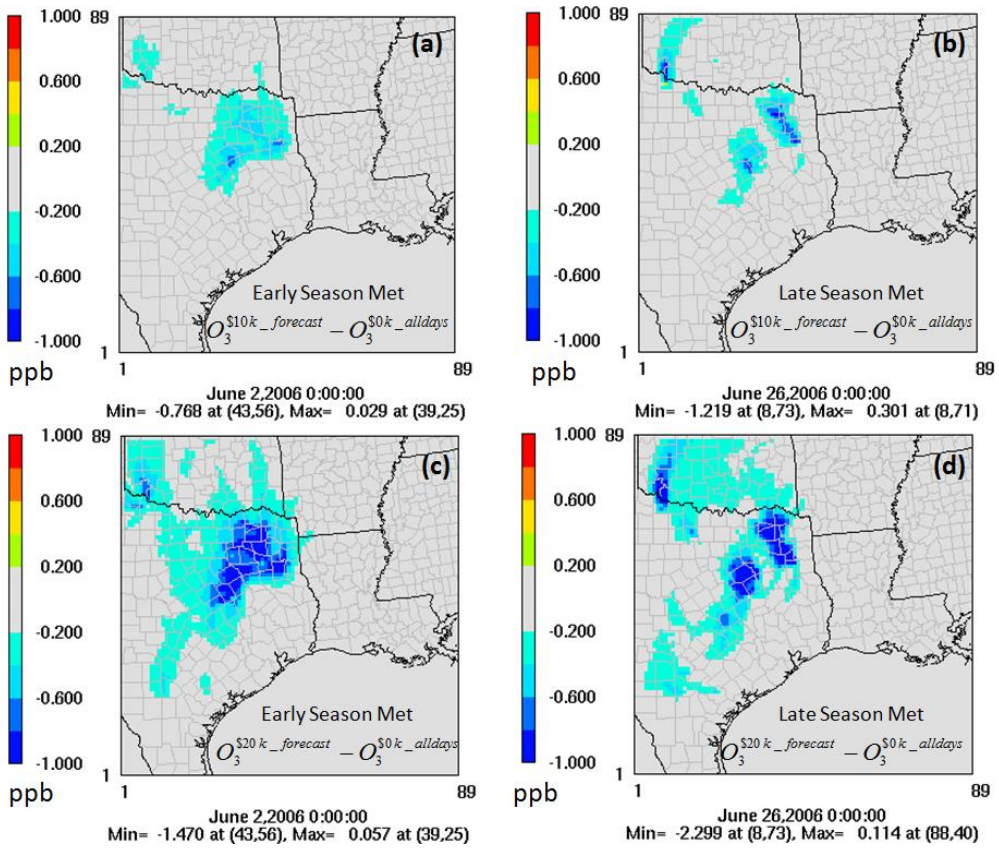

Figure 3-13. Comparison of the average reduction (blue color, negative values) in daily maximum 8h ozone concentration based on macro-scale meteorological conditions typically associated with early season high ozone days (6/2-6/15) and late season high ozone days (6/26-7/1) comparing either a $10k/ton (a, b) or $20k/ton (c, d) emissions price only on forecast high ozone days to a scenario without emissions pricing.

3.5.4 Ozone Exposure Metrics

Research (Bell 2006) has found health impacts associated with increased ozone concentrations even when ambient conditions were below current U.S. standards. Thus, the possibility exists that any ozone decreases would yield health benefits. For this work, several area and population-based exposure metrics were examined to compare the impacts of the emissions reductions associated with NO_x pricing scenarios. Detailed information on these metrics is available in existing literature (Nobel et al. 2001, Nobel et

al. 2002, Alhajeri et al. 2011b). All metrics shown below (Table 3-7) were calculated as the percent difference in the ozone metric between the scenario examined and the \$0k_alldays, which was the scenario without NO_x emissions trading, for the area of eastern Texas included in the 12 km by 12 km eastern Texas photochemical modeling domain over the 33 day photochemical modeling episode.

Time Integrated Area above a Threshold (Time Area):

$$A_{Time} = \sum_h \sum_g A_g x \delta_{g,h}$$

$$\delta_{g,h} = \begin{Bmatrix} 0, & C_{g,h} \le Threshold \\ 1, & C_{g,h} > Threshold \end{Bmatrix}$$

where A_g is the area of a grid cell g (km^2). This metric is calculated by determining whether the ground level 1-hr ozone concentration $C_{g,h}$ exceeded an ozone threshold value (65 or 75 ppb). If for any hour h during the 33 day episode, the threshold is exceeded, the area of the grid cell is added to the total. A time integrated population above a threshold metric (Time Population) can also be calculated by replacing the area of the grid cell A_g with the total population within the grid cell P_g based on census data.

Total Episode Area Exposure (Excess Area):

$$A_{Excess} = \sum_h \sum_g A_g x \delta_{g,h}$$

$$\delta_{g,h} = \begin{Bmatrix} 0, & C_{g,h} \le Threshold \\ C_{g,h} - Threshold, & C_{g,h} > Threshold \end{Bmatrix}$$

This metric is calculated differently from the Time Area metric above in that the area of the grid cell A_g is multiplied by the difference between the 1 hour ozone concentration $C_{g,h}$ and the chosen threshold value. This weighs grid cells with a larger excess value over the threshold more heavily than grid cells with a lesser exceedance. A total population exposure metric (Excess Population) can also be calculated by substituting the grid cell population P_g for the grid cell area A_g in this metric. While a 0 threshold in the

time area and time population metric is unlikely to have meaning with equal weighting of all grid cells, the weighting of the grid cell by the amount of the excess may yield insights.

	Time Area		Time Population		Excess Area			Excess Population		
Threshold	**65**	**75**	**65**	**75**	**0**	**65**	**75**	**0**	**65**	**75**
10k_alldays	-1.6%	-2.6%	-1.2%	-1.4%	-0.1%	-2.1%	-2.4%	-0.1%	-1.2%	-1.1%
10k_forecast	-1.5%	-2.4%	-1.1%	-1.2%	-0.1%	-1.9%	-2.3%	-0.1%	-1.1%	-1.0%
20k_forecast	-3.0%	-4.6%	-2.3%	-2.6%	-0.2%	-3.8%	-4.1%	-0.3%	-2.3%	-1.9%

Table 3-7. Comparison of ozone population and area exposure metrics. Percentages are reductions in the magnitude of the metrics in the portion of Texas in the 12 km by 12 km modeling domain for the emissions pricing scenarios over the 33 day photochemical modeling episode compared to the $0k_alldays case without NO_x emissions prices.

Different metrics and thresholds show a consistent pattern with regards to the effectiveness of the NO_x pricing strategies (Table 3-7), which is consistent with findings from previous research (Nobel et al. 2002). Despite applying emissions pricing on only 70% of the days in the 33-day photochemical modeling episode, changes in population and area exposure metrics in the $10k_forecast case are similar to the application of the same emissions pricing ($10k_alldays) on all episode days, while the $20k_forecast scenario yields reductions that are roughly double the reductions of the scenarios with $10,000 per ton NO_x pricing. Area exposure metrics tend to be dominated by large changes in ozone concentrations in northeastern Texas while population exposure metrics tend to be dominated by small changes in the urban areas of Texas.

3.5.5 Potential Co-Benefits

Shifting power generation based on NO_x emissions pricing from coal-fired, base load power plants to intermediate natural-gas plants offers other potential co-benefits.

Compared to coal-fired power plants, natural gas EGUs on average consume less water (Grubert et al. 2012) and have lower CO_2 and SO_2 emissions (deGouw et al. 2014). Over the 2006 ozone season, all scenarios offer net benefits in terms of SO_2 and CO_2 emissions as well as water consumption in ERCOT (Table 3-8). Despite only re-dispatching generation on 37% of days in the season, the co-benefits of the \$20k_forecast scenario approach the \$10k_alldays scenario, despite having a lesser increase in non-recoverable ERCOT cost (Table 3-2).

	33-Day Episode Daily Average			***Percent Change from 0k_alldays***		
Scenario	**SO_2 emissions (tpd)**	**Water Consumption (1000 m^3/d)**	**CO_2 emissions (1000 tpd)**	**SO_2 emissions**	**Water Consumption**	**CO_2 emissions**
\$0k_alldays	1485.8	1299.1	648.2	0.0%	0.0%	0.0%
\$10k_allday	1334.8	1271.4	613.6	-10.2%	-2.1%	-5.3%
\$10k_forecast	1433.4	1289.1	635.8	-3.5%	-0.8%	-1.9%
\$20k_forecast	1351.7	1274.5	621.1	-9.0%	-1.9%	-4.2%

Table 3-8. Potential environmental co-benefits to NO_x emissions pricing scenarios over 2006 ozone season.

From a program cost-benefit perspective in air quality, changes in fine particulate matter (PM) are important. For example, reductions in regional PM concentrations were the largest driver of health-based cost savings in the Acid Rain Program (Chestnut et al. 2005). Figure 3-14 shows the changes to episode average fine PM concentrations for each of the emissions pricing scenarios over the 33-day photochemical modeling episode. The magnitude and spatial extent of PM reductions is greater for the \$20k_forecast scenario than the \$10k_alldays scenario. This was largely driven by the fact that SO_2 emissions reductions during the modeling period were 24.2 tpd greater in the \$20k_forecast scenario compared to the \$10k_alldays scenario. Changes in PM were

explained by changes in particulate sulfate and associated ammonium ion titration, which is consistent with previous studies of PM changes related to changes in EGU emissions (Mueller et al. 2004; Pacsi et al. 2012, Pacsi et al. 2013a).

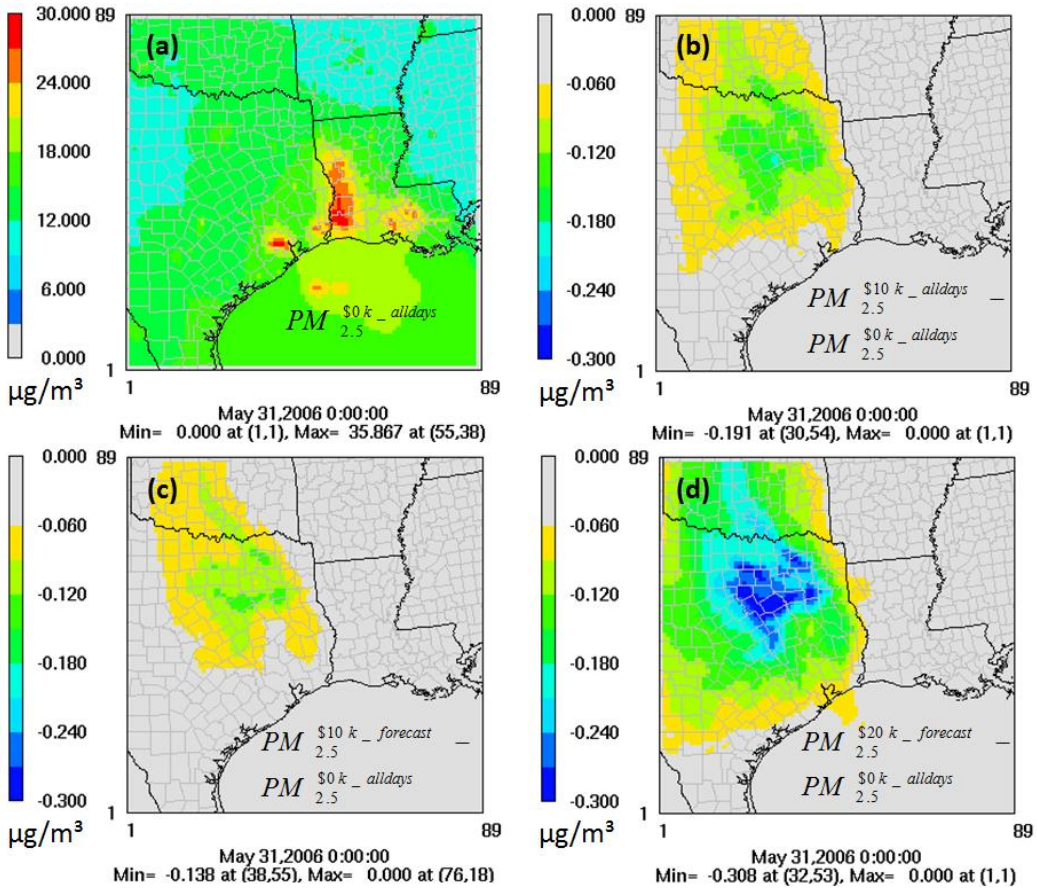

Figure 3-14. Changes to average fine PM concentration over the 33-day photochemical modeling episode compared to a scenario without NO_x emissions pricing (a). Negative values in plots b-d indicate reductions in episode average PM concentration.

3.5.6 Policy Implications

When considering an entire season, the cost of implementing a NO_x emissions pricing program in ERCOT is related to the abatement cost ($/ton pollutant) and the number of days that the cost is implemented. Over the course of the 2006 ozone season, it

would have been less costly to implement a $20,000 per ton emissions price on power plant NO_x emissions on forecast high ozone days than to implement a price of $10,000 per ton over the entire season. For a photochemical modeling episode with elevated ozone concentrations, greater reduction in 8 hour ozone concentrations was found by applying the higher price only on high ozone days than for applying a price to all days. This result was robust considering a variety of ozone metrics, PM reductions, macro-scale meteorological influences, and carry-over impacts. The efficiency of NO_x emissions trading programs in Texas could be improved through coupling with ozone forecasting, to target reductions on days when they would have the highest impact.

Chapter 4: Changing the Spatial Location of Electricity Generation to Increase Water Availability in Areas with Drought: A Feasibility Study and Quantification of Air Quality Impacts in Texas

Pacsi, A. P.; Alhajeri, N.S.; Webster, M. D.; Webber, M. E.; Allen, D. T. *Environmental Research Letters*. **2013**, *8*, doi:10.1088/1748-9326/8/3/035029

4.1 CONTEXT

Chapter 4 describes the expansion of the temporally-linked UT/MIT Integrated model from the use of a NO_x emissions price as the driver of changes in electricity dispatch to the consideration of a different driver of dispatch [the location of drought] (Objective 3). For this work, the feasibility, relative cost, and air quality impacts of using the spatial location of drought as a driver of ERCOT dispatch decisions is examined.

4.2 ABSTRACT

The feasibility, cost, and air quality impacts of using electrical grids to shift water use from drought-stricken regions to areas with more water availability were examined. Power plant cooling is a large portion of freshwater withdrawals in the United States, and shifting where electricity generation occurs can allow the grid to act as a virtual water pipeline, increasing water availability in regions with drought by reducing water consumption and withdrawals for power generation. During a 2006 drought, shifting electricity generation out of the most impacted areas of South Texas (~10% of base case generation) to other parts of the grid would have been feasible using transmission and power generation options available at the time, and some areas would experience changes in air quality. Although expensive, drought-based electricity dispatch is a potential parallel strategy that can be faster to implement than other infrastructure changes, such as air cooling or water pipelines.

4.3 INTRODUCTION

Over the past several decades, droughts in the United States have tended to become more extreme, (Dai et al. 2004) and drought is expected to become more frequent in many areas of the United States, including Texas (Strzepek et al. 2010). A drought in the western United States from 1998-2004 was nearly record setting in terms of decreased water availability (Andredais et al. 2005, Cook et al. 2007). Other short term droughts, such as in Texas in 2011 (Nielsen-Gammon 2012) and the Midwest in 2012 (Schnoor 2012), have also been severe. In the United States, cooling for electricity generating units (EGUs), which are commonly known as power plants, accounts for approximately 40% of freshwater withdrawals, (King et al. 2008a) which is defined as the total amount of water that is removed from a source (Kenny et al. 2009). Power plants also account for approximately 3% of total domestic water consumption (Averyt et al. 2013), which is defined as the portion of water that is not returned to the source from which it was removed (King et al. 2008a). Due to their critical need for cooling water, thermoelectric power plants are vulnerable to water shortages that can occur during drought. (Stillwell et al. 2011a) For example, in the summer of 2007, severe droughts in the southeastern United States forced localized reductions in nuclear power generation due to insufficient cooling water (Hightower et al. 2008; Manuel 2009). Thus, drought can increase stress on both the water and electricity generation infrastructures.

Texas makes a particularly interesting test-bed for examining the interconnectivity of water systems and electricity generation. From a water systems perspective, the state has large variability in precipitation from arid (west) to relatively wet (east) and several river systems that do not cross state boundaries. (Stillwell et al. 2011a) Texas also has a self-contained electric grid, the Electric Reliability Council of Texas (ERCOT), which services 23 million customers, which is small enough to model

effectively but large enough to have useful results for the national scale (Alhajeri et al. 2011a). The generation resources in ERCOT are a reasonable approximation of the national mix and include all major fuel types and prime mover technologies [such as combined cycle, steam turbine, and simple cycle combustion turbine natural gas-fired power plants] (Stillwell et al. 2011b). Texas also has experienced several severe droughts in recent history (NCDC 2014). Finally, future population and electricity demand growth in Texas is predicted to increase the stress on both the water and electricity infrastructures systems (King et al. 2008a; Sovacool et al. 2009), even during times with relatively more water availability.

Previous studies (Alhajeri et al. 2011a; Sun et al. 2012) have shown that changes in where electricity is generated can cause significant changes in both the magnitude and location of air pollutant emissions. Electricity generation can be dispatched, where dispatching refers to the process by which power plants are assigned generation by an electric grid operator like ERCOT, to minimize air quality impacts if the electric grid has sufficient flexibility in transmission and generation capacity. This work expands on these previous analyses of dispatching for air quality objectives, demonstrating that the grid can also be operated as a virtual water "pipeline" to "deliver" increased water availability in drought stricken regions by shifting power generation to other areas of the grid. These shifts in generation, while increasing water availability in targeted regions, can potentially increase electricity costs and change the spatial distribution of air pollutant emissions. Individual power plant factors such as fuel type (Grubert et al. 2012; Macknick et al. 2012), cooling system configuration (King et al. 2008a; Macknick et al. 2012), and prime movers (e.g. the power cycle) can affect water withdrawals and water consumption. Thus, changing the dispatch order may also impact the fuel mix for ERCOT, which can affect water usage in the electricity generation sector. Typical values

for fossil fuels EGUs range from 1,100-189,000 liters/MWh for water withdrawals and 1,000-1,800 liters/MWh for water consumption (King et al. 2008a). This work reports changes to both consumptive water use and withdrawals at power plants in Texas that would result from dispatching power generation away from drought stricken regions.

Recent studies (Feely et al. 2008; Zhai & Rubin 2010; Stillwell & Webber 2013a) have examined reducing the water footprint of electricity generation through the installation of air cooling technologies, which take years to deploy. Since the dispatch order can be adjusted on a daily or even faster basis, the approach outlined in this work offers the potential for rapid implementation and quick adaptation to shifts in the location of drought. The shifts may also have non-monetized costs associated with changes in the amount and location of emissions of nitrogen oxides (NO_x) and sulfur dioxide (SO_2). NO_x is a precursor for ozone formation, which has been linked to health impacts such as increased respiratory mortality (Bell et al. 2004; Anenberg et al. 2010). While SO_2 is one of many precursors for fine particulate matter (PM), it contributes to the formation of PM sulfate, which is the largest mass component of fine PM in Texas (Russell et al. 2004), and the most sensitive PM species to changes in electricity generation (Mueller et al. 2004; Bergin et al. 2007). Fine PM has been shown to increase instances of lung cancer and overall morbidity (Pope et al. 2002; Anenberg et al. 2010).

4.4 METHODS

4.4.1 Episode Selection

For this work, the potential impacts of drought-based electricity dispatch in ERCOT were examined using a 33-day episode from May 31-July 2, 2006. While Texas has experienced several periods of drought in the last decade, (NCDC 2014) this particular drought episode was chosen for this proof of concept work since it

corresponded with the period that the Texas Commission on Environmental Quality (TCEQ) had previously chosen for air quality planning in Texas (TCEQ 2010). In Texas, both the Dallas-Fort Worth and Houston areas are currently in non-compliance with the federal 8-hour ozone standard (EPA 2013), and policy changes that would negatively impact air quality in these areas would thus be difficult to implement. Therefore, it is important to characterize the potential air quality impacts of water availability-based changes in the electricity generation sector.

4.4.2 Power Plant Water Use Factors

The average water use per unit of generation at each power plant in ERCOT was characterized by a previously-developed consumption rate (King et al. 2008b) and withdrawal rate (Averyt et al. 2013). These data were used, rather than data from the U.S. Energy Information Administration (EIA 2012a) because recent research (Macknick et al. 2012; Averyt et al. 2013) has found numerous inaccuracies in water withdrawal data that is reported annually to the EIA. For the year 2008, Averyt et al. (2013) classified each power plant in the United States based on its fuel, generation technology, and cooling system type and assigned the median withdrawal rate for the configuration. (Macknick et al. 2012) Power plant-specific consumption rates were estimated by King et al. (2008b) using 2006 total water consumption data and total electricity generation that was reported to the TCEQ. King et al. (2008b) screened data for completeness and used average factors specific to fuel type and generation technology when incomplete or erroneous data was found. Both resources (King et al. 2008b; Averyt et al. 2013) provide estimates of the error bounds associated these factors, but a detailed discussion of error bounds is beyond the scope of this work.

4.4.3 Electricity Generation Model

For each hour in the episode, a PowerWorld model was used to determine the generation level (MWh) at each power plant in ERCOT that minimized the total cost of electricity generation subject to meeting demand and including line losses, transmission line capacity limits, and EGU maximum and minimum generation levels. A linear programming (LP) approach was used that allowed for all constraints to be met, including inequalities. More information on the implementation of this electricity generation model in ERCOT is available in prior publications (Alhajeri et al. 2011a; Pacsi et al. 2013). As shown in Table 4-1, the PowerWorld model was validated based on a comparison to industry data for June 2006 (EIA 2013), and performance was consistent with a similar model in peer-reviewed literature (Venkatesh et al. 2012). For each hour and each power plant, water consumption and withdrawals were calculated by multiplying the unit generation (MWh) by the matched water usage rates (m^3/MWh) that were described in the previous section.

	June 2006 Episode		**Venkatesh et al. (2012)**	
Fuel Type	**PowerWorld Model**	**Industry Data (EIA 2013)**	**Peer-Reviewed Model**	**Industry Data**
Coal	32%	32%	45%	40%
Natural Gas	52%	55%	36%	38%
Nuclear	10%	11%	13%	13%
Other	6%	2%	6%	9%

Table 4-1. Comparison of ERCOT fuel mix (MWh) for the PowerWorld electricity model used in this study to actual generation (EIA 2013) and to another model in the peer-reviewed literature (Venkatesh et al. 2012). This work focused on an episode from May 31-July 2, 2006, while Venkatesh et al. (2012) modeled the year 2010.

For the base case in this work, the PowerWorld model was executed with an objective of minimizing the total generation cost in ERCOT while excluding water-based constraints. The choice of a cost-minimized base case is consistent with ERCOT operations in which generation rights are assigned based on bidding by power plants while accounting for transmission and security constraints (Daneshi et al. 2011). In addition, four scenarios in which the grid was operated based on water consumption constraints were examined and are summarized in Table 4-2. The water consumption constraints applied to ERCOT were based on the spatial location of each power plant relative to the U.S. Drought Monitor intensity index for Texas on June 13, 2006, (USDM 2014) as shown in Figure 4-1. For this period, all of Texas was classified as being under drought conditions (USDM 2014), although the intensity varied geographically from abnormally dry (least intense) to exceptional drought (most intense) as shown in Figure 4-1. In practice, drought-based changes to the spatial location of electricity generation in Texas could be applied based on a number of different drought measurement techniques, but this work presents a proof of concept using the U.S. Drought Monitor intensity index.

Scenario Name	Constraints in Abnormally Dry and Moderate Drought Regions	Constraints in Severe Drought Regions	Changes in Extreme and Exceptional Drought Regions
Base Case	None	None	None
A	None	None	No water withdrawing electricity generation
B	None	0% net consumptive water increase from the base case	No water withdrawing electricity generation
C	None	5% net consumptive water decrease from the base case	No water withdrawing electricity generation
D	None	10% net consumptive water decrease from the base case	No water withdrawing electricity generation

Table 4-2. Summary of the drought-driven constraints on electricity generation for each scenario examined in this study.

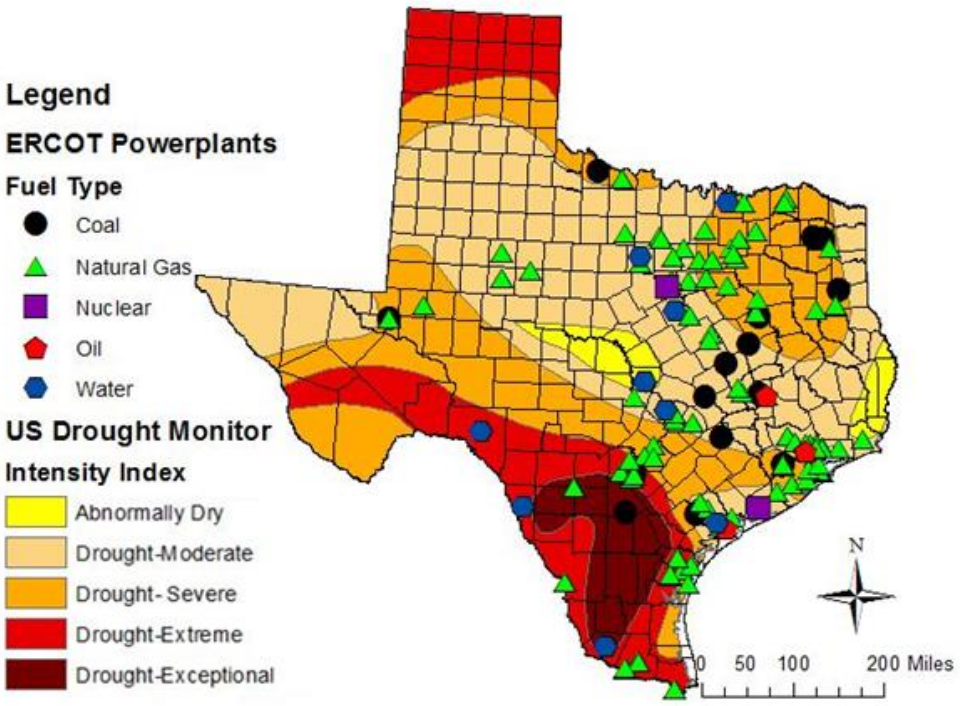

Figure 4-1. Location of ERCOT power plants requiring cooling water withdrawals and U.S. Drought Monitor intensity index for June 13, 2006. (USDM 2014) Drought intensity increases from abnormally dry (yellow) to drought-exceptional (dark red). Almost 10% of ERCOT base-load generating capacity was located in south Texas locations under extreme or exceptional drought.

The first scenario (Scenario A) involved eliminating water-withdrawing electricity generation in areas of South Texas with extreme and exceptional drought (as shown in Figure 4-1) and represented the minimum cost strategy for shifting water use from the highest drought areas. For Scenario A, the shifted electricity generation (7.7 GW of generation capacity and 9.9% of base case generation) was dispatched based on minimizing total additional cost in ERCOT. In order to prevent exporting water availability issues to other areas that were classified as having severe drought (the next

most intense drought class as show Figure 4-1), three additional scenarios were modeled in which no generation occurred in extreme and exceptional drought regions (the same constraint as Scenario A) and with another constraint that total cooling water consumption in severe drought areas either remained constant (Scenario B), decreased by 5% (Scenario C), or decreased by 10% (Scenario D) compared to the base case. The net consumptive water constraints in severe drought regions (Scenarios B-D) were enforced by reducing the maximum generation at each power plant in the region by a constant factor until the constraint was met. For example, in Scenario C, the maximum generation at all power plants in the severe drought region were reduced by 37% so that the sum of all water consumption in the severe drought region was 5% less than in the base case simulation. While more sophisticated approaches to reducing cooling water consumption in severe drought regions could be implemented in future work, the constant factor approach was chosen for its clarity as a proof of concept. Further reductions in water consumption (>10%) in severe drought regions violated capacity or transmission constraints within ERCOT. This work also reports changes to water withdrawals, which were not used to constrain grid operation. Using this 2006 episode, the results presented here are a first attempt at assessing the feasibility and relative cost of this strategy, rather than a full-scale implementation model.

4.4.4 Air Quality Model Description

The air quality model used in this work was developed for air quality planning in the Dallas-Fort Worth area by the Texas Commission on Environmental Quality (TCEQ) as part of the State Implementation Plan for compliance with the U.S. Environmental Protection Agency's National Ambient Air Quality Standard for ozone. The episode extended for 33 days from May 31-July 2, 2006, and includes days with elevated ozone

concentrations in Texas as well as days with a variety of electricity demand levels. More information on the evaluation of the model, on the comparison to observed concentrations, and emission inventory development are available through the TCEQ (TCEQ 2010). With the exception of emissions from EGUs in ERCOT, which will be described below, the TCEQ base case assumptions for anthropogenic and biogenic emissions were maintained in this research.

The data for the episode was developed for use with the Comprehensive Air Quality Model with Extensions [CAMx] (ENVIRON 2011). For this work, CAMx version 5.40 with CF aerosol chemistry and plume-in grid treatment of large point source emissions was utilized. The modeling domain (Figure 4-2) included the eastern United States at 36 km by 36 km resolution with finer resolution over eastern Texas (12 km by 12 km) and the Dallas-Fort Worth region (4 km by 4 km). Air quality results for this study were shown in the 12 km by 12 km eastern Texas domain, which includes the ERCOT power plants with changing generation levels.

In order to obtain hourly emissions of NO_x and SO_2 from each EGU in ERCOT for each scenario, the generation output from the PowerWorld model was multiplied by an annual average emissions factor for the power plant from the Emissions & Generation Resource Integrated Database (eGRID) for 2005 (EPA 2012a). Estimates for emission factors for volatile organic compounds (VOC) and carbon monoxide (CO) emissions were made by scaling the original ratio of the pollutant to NO_x emissions by the eGRID NO_x emissions rate. For non-EGU SO_2 emissions in Texas, TCEQ emissions estimates (TCEQ 2014a) were used based on daily average emissions over the episode. Emissions of SO_2 outside of Texas and primary PM throughout the domains were assumed to be unchanged throughout all scenarios and were based on inventories developed by Simon et al (2008).

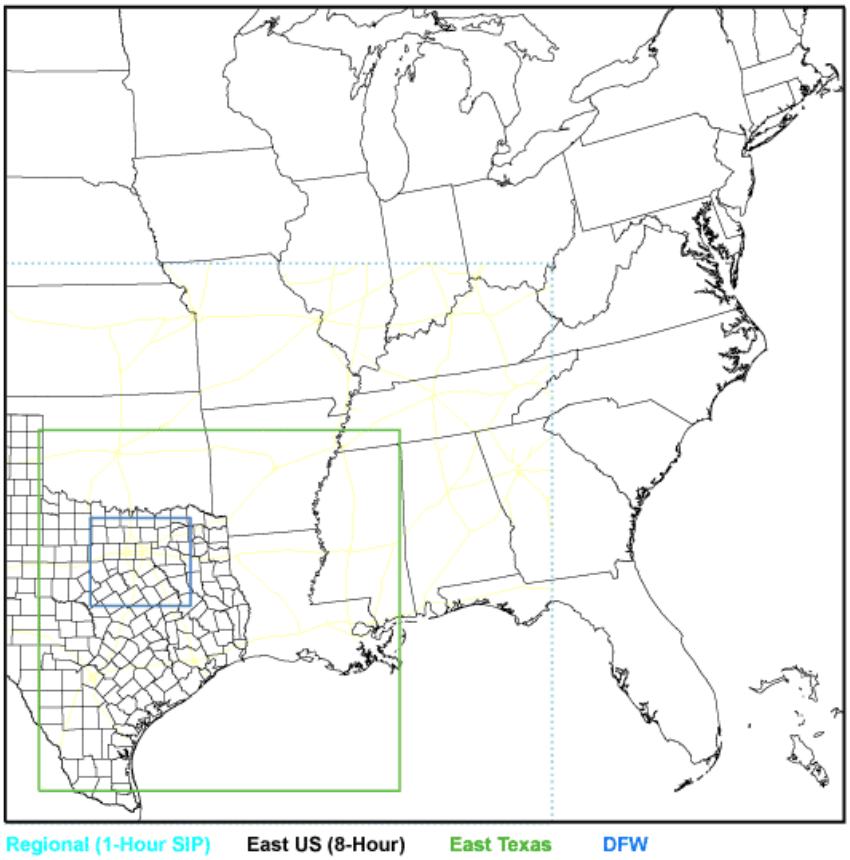

Figure 4-2.Air quality modeling domain used in this study. (TCEQ 2010) While the 36 km by 36 km domain over the eastern U. S. (black box) and 4 km by 4 km domain over the Dallas-Fort Worth area (blue box) were available, results are given in the 12 km by 12 km domain over eastern Texas (green box).

4.5 Results and Discussions

4.5.1 Drought-Based Grid Changes and Costs

All scenarios offered an average reduction of consumptive water use of 188,000 m^3/day and withdrawal reductions of 1,740,000 m^3/day in areas with extreme and exceptional drought (Tables 4-3 and 4-4). The avoided water consumption in extreme and exceptional drought regions would be enough for the personal use of 360,000 people based on average domestic water usage in Texas (Kenny et al. 2009), for the production of ethanol for 1.8 million miles of driving from corn grain in irrigated fields (King et al.

2008c), or to produce 16 billion cubic feet per day of the average Texas shale gas (Grubert et al. 2012). For Scenario D, in which water consumption in the severe drought region is reduced by 10% from the base case, the electric grid offers enough flexibility to avoid additional water consumption of 47,000 m^3/day in the regions with severe drought in this episode. While cooling water consumption in the rest of ERCOT (abnormally dry and moderate drought regions as shown in Figure 4-1) increases by 10%-34% for the four scenarios (A-D) compared to the base case, total cooling water consumption in ERCOT (Table 4-3) decreases in all scenarios compared to the base case. The maximum of 7% reduction in total ERCOT cooling water consumption occurs in Scenario A, in which electricity dispatch is unconstrained in the severe drought regions. The reduction in cooling water consumption in Scenario A is driven by decreased coal-fired electricity generation in ERCOT (Table 4-5), which typically has a higher water consumption rate than the natural gas facilities (Feely et al. 2008; Grubert et al. 2012) that our model indicates would replace the coal-fired generation. The total savings in cooling water consumption are reduced with increasing constraints in the severe drought region due to the increased use of less efficient peaking natural gas plants in ERCOT. Total water withdrawals increase 5%-23% in ERCOT versus the base case scenario (Table 4-4) and increase with increasing grid constraints. The increases in ERCOT total cooling water withdrawals are driven by more use of less efficient natural gas plants, which often have once-through cooling water systems in Texas.

	Total Daily Cooling Water Consumption (m^3/day)				Percent Change from Base Case			
	Extreme and Exceptional Drought	Severe Drought	Moderate and Abnormally Dry	All Regions	Extreme and Exceptional Drought	Severe Drought	Moderate and Abnormally Dry	All Regions
Base Case	188327	466312	578943	1,233,582	0%	0%	0%	0%
A	0	511397	638148	1,149,545	-100%	10%	10%	-7%
B	0	465936	710846	1,176,781	-100%	0%	23%	-5%
C	0	443275	742732	1,186,007	-100%	-5%	28%	-4%
D	0	419811	776720	1,199,531	-100%	-10%	34%	-3%

Table 4-3. Episode average daily water consumption in aggregate and by drought class for each scenario.

	Average Daily Withdrawals (m^3/day)				Percent Change in Daily Withdrawals			
Scenario	Extreme and Exceptional Drought	Severe Drought	Moderate Drought and Abnormally Dry	All Regions	Extreme and Exceptional Drought	Severe Drought	Moderate Drought and Abnormally Dry	All Regions
Base Case	1,736,017	9,851,391	8,681,871	20,269,278	0%	0%	0%	0%
A	0	10,990,183	10,237,919	21,228,102	-100%	12%	18%	5%
B	0	10,586,927	12,935,120	23,522,047	-100%	7%	49%	16%
C	0	10,072,940	14,117,892	24,190,832	-100%	2%	63%	19%
D	0	9,463,393	15,401,885	24,865,279	-100%	-4%	77%	23%

Table 4-4. Episode average daily cooling water withdrawal in aggregate and by drought class for each scenario.

	Base Case	A	B	C	D
Nuclear	10%	10%	10%	10%	10%
Coal	32%	30%	28%	27%	26%
Natural Gas	52%	54%	56%	57%	58%
Oil	0%	0%	0%	0%	0%
Other	5%	5%	5%	5%	5%

Table 4-5. Episode percentage of total ERCOT generation by fuel type under each scenario.

The shifting of 9.9% of the ERCOT episode base case generation from EGUs in areas of extreme and exceptional drought in South Texas causes electricity generation to become more expensive by dispatching generation to higher cost power plants in other locations. Scenario A would increase the average cost of electricity generation by $1.28/MWh, a 5% increase over the base case scenario. Further restricting water consumption in severe drought regions (Scenarios B-D), as shown in Table 4-6, would increase the average ERCOT generation cost per MWh by up to 13%. While average prices can illustrate the magnitude of the cost associated with a change, electricity is priced based on marginal cost, which varies with demand level. In this episode, cost increases associated with drought-based electricity dispatch in ERCOT were modeled to range from $0.51/MWh to $0.83/MWh for base load conditions (2%-3% increase from the base case) and $3/MWh to $15/MWh (9%-45% increase from the base case) for the episode peak demand hour.

	Average Daily Cost ERCOT ($)	Change in Cost from Base Case ($)	Percent Increase in Cost over Base Case	Episode Average Cost ($/MWh)
Base Case	28,360,400	-	0%	28.42
A	29,640,157	1,279,757	5%	29.71
B	30,753,839	2,393,439	8%	30.82
C	31,296,193	2,935,794	10%	31.37
D	32,091,068	3,730,669	13%	32.16

Table 4-6. Average daily cost of shifting power generation based on drought.

Past research has characterized the cost of changing the electricity dispatch for ERCOT based on NO_x emissions pricing (Alhajeri et al. 2011a) and fuel costs (Pacsi et al. 2013a, Venkatesh et al. 2012). This work characterizes the range of price incentives ($/MWh) that would need to be given to electricity producers in less drought-affected regions of ERCOT in order to shift generation to some of the more expensive facilities in those areas. In practice, these price incentives could either be given as a subsidy to facilities at which more generation is desired or as an additional cost to facilities in drought-stricken regions in order to change the relative dispatch order in ERCOT. However, this strategy might have additional costs associated with compensating EGUs that would be forced to eliminate or decrease generation, but estimating these costs is beyond the scope of this work. In addition, the change from a zonal to a nodal based pricing system, undertaken by ERCOT in 2010 to improve dispatch efficiencies and price signals (Daneshi et al. 2011) may alter costs.

Recently, Texas has built physical pipelines as a method of increasing water availability in some regions with prolonged water scarcity concerns. For example, a planned 240 mile pipeline to deliver 370,000 m^3/day from Lake Palestine to the Dallas-

Fort Worth area would have a total capital cost of $888 million and an estimated cost of $0.63/$m^3$ water (TWDB 2012). If a similar pipeline were constructed to deliver water for the power generation sector in a region and was used only during drought years, the unit cost would double to $1.26/$m^3$ water, assuming the frequency of drought in Texas remained the same as from 1990-2010 (NCDC 2012). By comparison, the drought-based dispatch strategies would cost $6.80-$15.89/m^3 water for consumptive water reductions in extreme, exceptional, and severe drought regions and $0.74-$2.15/m^3 water for targeted withdrawal reductions in extreme and exceptional drought regions.

Another proposed policy for cooling water reductions would be to install air cooling systems at the 38 EGUs in areas of extreme and exceptional drought in this episode. The cost of air cooling is largely driven by the parasitic loss of electricity generation at the power plant caused by the technology. Assuming an average 2% parasitic loss, (Zhai et al. 2010) the estimated range of the cost of this air cooling strategy was found to be $0.09/MWh to $0.43/MWh for the episode average and maximum electricity price, respectively, in the ERCOT South Zone (ERCOT 2006a) based on methods in Stillwell and Webber (2013a). Parasitic losses can vary from nearly 0% to 10% based on factors such as temperature and humidity (Stillwell & Webber 2013a). At the upper limit of 10% for parasitic loss, the cost of air cooling would be $0.37/MWh and $68.11/MWh, at the episode average and maximum electricity price in the South Zone, respectively. While the cost of drought-based grid dispatching appears to be substantially more than air cooling with the exception of cases of high parasitic loss or electricity cost, the strategy could be implemented without making new capital investments at power plants and could respond to changes in the spatial extent of drought. Cost comparisons for drought-based dispatching and other infrastructure changes are summarized in Table 4-7. This policy could be rapidly deployed while other physical adjustments—such as

adding air cooling systems, building or expanding reservoirs, or building water pipelines—are conducted in parallel. However, it is possible that optimization in future work could improve the economics of drought-based dispatching.

Consumptive Water Change Method	Episode Average Cost ($/MWh)	Episode Peak Hour Cost ($/MWh)
Scenario A	1.29	3.01
Scenario B	2.40	5.11
Scenario C	2.95	10.24
Scenario D	3.74	15.38
Air Cooling, 2% parasitic loss rate	0.09	0.43
Air Cooling, 10% parasitic loss rate	0.37	68.11
Pipeline Installation (used always)	0.79	N/A
Pipeline Installation (used only in times of drought)	1.58	N/A

Table 4-7. Summary of unit costs of drought-based electricity dispatch scenarios compared to alternative plans to increase water availability. Note that comparison were based on the cost of targeted consumptive water reductions in extreme, exceptional, and severe drought regions in the scenarios examined in this work. Pipeline values have been converted from the $\$/m^3$ basis reported in the paper based on the average cooling water consumption rate for ERCOT (1.26 m^3/MWh) for the base case in this study.

4.5.2 Effect on Regional Air Quality

Changing the spatial distribution of power generation in ERCOT would not only change the location of cooling water usage but also the location of air pollutant emissions in the power generation sector. Total SO_2 emissions from ERCOT power plants (Table 4-8) decrease 3-21% from the base case. In Scenario A, the reduction in SO_2 occurs because the generation from several coal EGUs in South Texas is replaced with a less sulfur-intensive power generation mix (Table 4-5). In Scenarios B-D, additional SO_2 reductions are modeled based on decreased coal-fired power generation in the severe drought region. However, other areas (abnormally dry and moderate drought regions as shown in Figure 4-1) experience 5-13% increases in SO_2 emissions compared to the base case (Table 4-8). The impact on total ERCOT NO_x emissions (Table 4-9) was more complicated than for SO_2 emissions, with changes from the base case ranging from -2% (Scenario A) to +8% (Scenario D). In Scenarios B-D, NO_x emissions reductions in exceptional and extreme drought regions from decreased coal-fired power generation (Table 4-5) were offset by the increased use of higher emitting natural gas peaking units as constraints on where generation could occur the grid were increased.

	Daily Average SO_2 (short tons/day)					Percent Change from Base Case			
Drought Zone	**Base Case**	**A**	**B**	**C**	**D**	**A**	**B**	**C**	**D**
Abnormally Dry	0	0	0	0	0	3%	3%	3%	3%
Moderate Drought	282.4	296.8	310.2	314.3	317.8	5%	10%	11%	13%
Severe Drought	765.8	824.4	718.6	658.5	601.6	8%	-6%	-14%	-21%
Extreme Drought	75.5	0	0	0	0	-100%	-100%	-100%	-100%
Exceptional Drought	38.1	0	0	0	0	-100%	-100%	-100%	-100%
Total	**1161.8**	**1121.2**	**1028.8**	**972.8**	**919.3**	**-3%**	**-11%**	**-16%**	**-21%**

Table 4-8. Episode average daily SO_2 emissions from ERCOT power plants in aggregate and by drought classification for each scenario.

	Daily Average NO_x (short tons/day)					Percent Change from Base Case			
Drought Zone	**Base Case**	**A**	**B**	**C**	**D**	**A**	**B**	**C**	**D**
Abnormally Dry	0.2	0.2	0.2	0.2	0.2	3%	3%	3%	3%
Moderate Drought	130.3	149.1	179	193.4	209.3	14%	37%	48%	61%
Severe Drought	188.5	206	199.1	191.7	181.4	9%	6%	2%	-4%
Extreme Drought	33	0	0	0	0	-100%	-100%	-100%	-100%
Exceptional Drought	11.2	0	0	0	0	-100%	-100%	-100%	-100%
Total	**363.2**	**355.3**	**378.3**	**385.2**	**390.9**	**-2%**	**4%**	**6%**	**8%**

Table 4-9. Episode average daily NO_x emissions from ERCOT power plants in aggregate and by drought classification for each scenario.

Since the secondary formation of ozone (Nobel et al. 2001; Mauzerall et al. 2005) and PM (Brock et al. 2002) can vary significantly based on geographic location of changes in precursor emissions, photochemical modeling was used to resolve the average PM and ozone concentration changes over the episode (Figure 4-3 and 4-4). The maximum of the episode average changes from the base case for ozone were +0.2 ppb (increase from the base case) to -0.55 ppb (decrease from the base case). Maximum changes in fine PM were highly localized and on the order of ±0.25 µg/m³. A surprising result (Figure 4-4) was the maximum changes for fine PM that occurred in the Scenario A in the region northwest of Houston. This maximum increase was driven by locally increased generation at a facility with multiple EGUs. This area of increased PM formation was limited in Scenario B-D since generation was restricted at that facility.

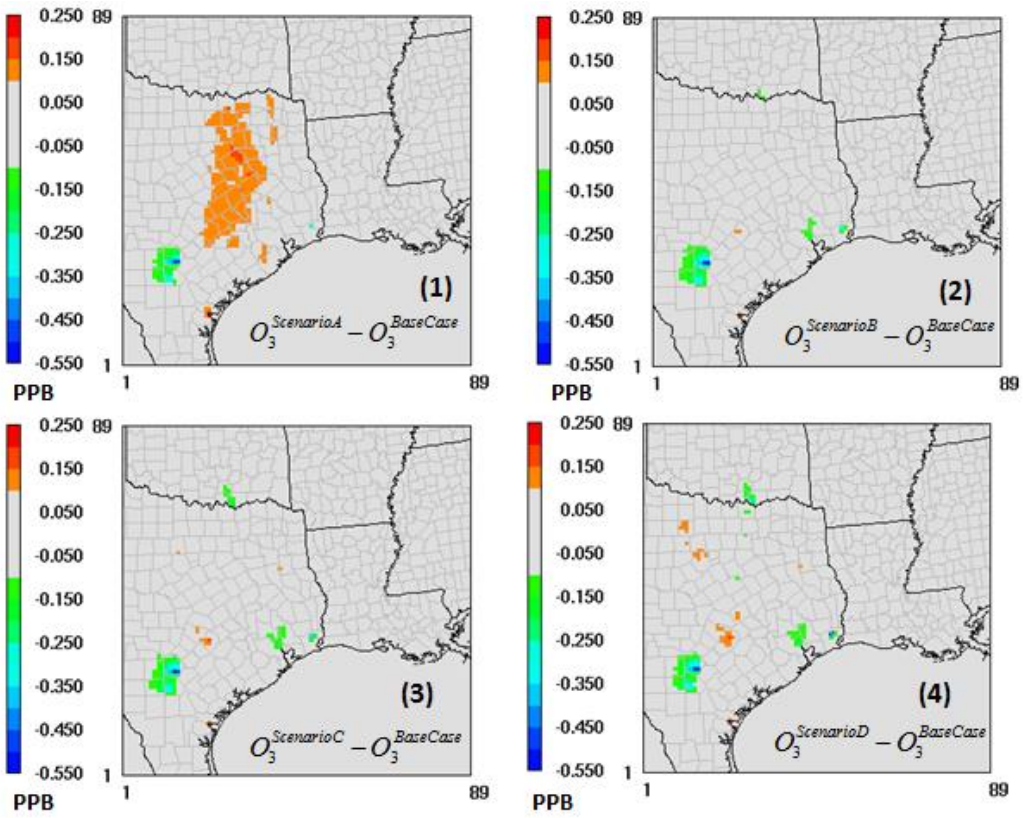

Figure 4-3. Changes in episode average ozone concentration from the base case for the drought scenarios examined in this work. Scenario A (1) involved shifting all generation from extreme and exceptional drought regions. Scenarios B (2), C (3) and D (4) both included the constraint of no generation in exceptional and extreme drought regions and the constraint that net water consumption in severe drought regions would remain constant (Scenario B), be reduced by 5% (Scenario C), or be reduced by 10% (Scenario D) relative to the base case.

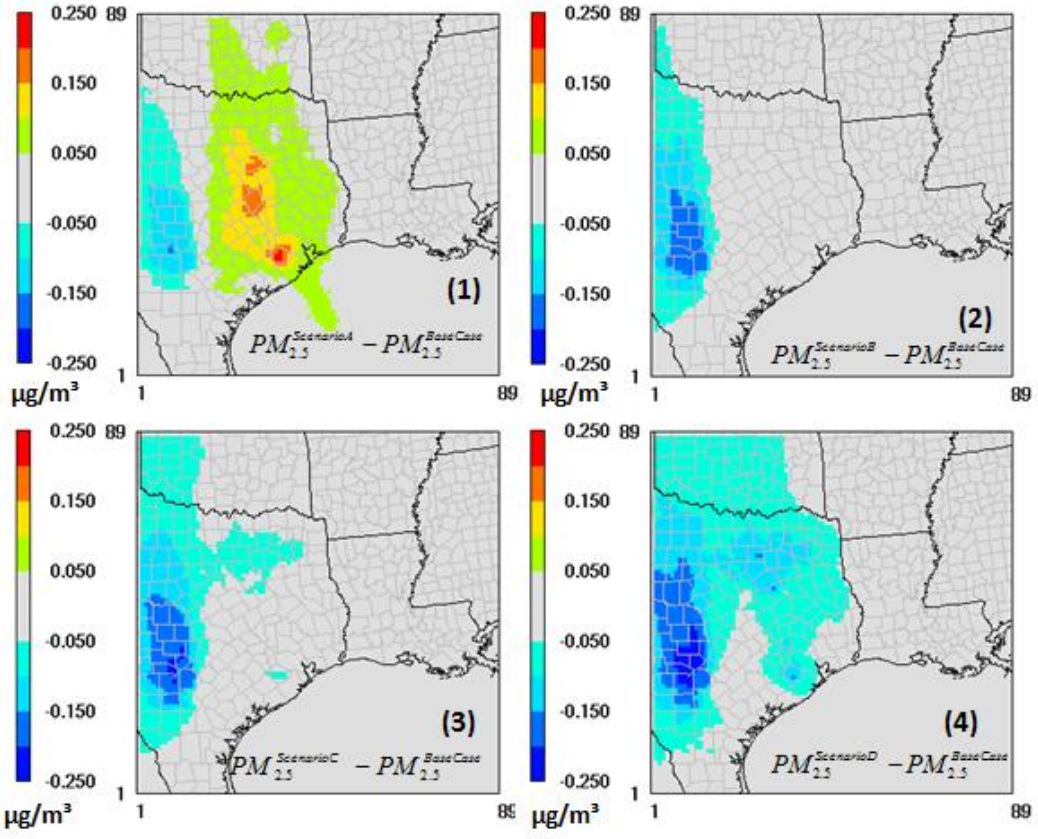

Figure 4-4. Changes in episode average fine particulate matter (PM2.5) from the base case for the drought scenarios examined in this work. Scenario A (1) involved shifting all generation from extreme and exceptional drought regions. Scenarios B (2), C (3) and D (4) both included the constraint of no generation in exceptional and extreme drought regions and the constraint that net water consumption in severe drought regions would remain constant (Scenario B), be reduced by 5% (Scenario C), or be reduced by 10% (Scenario D) relative to the base case.

4.6 CONCLUSIONS

The electric grid in Texas (ERCOT) can be used as a means of changing the spatial distribution of cooling water consumption and withdrawals in the state. This method was demonstrated with a model for an historical episode from 2006 in which 7.7 GW of generation capacity that were located in intensive drought regions were removed from the dispatch order. The approach demonstrated here would reduce cooling water

consumption by 188,000 m^3/day in the worst-hit drought areas, which is enough water for the average daily water use of 360,000 Texans. In addition, this strategy decreased over all cooling water consumption in the state at a price that is cost competitive with air cooling at the upper end of observed electricity prices in the region, and could be a potential parallel strategy while other physical adjustment to water infrastructures are completed.

Chapter 5: Regional Air Quality Impacts of Increased Natural Gas Production and Use in Texas

Pacsi, A. P.; Alhajeri, N.S.; Zavala-Araiza, D.; Webster, M. D.; Allen, D. T.
Environmental Science & Technology. **2013**, *47*, 3521-3527.

5.1 CONTEXT

Chapter 5 includes the expansion of the UT/MIT Integrated Model to include changes in the price of natural gas as the driver of changes in the power sector emissions (Objective 4) and adds upstream production emissions from the Barnett Shale to the model framework (Objective 5). The ozone and fine PM impacts of different natural gas prices for the power sector and production levels in the Barnett Shale are considered.

5.2 ABSTRACT

Natural gas use in electricity generation in Texas was estimated, for gas prices ranging from $1.89 to $7.74 per MMBTU, using an optimal power flow model. Hourly estimates of electricity generation, for individual electricity generation units, from the model were used to estimate spatially resolved hourly emissions from electricity generation. Emissions from natural gas production activities in the Barnett Shale region were also estimated, with emissions scaled up or down to match demand in electricity generation as natural gas prices changed. As natural gas use increased, emissions decreased from electricity generation and increased from natural gas production. Overall, NO_x and SO_2 emissions decreased while VOC emissions increased as natural gas use increased. To assess the effects of these changes in emissions on ozone and particulate matter concentrations, spatially and temporally resolved emissions were used in a month-long photochemical modeling episode. Over the month-long photochemical modeling episode, decreases in natural gas prices typical of those experienced from 2006 to 2012, led to net regional decreases in ozone (0.2-0.7 ppb) and fine particulate matter (PM) (0.1-

0.7 μg/m^3). Changes in PM were predominantly due to changes in regional PM sulfate formation. Changes in regional PM and ozone formation are primarily due to decreases in emissions from electricity generation. Increases in emissions from increased natural gas production were offset by decreasing emissions from electricity generation for all the scenarios considered.

5.3 INTRODUCTION

Production of natural gas in the United States has increased significantly due to technological advances in horizontal drilling and hydraulic fracturing in shale formations. The annual production of dry natural gas from shale formations (shale gas) is expected to increase nationally from 4.99 trillion cubic feet (tcf) in 2010 (23% of total natural gas production in the United States) to 13.63 tcf in 2035 (49% of total projected natural gas production) [EIA 2012]. Shale gas developments are of particular importance in Texas, which accounted for 29% of domestic natural gas production in 2010 (EIA 2014a). The Barnett Shale in north central Texas, the Eagle Ford Shale in south central Texas, and the Haynesville Shale in eastern Texas along the Louisiana border are among the areas with the most extensive activity. Currently, the Barnett, Haynesville, and Eagle Ford shales are estimated to contain 6%, 10%, and 3% of the undeveloped dry shale gas reserves in the lower 48 states (EIA 2011).

A variety of studies have been undertaken to understand the environmental impacts of new natural gas developments, including impacts on water quality and availability (Kargbo et al. 2010; Osborn et al. 2011) and greenhouse gas emissions (Howarth et al. 2011; Jiang et al. 2011; Venkatesh et al. 2012). This paper focuses on the regional air quality impacts of natural gas developments. The approach to be used in analyses presented in this work will be to consider spatially and temporally resolved air

pollutant emissions along the supply chain of natural gas, from production to use. Increased natural gas production in Texas will result in emissions of ozone (O_3) and particulate matter (PM) precursors, but when that natural gas is used in generating electrical power, increased natural gas use results in decreases in ozone and particulate matter precursor emissions (Alhajeri 2012). Previous studies (Jaramillo et al. 2007; Venkatesh et al. 2012) have found net reductions in the overall emissions of the ozone precursor NO_x and the fine particulate matter precursor SO_2 when natural gas is used as a replacement for coal-fired electricity generation. The analyses presented here will extend those analyses by considering the spatial and temporal patterns of the emissions and by using that information in air quality models to predict the spatially and temporally resolved impacts of the emissions. Emissions from natural gas production occur at a relatively constant rate and occur in natural gas production regions. Emissions from electricity generation have a strong diurnal variability and occur at sites that are relatively remote from the production emissions. This work will examine the net impact of these spatial and temporal patterns of emissions on ozone and particulate matter formation. In addition, since the extent of use in electricity generation depends on the relative prices of natural gas and coal, this work also will examine the sensitivity of air quality impacts to natural gas prices.

The maximum extent of changes to the electricity generation is limited by the natural gas capacity of the grid. In 2011, the Electricity Reliability Council of Texas (ERCOT), which is the grid that services the majority of Texas, utilized a fuel mix that was 39% coal, 40% natural gas, 12% nuclear, and 8.5% wind (ERCOT 2012). Coal is typically used for base load electricity generation, with natural gas used to meet peak loads. Overall generation capacity in ERCOT is 23% coal, 57% natural gas, 7% nuclear, and 13% wind (ERCOT 2012), so available natural gas capacity exists in the current

operation of the grid. The combination of extensive natural gas production, pipeline capacities that limit the ability to distribute natural gas, and excess natural gas electricity generation capacity makes Texas an interesting test bed for modeling the air quality impacts of natural gas production.

5.4 METHODS

The overall goal of this work is to estimate impacts, on regional air quality, of increases in natural gas production, coupled with changes in electricity generation driven by changes in natural gas prices. The sections below describe (1) the air quality model used to assess regional air quality impacts and (2) the methods used to estimate changes in emissions driven by increased natural gas use in electricity generation, and the changes in emissions due to increases in natural gas production.

5.4.1 Air Quality Model Development

The air quality model used in this work was developed by the Texas Commission on Environmental Quality (TCEQ) for evaluating air quality management plans for the Dallas-Fort Worth area. The air quality episode was used in the State Implementation Plan (SIP) modeling and employs meteorology from May 31-July 2, 2006. Performance evaluations of the model, comparing observed air pollutant concentrations in 2006 to predictions of the model using 2006 emissions, are reported by the TCEQ (TCEQ 2010). In this work, meteorology and biogenic emissions from 2006 will be used, together with estimates of 2012 anthropogenic emissions, to project estimated 2012 air pollutant concentrations. Most of the estimated 2012 anthropogenic emissions, such as on-road and area source emissions, are extrapolations of 2006 emissions, performed by the TCEQ as part of the SIP development process. As described below, in this work, emissions

from natural gas production and electric generation units (EGUs) will be modified to estimate impacts of changes in natural gas production and use.

The air quality simulations were performed with the Comprehensive Air Quality Model, with extensions (CAMx). CAMx is a three-dimensional Eulerian model which calculates the effects of emissions, chemistry, deposition, advection, and dispersion on chemical concentrations in the atmosphere. A detailed description of the model treatment of these processes as well as the computation schemes can be found in the CAMx User's Guide (Environ 2011). CAMx version 5.40 with CF aerosol chemistry and plume-in-grid (PiG) treatment for large point source plumes was the version employed. The CAMx domain (Figure 4-2) has 36 by 36 km grid cells over the eastern United States and finer grid resolution over eastern Texas (12 km by 12km) and the Dallas-Fort Worth area (4 km by 4 km).

5.4.2 Emissions Inventory Development

The emissions used in this work were 2012 Future Year projections of the 2006 episode, developed by the TCEQ for the Dallas-Fort Worth SIP (TCEQ 2010). A brief description of the model performance is available in Section 5.4.3. The changes made, in this work, to the publicly available CAMx-ready emissions files (TCEQ 2012a) are described below.

5.4.2.1 Particulate Matter

The SIP emission inventory, used to develop plans for reducing ozone concentrations, did not contain estimates of primary particulate matter (PM) emissions. In this work, a primary PM emission inventory developed by Simon et al. (2008) was used. The inventory is based on a year 2000 inventory and used size bins associated with the CMU aerosol chemistry mechanism for CAMx. For this work, the CMU species

were converted to CF aerosol chemistry species, and it was assumed that primary PM emissions remained constant over time. Since the air quality impacts reported in this work focus on differences in PM concentrations between different natural gas production and use scenarios, and since primary PM emissions from EGUs are small relative to changes in PM formation due to SO_2 emissions, the assumptions made in the primary PM inventory have negligible impact on the results reported here.

5.4.2.2 Sulfur Dioxide

As with primary PM emissions, the SIP emission inventory did not contain SO_2 emissions. In the modeled domain, SO_2 emissions are primarily due to EGUs, and the methods used to estimate EGU SO_2 emissions are described separately. For SO_2 emissions from other sources (e.g., diesel vehicles), an inventory developed by Simon et al. (2008) was used. Again, this inventory was for 2000, and because of changes in sulfur concentrations in diesel fuels, the 2000 non-EGU SO_2 inventory was multiplied by a factor of 0.094 to estimate 2012 emissions. This factor was determined based on the difference in low level SO_2 emissions between a TCEQ non-EGU SO_2 inventory for 2006 (TCEQ 2014a) and the year 2000 inventory that was used in this study (Simon et al. 2008) over an overlapping section of the inventory domains in eastern Texas.

5.4.2.3 EGU Emissions

The response of electric power generation and EGU emissions to changes in natural gas pricing was estimated using PowerWorld Simulator 16 (PowerWorld 2012). The model determined hourly generation in each EGU, using a nonlinear optimization algorithm that minimizes operating cost subject to meeting demand, enforcing transmission line constraints, generator unit minimum and maximum power levels, and accounting for line losses. A linear programming (LP) approach was used, which allowed

the inclusion of inequality constraints. Electricity demand used in the PowerWorld simulations was the day specific generation in the Electric Reliability Council of Texas (ERCOT) grid from May 31-July 2, 2006, (ERCOT 2006a) grown by 2.1% per year (ERCOT 2006b) to 2012 (Figure 5-1). Additional details of the PowerWorld modeling framework used in this work for applying price signals to dispatch electricity generation within ERCOT can be found in Alhajeri (2012) and Alhajeri et al. (2011a). Emissions for SO_2 and NO_x were based on emission factors (lb/MWh) developed using the Emissions and Generation Resource Integrated Database (eGRID) 2007 (EPA 2012a).

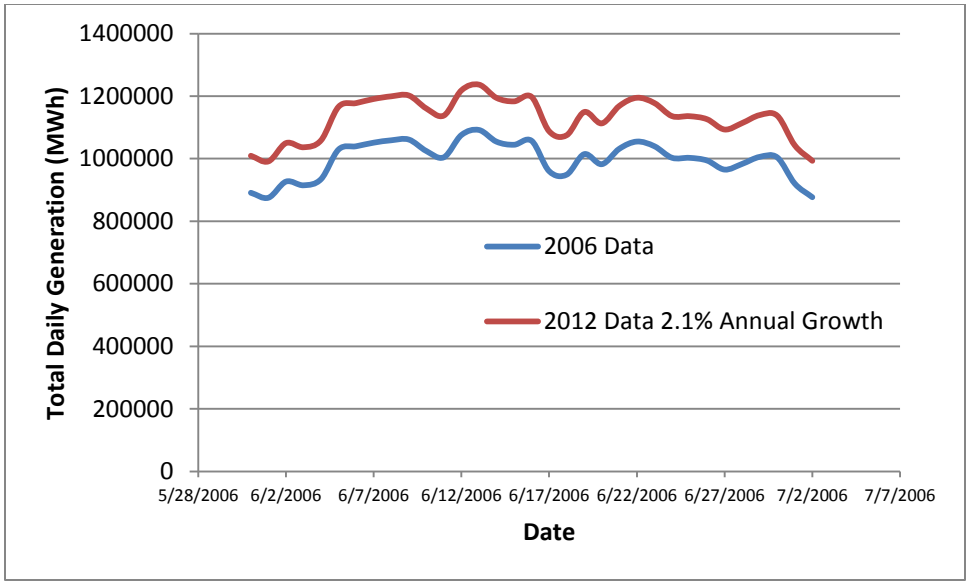

Figure 5-1. Total daily electricity generation in ERCOT over 5/31-7/2 for 2006 and projected for 2012.

In this work, the response of EGU emissions to changes in the relative prices of coal and natural gas was estimated. Four scenarios, with natural gas prices of $1.89, $2.88, $3.87, and $7.74 per Million British Thermal Units (MMBTU), and all with a coal price of $1.89 per MMBTU, were used. The $7.74 per MMBTU pricing scenario

assumed that the natural gas price remained roughly the same as in 2006. The $3.87 per MMBTU case assumes that prices remain similar to levels before the new shale gas plays brought additional natural gas to market in Texas. The $2.88 per MMBTU case was chosen since it is roughly equal to the actual price of natural gas in early 2012. Finally, the $1.89 per MMBTU was chosen to simulate a scenario in which natural gas price is equal to that of coal on a heat input basis. Overall, for these pricing scenarios, natural gas use in electricity generation increases relative to coal as the price of natural gas decreases.

For each hour in the episode and for each pricing scenario examined, the Power World model solves for the hourly generation at specific EGUs (MWh) within ERCOT. For NO_x and SO_2 emissions from EGUs, the hourly generation at each EGU was multiplied by a yearly average emissions factor (tons/MWh) for that same EGU from the eGRID2007 database (EPA 2012a). Previous research (Alhajeri et al. 2011a) has indicated little difference in grid level total emissions of NO_x and SO_2 between the use emission rates from eGRID2007 and eGRID2010. Since the eGRID database did not contain emissions of CO and VOCs, a ratio of VOC and CO to NO_x was created from the TCEQ inventories for each EGU. The NO_x emissions for a specific hour were then multiplied by these factors to obtain the VOC and CO emissions. The hourly EGU emissions for each scenario were used to generate new day-specific point source emission files for the CAMx model.

5.4.2.4 Oil and Gas Emissions in Texas

Emissions from oil and gas production were estimated using both a base case (assuming current pricing of natural gas at $2.88 per MMBTU), and scenarios in which

natural gas production might increase or decrease based on natural gas pricing. For the base case, recently developed emission inventories from the TCEQ were employed.

In the 2012 future year projections used in the SIP air quality modeling, the TCEQ included estimates for the growth of oil and gas in Texas. As a starting point, TCEQ developed a 2010 emission inventory for oil and gas operation, then grew the emissions by 10% between 2010 and 2012. The exceptions to the 10% growth rate were the Eagle Ford and Haynesville shale production regions, which were expected to grow by 20%. The 2010 base inventory contained county-level totals of NO_x, VOC, and CO emissions, and the TCEQ gridded these emissions to the CAMx domain based on the fraction of county-wide production that occurred in 2010 in a specific grid cell. The TCEQ assumed a single split factor for VOC speciation from oil and gas production regardless of the type of source (engine, flare, etc.). This profile (Figure 5-2) assumes that VOCs are predominantly paraffinic hydrocarbons (PAR) and non-reactive species (UNR). Primary PM emissions from oil and gas operations were not considered in this study and are expected to be small compared to secondary PM formation.

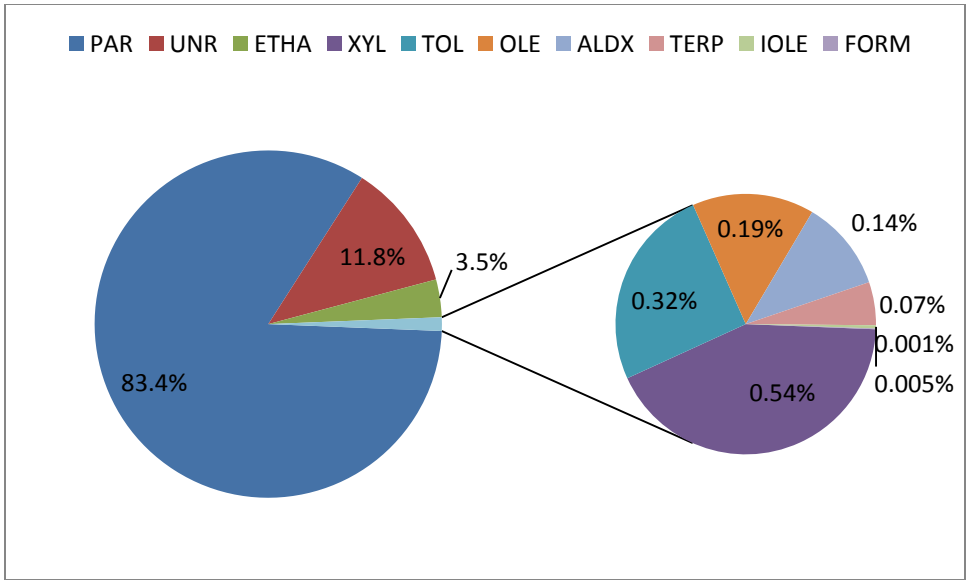

Figure 5-2. Mass percent of VOC for natural gas production emissions by lumped chemical species used in the Carbon Bond chemical mechanism (CB05) including higher aldehydes (ALDX), ethane (ETHA), formaldehyde (FORM), internal (IOLE) and terminal (OLE) olefins, paraffinic carbon (PAR), terpene (TERP), toluene (TOL), unreactive carbons (UNR), and xylene (XYL).

The primary modifications, made in this work, to the TCEQ SIP inventory were in the Haynesville Shale and Barnett Shale production regions. While the TCEQ inventory assumed that gas production would increase by 20% in the Haynesville Shale between 2010 and 2012, the actual rate of growth between 2010 and 2011 was 51% with production expected to level off in 2012 at 2011 levels (TXRRC 2014c). Thus, a 51% growth in NO_x, CO, and VOC emissions in the Haynesville Shale from 2010 values was assumed. The same spatial profile and VOC composition profile was retained.

In the Barnett Shale production region, the TCEQ undertook a large data gathering campaign to obtain better spatial resolution of 2009 emissions associated with natural gas production (TCEQ 2011). NO_x and VOC emission data on approximately 20,000 individual sources were assembled. In this work, this 2009 Barnett Shale Special

Inventory was used with emissions grown by 5% per year, based on production data retrieved from the Texas Railroad Commission (TXRRC 2014c). The differences between the Barnett Shale Special Inventory and the existing inventory were (1) revised emission estimates for VOC and NOx and (2) latitude and longitude spatial locators, rather than county emissions, for 60% of the emissions. The enhanced spatial distribution information was used to create spatial distributions of NOx and VOC emissions, shown in Figure 5-3. Since CO emissions were not available in the Special Inventory, CO emissions in this work were based on NO_x emissions and CO to NO_x ratios, by source type, in the original TCEQ inventory. For sources that did not have latitude and longitude locators, the relative spatial distributions by grid cell were assumed to be the same as for the sources that did have latitude and longitude locators. A performance evaluation of this inventory has been conducted, comparing observed hourly VOC concentrations at a location near the center of the production region, and VOC concentrations predicted based on the inventory and Lagrangian and Eulerian air quality modeling. The performance evaluation indicates that the inventory led to ambient VOC concentration predictions that had little (<10-20%) bias (Zavala-Araiza et al. 2012).

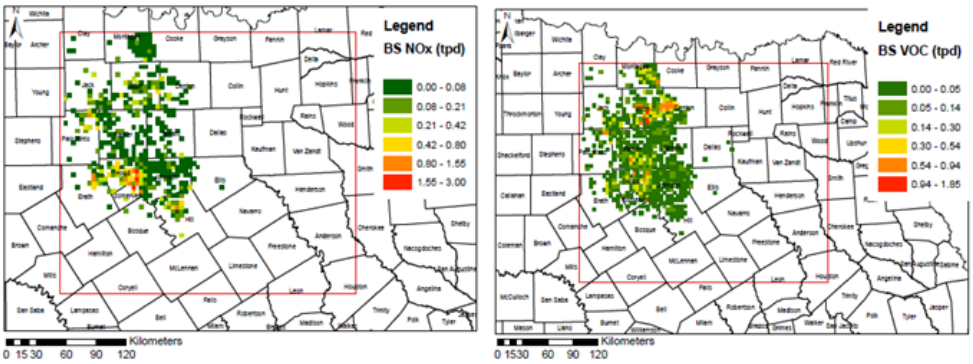

Figure 5-3. Gridded special inventory emissions for NO_x (left) and VOC (right) for natural gas production in the Barnett Shale projected for 2012 (tons per day).

This base case emission inventory for oil and gas production is consistent with the current pricing for natural gas (roughly equivalent to the $2.88 per MMBTU scenario). Additional oil and gas production emission scenarios were developed to be consistent with the electricity generation scenarios associated with higher and lower natural gas prices. For these scenarios, the difference in demand for natural gas in electricity generation, between the base gas and the scenario was determined, and the Barnett Shale was assumed to increase production with changing natural gas demand from ERCOT. For example, at a natural gas price of $1.89 per MMBTU, approximately 6.9 billion standard cubic feet (scf) per day of natural gas is used in electricity generation, as compared to 5.8 billion scf per day that is predicted to be used with natural gas at $2.88 per MMBTU. To meet this 19% increase in natural gas demand from ERCOT, production levels in the Barnett Shale, would need to increase by 1.1 billion scf per day (20%); so, emissions in the Barnett Shale due to natural gas production were assumed to increase by 20%. Similar modifications were made for natural gas prices higher than $2.88 per MMBTU. In this case it is assumed that natural gas scarcity is driving higher prices, suggesting production is lower and assumed emissions decrease. These assumed changes in production are simplifications of actual total changes but do reflect the magnitude of changes that would be expected from changes in natural gas use in electricity production.

5.4.3 CAMx Model Performance and Episode Selection

The Texas Commission on Environmental Quality (TCEQ) created the model used in this work as part of the State Implementation Plan (SIP) for the 8-hour ozone standard in the Dallas-Fort Worth (DFW) region. This episode was chosen by the TCEQ for SIP modeling since it had multiple observed high ozone days (17 out of 33 episode

days) and coincided with a large air quality data gathering campaign (TexAQSII) in the state of Texas. The campaign allowed for additional comparisons of model performance based on measurements only taken during that time period. In addition, the Dallas- Fort Worth region typically experiences an increase in high ozone concentrations in June (as well as August). Due to its proximity to the Barnett Shale, the DFW regional model was chosen versus other possible areas, such as Houston, to examine the impact of natural gas production emissions and natural gas price. High ozone days in June in the Dallas-Fort Worth region are typically related to meteorological conditions with low wind speed out of the east and southeast, which carry air masses with elevated background ozone concentrations into the DFW region. Combined with urban emissions from DFW, the slow moving air masses tend to cause elevated ozone concentrations in the region.

The discussion presented here is a summary of the performance metrics that were completed for the June 2006 episode by the TCEQ (TCEQ 2010). The TCEQ conducted a variety of statistical analyses on the 8-hour averaged ozone concentrations to compare observed and modeled results. For Unpaired Peak Accuracy (UPA), 26 of the 33 episode days performed within the EPA guidance of ±20%. Days with UPA values outside the recommended range tended to have ozone concentrations below the 8-hour standard, which the model tended to underpredict. The average mean normalized bias (MNB) and mean normalized gross error (MNGE) were -0.3% and 14.7%, which were well within recommended EPA guidelines. The TCEQ report (2010) summarizes the model performance at regulatory monitoring locations in the Dallas-Fort Worth area, showing general good performance in predicting the location of episode high ozone concentrations though generally underpredicting the magnitude of the peak 8-hour ozone concentration values.

5.5 Results and Discussions

For purposes of this work, the $2.88 per MMBTU natural gas pricing scenario (which is roughly equivalent to the 2012 price for natural gas for electricity generation in Texas) will be referred to as the base case against which the other scenarios ($1.89, $3.87, and $7.74 per MMBTU) are compared.

5.5.1 Electricity Generation

Different prices for natural gas led to changes in the dispatch order of power plants in ERCOT. The average percent generation by fuel type, for the four natural gas price scenarios, over the 33 day episode, is shown in Figure 5-4. As the price of natural gas decreases, the generation in ERCOT from natural gas increases while the generation from coal-fired EGUs decreases. This is similar to the response of generation in ERCOT predicted by Alhajeri (2012) in response to increased NO_x emissions prices. The $1.89 case (73% of generation from natural gas) and the $7.74 case (34.6% of generation from coal) represented extremes in grid operation based on fuel type.

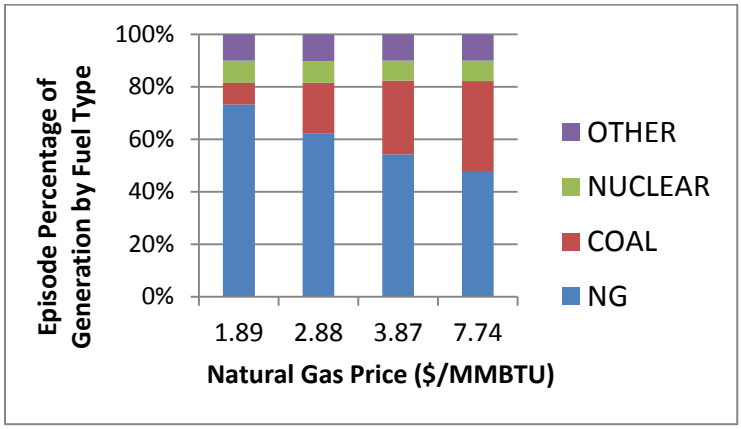

Figure 5-4. Percentage of electricity generation by fuel type for four natural gas pricing scenarios.

Figure 5-5 shows the changes in the average daily spatial patterns of electricity generation as natural gas prices increase. Decreases in natural gas use as price increases are distributed throughout the eastern half of the state; coal use increases with increasing natural gas price, again with changes distributed throughout the eastern half of the state.

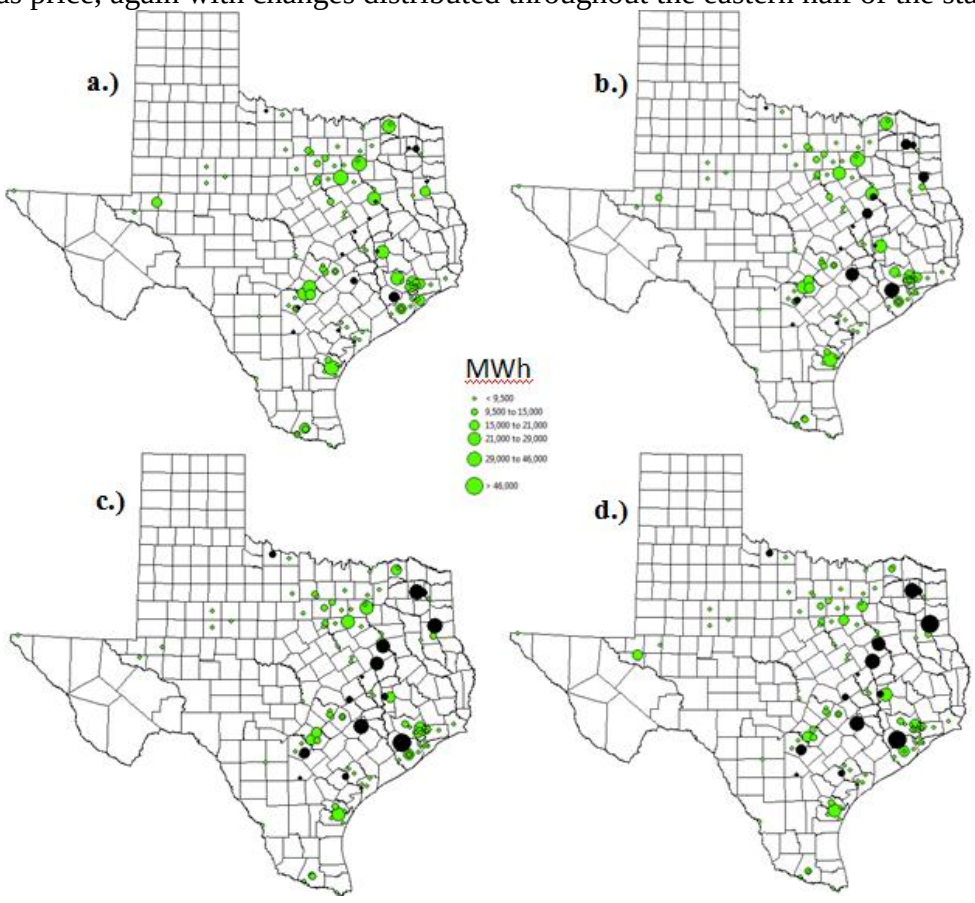

Figure 5-5. Predicted changes in spatial distribution of episode daily average electricity generation from natural gas (green) and coal (black) EGUs as natural gas prices change a.) Natural gas price of $1.89/MMBTU; b.) Natural gas price of $2.88/MMBTU; c.) Natural gas price of $3.89/MMBTU; d.) Natural gas price of $7.74/MMBTU

5.5.2 Emissions

The switch from coal-fired EGUs to natural gas EGUs changes emissions from electricity generation, since coal and natural gas EGUs in ERCOT have different

emission rates per MWh of generation (Alhajeri 2012). Figure 5-6 shows total emissions from EGUs in ERCOT under the four natural gas pricing scenarios. As natural gas price decreases, emissions of NO_x, SO_2, and CO decrease. Figure 5-7 shows total emissions of NO_x, CO, and VOC from the natural gas production in the Barnett Shale assuming production increases or decreases to meet demand for natural gas EGUs in ERCOT.

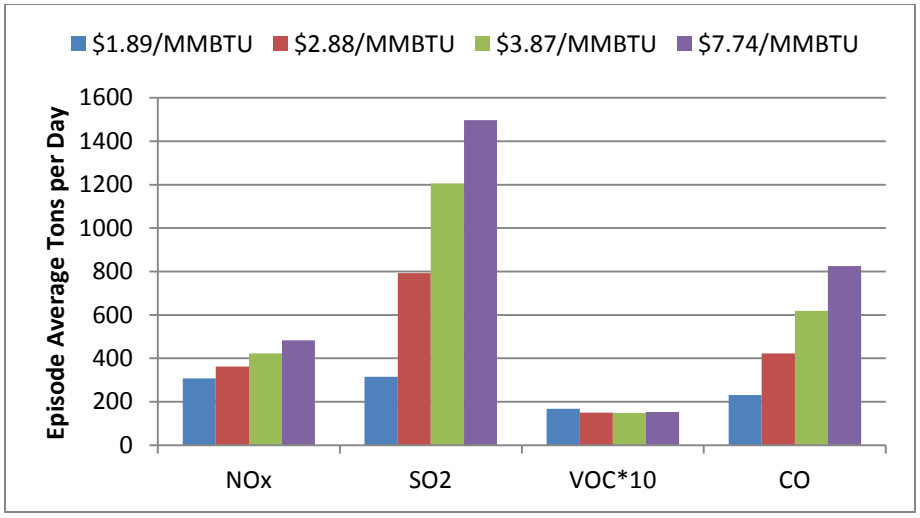

Figure 5-6. Daily average ERCOT EGU primary emissions (tons/day) at each natural gas price. Note that the VOC emissions have been multiplied by a factor of 10 for visibility in the figure.

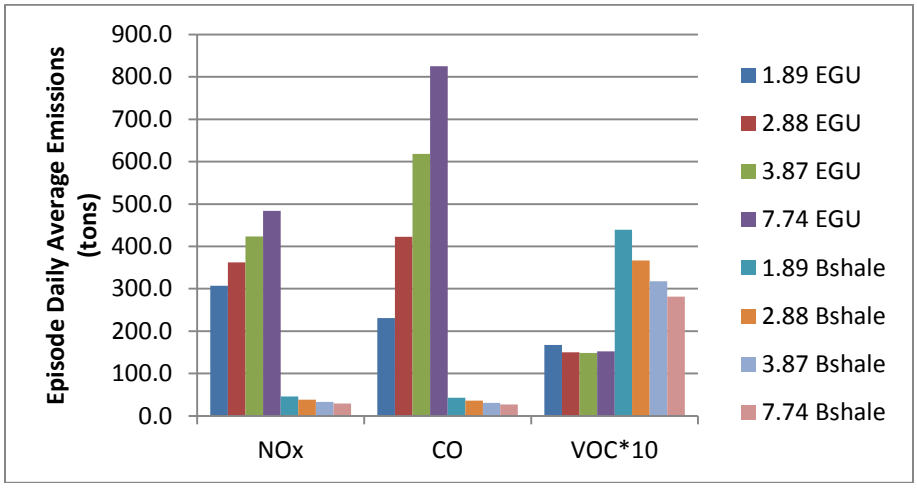

Figure 5-7. Comparison of the magnitude of the average daily emissions from Barnett Shale (Bshale) natural gas production and ERCOT EGU primary emissions for each natural gas price. Note that the VOC emissions have been multiplied by a factor of 10 for visibility in the figure.

Potential changes in emissions from changes in natural gas production and use are shown in Table 5-1 and Figure 5-7**.** These calculations assume that as natural gas demand for electricity generation changes with price, production in the Barnett Shale is raised or lowered to meet demand. Shown in the Table are changes in CO, VOC, and NO_x emissions assuming that the increased natural gas emissions are in the Barnett Shale.

	$1.89/MMBTU			$2.88/MMBTU			$3.87/MMBTU			$7.74/MMBTU		
	NOx	CO	VOC	NOx	CO	VOC	NOx	CO	VOC	NOx	CO	VOC
ERCOT EGU Emission (ton/day)	307.0	230.6	16.8	362.5	422.7	15.0	423.2	618.1	14.8	483.5	824.8	15.2
Barnett Shale Production Total Emissions (ton/day)	46.3	43.0	44.0	38.7	35.9	36.7	33.5	31.0	31.7	29.7	27.5	28.2
Total Emission (ton/day)	353.4	273.6	60.7	401.1	458.6	51.7	456.7	649.1	46.6	513.2	852.4	43.4
Total Change in Emissions from Base Case (ton/day)	-47.7	-185.0	9.0	0.0	0.0	0.0	55.5	190.6	-5.1	112.1	393.8	-8.3
Percent Change in Emissions from Base Case	-12%	-40%	17%	0%	0%	0%	14%	42%	-10%	28%	86%	-16%

Table 5-1. Predicted changes in emissions from natural gas production in the Barnett Shale based on changes in demand in the ERCOT grid.

An additional factor that was considered in the emission estimates is that as natural gas use in electricity generation increases, coal and lignite use decrease. In Texas, most of the coal used in electricity generation is from the Powder River Basin in Wyoming and Montana; however, many of the EGUs are located at lignite mines. Changes in NO_x emissions due to lignite production would occur in the air quality modeling domain and were accounted for using an emissions factor of $1.03 \cdot 10^{-4}$ tons NO_x/ton lignite (NREL 2013). Other emissions were not considered due to their small impact on the end points being considered in this study, PM and ozone. Changes in the use of lignite were estimated based on the additional lignite required to meet to needs of EGUs using lignite for each natural gas pricing scenario. Results are shown in Table 5-2,

comparing changes in NO_x emissions from lignite production to other changes in NO_x emissions considered in this work. The NO_x changes associated with lignite mining were much less than changes in emissions from ERCOT EGUs.

Life Cycle Assessment for NOx (tons/day)				
	Natural Gas Price for Electricity Generation ($/MMBTU)			
Activity	**$1.89**	**$2.88**	**$3.87**	**$7.74**
Electricity Generation	307.04	362.46	423.19	483.53
Lignite Mining	2.31	6.49	10.10	13.51
Natural Gas Activities	74.23	61.93	53.61	47.55
Total	**383.59**	**430.88**	**486.90**	**544.58**
Difference from $2.88	-10.98%	0.00%	13.00%	26.39%

Table 5-2. Assessment of proportioned regional NO_x emissions from new natural gas developments.

5.5.3 Comparison to Existing LCA Inventory

The emissions data in Table 5-1 can be compared to average emissions associated with natural gas production in the United States, as reported in the U.S. Life Cycle Inventory database (NREL 2013). This comparison is shown in Table 5-3. The emissions of criteria air pollutants per unit of natural gas production reported in this work is substantially higher than that reported in the NREL LCI. This is due to a variety of reasons. One reason for the difference is that the NREL LCI data are national averages including both conventional and unconventional natural gas production. In contrast, the Barnett Shale inventory is primarily for unconventional production using hydraulic fracturing, where compression and pumping duties can be significantly higher than in conventional production. In addition, in this work, all of the emissions are assigned to natural gas production, with no allocation of emissions to the production of oil and

natural gas liquids. While many parts of the Barnett Shale produce relatively dry gas, this approach necessarily over-allocates the emissions burdens to natural gas production.

	$1.89/MMBTU			$2.88/MMBTU			$3.87/MMBTU			$7.74/MMBTU		
Assumed Total Natural Gas Production in Barnett Shale (billion scf/d)	6.69			5.55			4.77			4.21		
	NOx	CO	VOC	NOx	CO	VOC	NOx	CO	VOC	NOx	CO	VOC
Special Emission Inventory Average Emissions (tons/day)	46.3	43.0	44.0	38.7	35.9	36.7	33.5	31.0	31.7	29.7	27.5	28.2
NREL LCI data Average Emissions (tons/day)	13.0	5.7	3.6	10.8	4.8	3.0	9.3	4.1	2.6	8.2	3.6	2.3
Special Emissions Inventory estimate/NREL Estimate	3.6	7.5	12.2	3.6	7.5	12.2	3.6	7.6	12.2	3.6	7.6	12.2

Table 5-3. Comparison of total NO_x, VOC, and CO emissions from Barnett Shale Special Emissions Inventory compared to NREL U.S. Life Cycle Inventory Database (NREL 2013).

5.5.4 Ozone Impacts

Figure 5-8 shows the changes in average ozone concentration for the natural gas pricing scenarios. These results shown in Figure 5-8 contain only the changes in emissions due to electricity generation. Results are shown as differences between the results for a $2.88 per MMBTU price for natural gas (base case) and the other cases. For the $1.89 per MMBTU case (Figure 5-8, top and right), the average ozone concentration decrease was modeled to be 0.2-0.5 ppb over all hours during the 33 days in the episode. Increases in the episode average ozone concentration of 0.2-0.4 ppb and 0.2-0.7 ppb were observed in the $3.87 and $7.74 cases, respectively. The maximum increases (dark red)

and decreases (dark blue) in the episode average hourly ozone concentration tended to correspond to the location of coal-fired power plants in Texas (Figure 5-9).

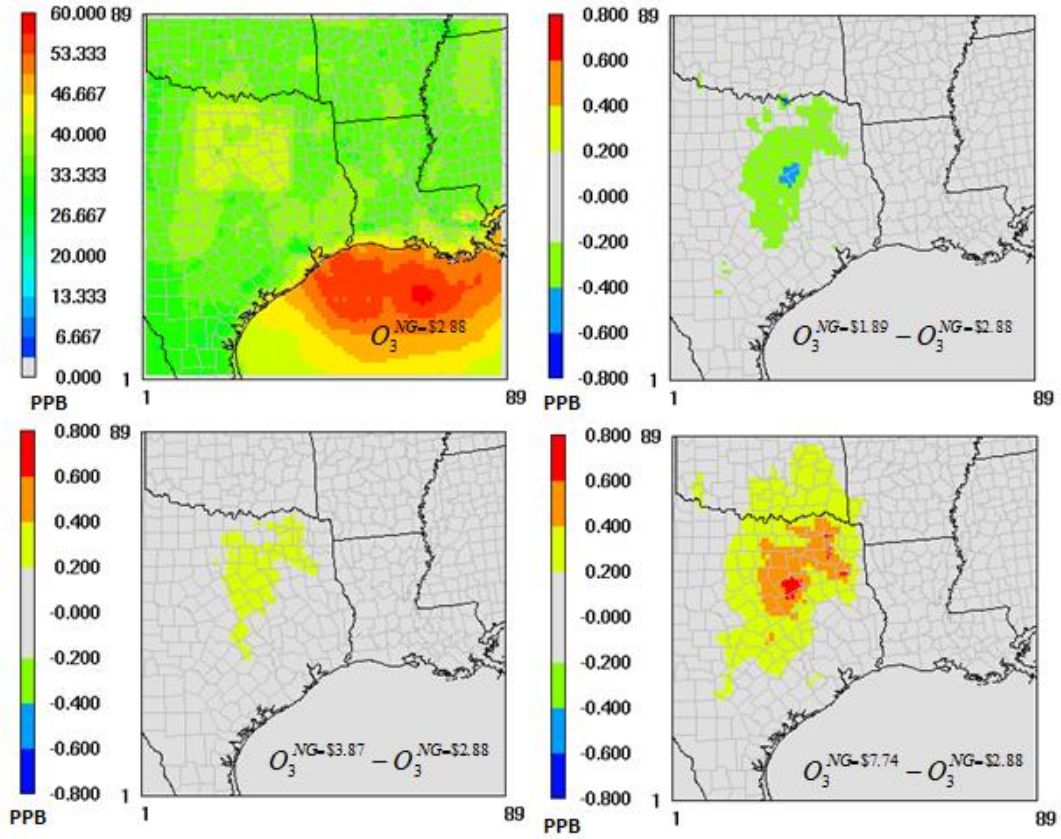

Figure 5-8. Average ozone concentration over the 33 day episode for the $2.88 case (top left) and average ozone increases (positive values) and decreases (negative values) in other pricing scenarios with constant natural gas production.

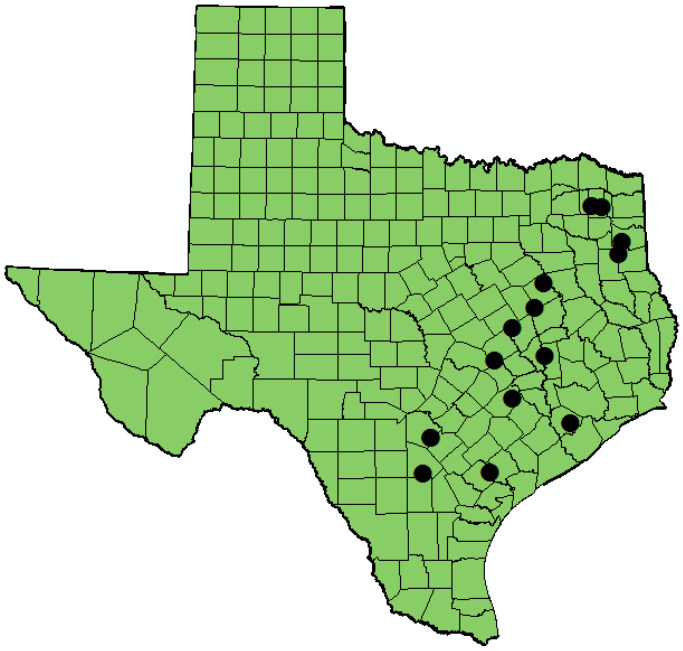

Figure 5-9. Location of coal-fired EGUs in eastern Texas.

When changes in the natural gas production emissions in the Barnett Shale are included (Figure 5-10), the overall trends in ozone formation are similar to scenarios with constant natural gas production emissions. Ozone decreases regionally with decreasing natural gas price. For example with the $1.89 per MMBTU natural gas price scenario, the 19% increase in emissions in the Barnett Shale from increased natural gas usage in electricity generation in ERCOT, considered alone, could cause localized ozone increases near the production sites. In fact, the 19% increase in emissions in Barnett Shale actually causes a decrease in the monthly average ozone concentration (Figure 5-11), due to increased titration of ozone during morning and evening near the production sites.

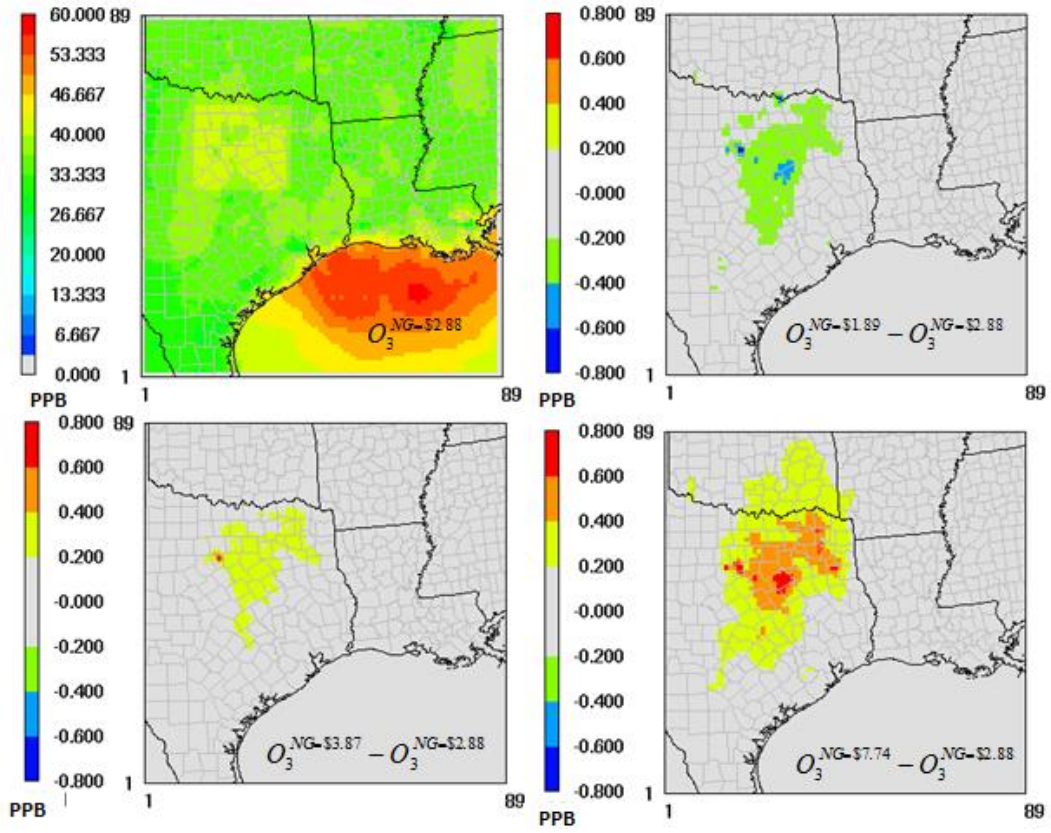

Figure 5-10. Average ozone concentration over the 33 day episode for the $2.88 case (top left) and average ozone increases (positive values) and decreases (negative values) in other pricing scenarios with changing electric generation and natural gas production emissions.

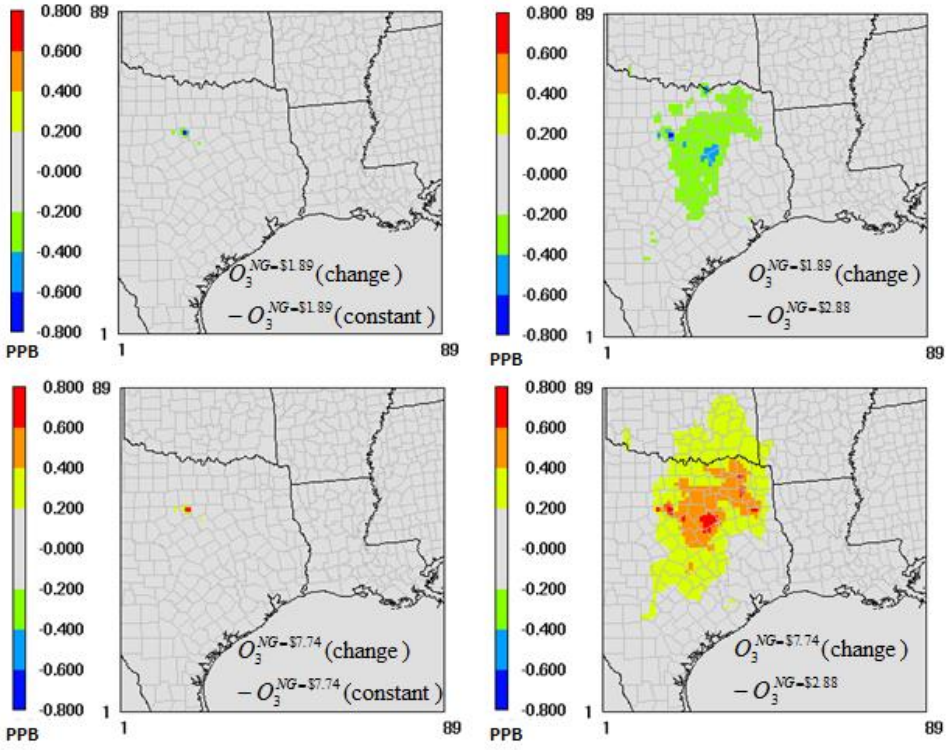

Figure 5-11. Left: Average ozone increases (positive values) and decreases (negative values) for the changes in natural gas production emissions in the Barnett Shale; Right: total changes in ozone concentrations due to changes in emissions in both electricity generation and natural gas production.

While the episode average concentrations are important indicators for ozone concentration changes, the policy relevant ozone concentrations (maximum daily values) occur during the afternoon. Therefore, the diurnal pattern of changes in ozone concentrations is important. Figure 5-12 shows the diurnal pattern of changes in ozone concentrations for grid cell (25,58) in the 12km by 12km eastern Texas domain, located in the southwest corner of Dallas County in an area that sees large average changes due to changes in natural gas production and use. The ozone concentration differences both with constant and changing emissions from natural gas production in the Barnett Shale peak in the afternoon, when ozone levels in Texas tend to be the highest and most

relevant for the 8-hour ozone standard. Grid-wide analysis of the episode average changes in daily maximum 8-hour ozone concentration (Figure 5-13) shows a similar spatial pattern as the average ozone changes, but with a larger magnitude. Thus, changes in natural gas price will likely have a larger impact on the 8-hour ozone standard than the episode average concentration suggests.

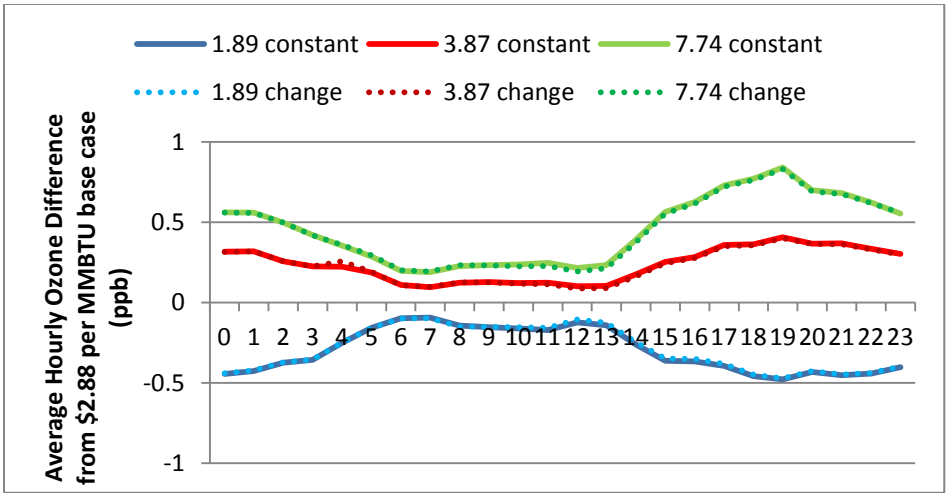

Figure 5-12. Difference in episode average hourly ozone concentrations in southwest Dallas County grid cell from base case ($2.89 per MMBTU natural gas price) for scenarios with changing natural gas production based on electricity demand (change) and with the same natural gas production levels as the base case (constant).

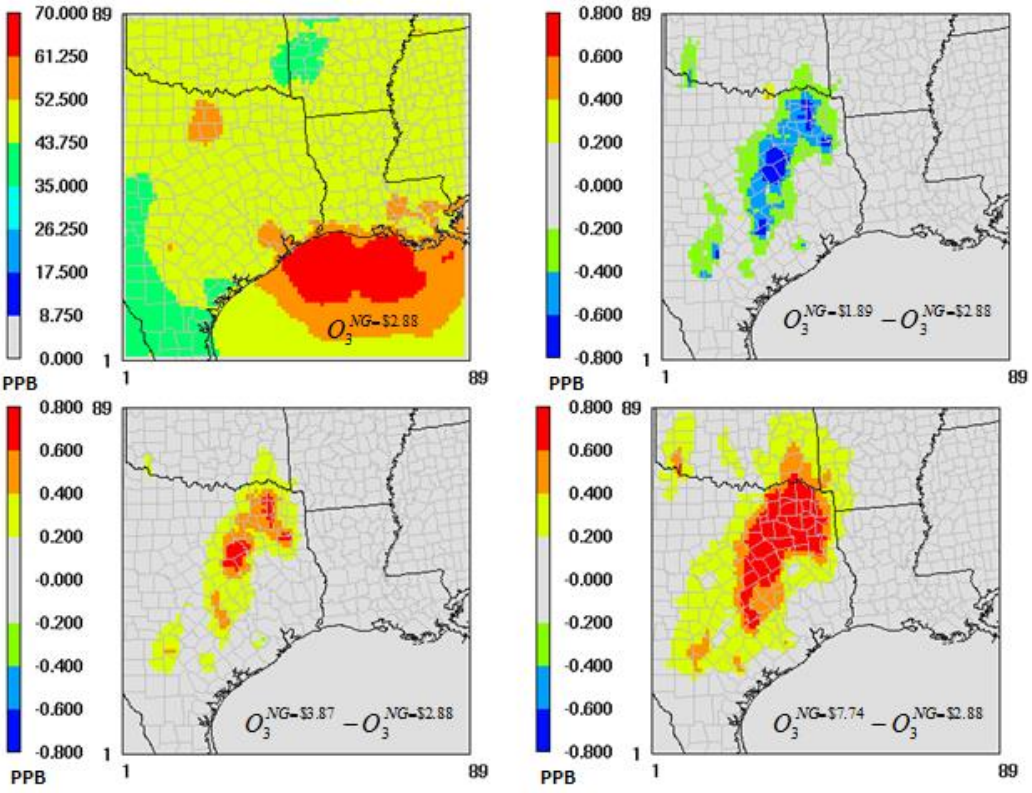

Figure 5-13. Average Reduction in 8-hour daily maximum ozone concentration over the 33 day episode for the $2.88 case (top left) and average 8-hour daily maximum ozone increases (positive values) and decreases (negative values) in other pricing scenarios with constant natural gas emissions from the Barnett Shale.

5.5.5 PM Impacts

Figure 5-14 shows the changes in average fine PM and particulate sulfate concentration for the natural gas pricing scenarios. These results contain only the changes in emissions due to electricity generation. Results are virtually identical for simulations that include changes in emissions due to natural gas production (differences <0.02 µg/m³). Results are shown as differences between the results with a $2.88 per MMBTU price for natural gas (base case) and the other cases. For the $1.89 per MMBTU case (Figure 5-14, top and right), PM reductions were on the order of 0.1-0.5

µg/m³ with increases of 0.1-0.4 µg/m³ and 0.1-0.7 µg/m³ for the $3.87 and $7.74 cases, respectively. The episode average trends in PM changes are similar in spatial extent and magnitude to the changes in PSO_4 and associated ammonium ion titration, which is reasonable given the large emissions reductions in the precursor SO_2.

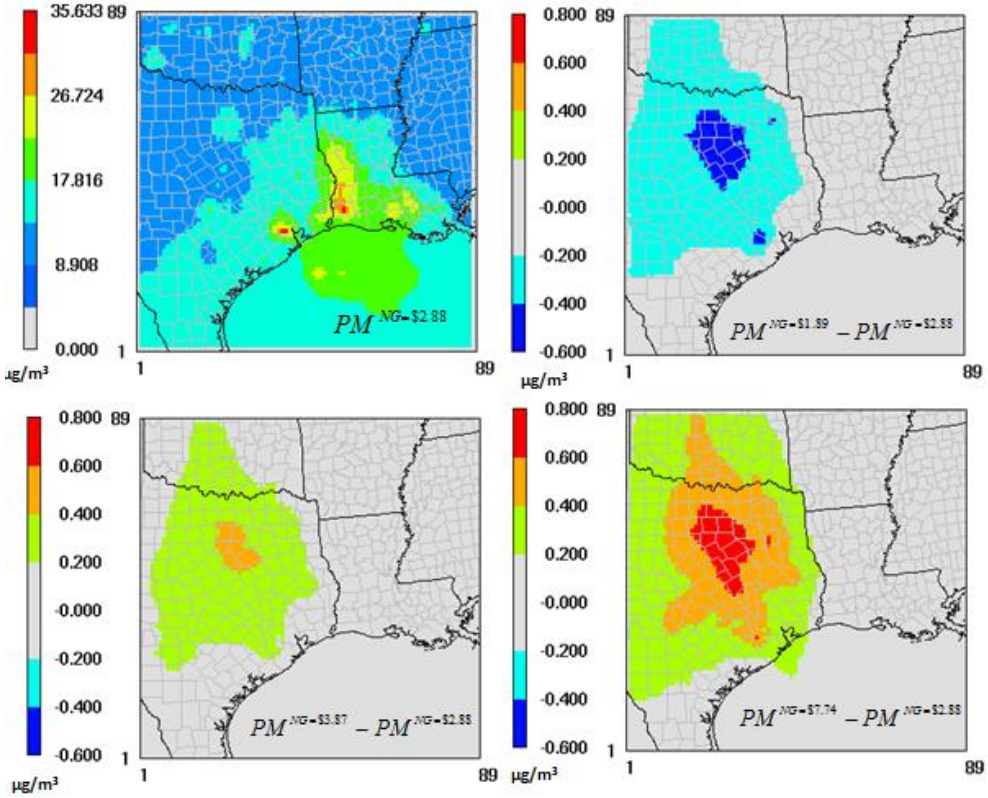

Figure 5-14. Average fine PM concentration over the 33 day episode for the $2.88 case (top left) and average PM increases (positive values) and decreases (negative values) in other pricing scenarios.

The regional air quality impact of increased natural gas development in Texas were examined under natural gas pricing scenarios from $1.89 to $7.74 per MMBTU based on historic price levels from 2006 to 2012. For a month long photochemical modeling episode, total regional emissions of NO_x and SO_2 were dominated by price-

driven changes in the coal and natural gas fractions of electricity generation in ERCOT. Under both assumptions of constant natural gas production at all price levels and of assumptions of changing natural gas production based on demand for natural gas in the electricity generation sector, regional emissions of NO_x and SO_2 decrease with decreasing natural gas price. Localized ozone formation increases near sites with increased NO_x emissions from gas production in the Barnett Shale are offset by NO_x emission reductions from ERCOT power plants. Regional PM concentrations decrease with decreasing natural gas price and are dominated by changes in PM sulfate formation from ERCOT SO_2 emissions.

Chapter 6: Regional Ozone Impacts of Increased Natural Gas Development in the Eagle Ford Shale and Use in the Texas Power Sector

6.1 Context

Chapter 6 applies the framework developed for the Barnett Shale in Chapter 5 to a different shale gas production region in Texas (the Eagle Ford) in order to examine the extent to which region-specific practices and locations of emissions affect conclusions about the ozone impacts of increased natural gas development and use in Texas (Objective 6).

6.2 Abstract

Emissions from the Texas electricity generation sector were estimated at natural gas prices between $1.89 and $7.74 per MMBTU. Emissions from the Eagle Ford Shale in south Texas were estimated and scaled up or down to match the demand for natural gas from the power sector. The ozone impacts of these emission changes were resolved using a photochemical model for a month-long episode that has been used in Texas for state planning associated with the Federal ozone standard. The increased use of natural gas in the power sector in place of coal-fired power generation drove reductions in the episode average daily maximum 8-hr ozone concentration of 0.5 ppb to 1.8 ppb in northeastern Texas while the associated increase in Eagle Ford Shale upstream oil and gas production emissions caused an estimated local increase of 0.1 ppb to 0.4 ppb in the same ozone metric.

6.3 Background

Overall natural gas production in the United States is expected to increase by 56% between 2012 to 2040, and shale gas production is expected to account for 53% of total natural gas production by 2040 (EIA 2014f). Development in shale gas production

regions has occurred while its impact on environmental concerns such as greenhouse gas emissions (Allen et a. 2013; Brandt et al. 2014) and regional water resources (Nicot et al. 2012; Laurenzi et al. 2013) are being examined.

Emissions from natural gas production activities may influence regional ozone concentrations, which are important due to their impacts on human health. Ozone is formed through atmospheric reactions of nitrogen oxides (NO_x) and volatile organic compounds (VOC), and emissions of NO_x and VOC can occur from natural gas production activities. While NO_x emissions from individual natural gas production facilities are generally small, aggregated emissions from the oil and gas sector in counties with extensive production activities can be substantially larger than the threshold for minor point sources (Litovitz et al. 2013). The regional ozone impacts associated with the dispersed NO_x and VOC emissions from natural gas production activities, however, can vary based on the timing and location of the emissions. For example, elevated wintertime ozone concentrations were observed in the Green River Basin in Wyoming during period with snow cover and stagnant atmospheric conditions (Schnell et al. 2009; Carter et al. 2012) but not during a winter season with different atmospheric conditions and no snow cover in a nearby basin (Edwards et al. 2013).

When coupled with lower prices, the production of natural gas may impact emissions levels from the power sector by increasing the utilization of natural gas-fired generation resources in place of coal-fired power plants (Venkatesh et al. 2012; Pacsi et al. 2013a) due to price-based changes in the dispatch order of electricity generating units (EGUs). Compared to the mix of coal-fired EGUs used nationally in 2007, natural gas EGUs had 84% lower NO_x emissions per MWh (EPA 2012a), leading to the possibility that some of the NO_x emissions increases from natural gas production could be offset by decreased emissions in the power sector. NO_x emissions from the power and natural gas

production sectors, however, are not necessarily co-located geographically or temporally. In a photochemical modeling study of the Barnett Shale in Texas, Pacsi et al. (2013a) found that the maximum regional ozone impacts associated with combined changes in the power and production sectors were largely driven by emission changes from coal-fired power plants rather than changes in emissions in the production region.

This study examines the regional ozone impacts associated with increased natural gas production in the Eagle Ford Shale in Texas and the increased use of natural gas generation resources in the Electricity Reliability Council of Texas (ERCOT) in order to determine whether the changes in the power sector are the primary driver of regional ozone concentrations as was the case with the Barnett Shale (Pacsi et al. 2013a). The Eagle Ford shale is an interesting test case since it is a newer shale gas play with rapidly expanding production. The total production in the Eagle Ford Shale increased from 2 million standard cubic feet per day (MMscf/day) in 2008 to 3,800 MMscf/day in 2013 (TXRRC 2014b). In addition, the Eagle Ford Shale is located in a different area of Texas than the regions in northeast Texas with the largest changes in power generation associated with low natural gas prices (Pacsi et al. 2013a).

6.4 Materials and Methods

The purpose of this work is to assess the combined impacts on regional ozone concentrations of price-based changes in utilization of coal-fired and natural gas-fired EGUs in ERCOT with changes in the upstream natural gas production emissions from the Eagle Ford Shale in Texas. The following sections will discuss the air quality model used in this work and the development of emissions inventories for ERCOT and for the oil and gas sector in Texas.

6.4.1 Air Quality Model

The air quality model used in this work was developed by the Texas Commission on Environmental Quality (TCEQ) for evaluating air quality management strategies for reducing ozone concentrations in the Dallas-Fort Worth area (TCEQ 2010). The original 33-day model was developed using meteorological and emissions data for the year 2006 (May 31-July 2) during a period with several high ozone episodes throughout eastern Texas. This work utilizes the 2012 projection of the 2006 episode (which contained estimates for emission changes from many sources, including vehicular emissions). This work utilizes the 12-km domain over eastern Texas and the 36-km domain over the eastern United States (Figure 4-2) from that model. Descriptions of the assumptions made for model development (Section 5.4.1) and the base case model performance (Section 5.4.3) are available in the previous Chapter. Changes to emissions estimates for ERCOT EGUs and oil and gas development areas will be discussed in depth in the next two sections.

6.4.2 EGU Emissions

The ERCOT PowerWorld simulations developed for the Barnett Shale air quality study in the previous Chapter (Section 5.4.2.3) were used in this study. Briefly, the hourly generation at each EGU in ERCOT required in order to meet total electricity demand was determined at natural gas prices of $1.89, $2.88, $3.87, and $7.74 per million British thermal units (MMBTU) using the PowerWorld model. Total ERCOT demand was estimated as the actual hourly demand in ERCOT in 2006 (ERCOT 2006a) with a 2.1% annual growth assumption, which was based on ERCOT planning and growth estimates (ERCOT 2006b). The hourly emissions of NO_x from each EGU were determined by scaling the hourly generation from the PowerWorld model by the annual average emissions factor (tons per MWh) for the power plant from the eGRID database

for the year 2007 (EPA 2012a). The emissions of NO_x were then mapped to specific stack locations in the air quality model. Since the eGRID database does not contain VOC or carbon monoxide (CO) emission rates, the emissions rate of these species for each hour was determined by multiplying the hourly NO_x emissions rate (as determined by the generation level from the PowerWorld model) by the ratio of the pollutant to NO_x in the original stack entry for the EGU.

For this work, the $2.88 per MMBTU natural gas price simulation will be considered the base case since it is based on the average purchase price of natural gas for Texas power producers in early 2012 (EIA 2014d) and is, thus, an estimate of the actual power sector operation during the period of the study. The $7.74 per MMBTU pricing scenario assumed that the natural gas price remained roughly the same as in 2006, and is higher than current projections for natural gas prices in the United States (EIA 2012f). The $3.87 per MMBTU case is roughly in line with current natural gas short term price projections in the United States (EIA 2014f). Finally, the $1.89 per MMBTU was chosen to simulate a scenario in which natural gas price is equal to that of coal on a heat input basis. The $1.89 per MMBTU price is below historic natural gas prices that have been seen in Texas since the development of shale gas resources.

6.4.3 Oil and Gas Emissions outside the Eagle Ford

For this work, emissions from other natural gas production regions were estimated in a variety of ways, which are described in detail in Section 5.4.2.4 in the previous chapter, but were kept constant between different natural gas pricing scenarios. For the Barnett shale, the base case inventory that was developed in Pacsi et al. (2013a) for a natural gas price of $2.88 per MMBTU was used in this study, representing an estimate of the actual development (and emissions) from the upstream oil and gas productions

sector in that region. For the Haynesville Shale in northeastern Texas, the base case assumption used in Pacsi et al. (2013a) was retained for this study. This meant that emissions from the Texas portion of the Haynesville shale were increased by 51% from the TCEQ SIP Inventory (TCEQ 2010) to account for the growth in production in the region between the year 2010, for which the inventory was developed, and 2012, which was the year that was inventoried in this work. All other natural gas production emissions from outside the Eagle Ford shale in the TCEQ SIP Inventory (TCEQ 2010) were grown by 10% to account for increased production between 2010 and 2012. For this work, all oil and gas emissions (including the Eagle Ford) were assigned the default VOC speciation profile assigned by the TCEQ to all oil and gas production sources (Figure 5-2), which assumes that the VOC emissions are predominantly paraffinic hydrocarbons and non-reactive species. In addition, average daily emissions from oil and gas production activities were divided equally for each hour of the day.

6.4.4 Oil and Gas Emissions from the Eagle Ford

Determining the relative ozone impact of changes in upstream natural gas production emissions from the Eagle Ford shale is a primary focus of this chapter, and the emissions inventory used in this work will be discussed in depth. It is important to note that the purpose of this Eagle Ford emissions inventory is to estimate the regional ozone sensitivity to the approximate level of emissions from upstream oil and gas production in the region rather than to estimate the exact 8-hour ozone impact on areas such as Austin or San Antonio. Future work will be undertaken in order to refine the emissions inventory and to improve on the proof of concept inventory presented in this work. Before adding the new emissions inventory for the Eagle Ford shale, all emissions (NO_x,

VOC, and CO) associated with oil and gas production in the TCEQ SIP Inventory (TCEQ 2010) were removed from the 29 counties that are part of the Eagle Ford shale in Texas.

For this proof of concept inventory for the Eagle Ford shale, the assumption was made that the emissions per well in the Eagle Ford were equivalent to the average upstream VOC and NO_x emissions per well from the TCEQ Barnett Shale Special Emissions Inventory (TCEQ 2011). Since CO was not inventoried in the Special Emissions Inventory (TCEQ 2011), CO emissions were estimated by the ratio of total NO_x emissions to total CO emissions from the Barnett Shale production activities in Pacsi et al. (2103a). The average emissions per well used in this work for the Eagle Ford Shale were calculated as be $3.22 \cdot 10^{-3}$ tons per day (tpd) NO_x, $3.47 \cdot 10^{-3}$ tpd VOC, and $3.52 \cdot 10^{-3}$ tpd CO. For the base case ($2.88 per MMBTU natural gas price) in this work, the per well emissions were summed in each county based on the total number of wells in the county by the end of 2012 and were spatially distributed within each grid cell in each county based on the distribution of wells in the county at the end of 2013 (Figure 6-1). The distribution of county emissions was made based on the location of wells in 2013 so that any emission growth scenarios assume the same locations of production emissions as in 2013.

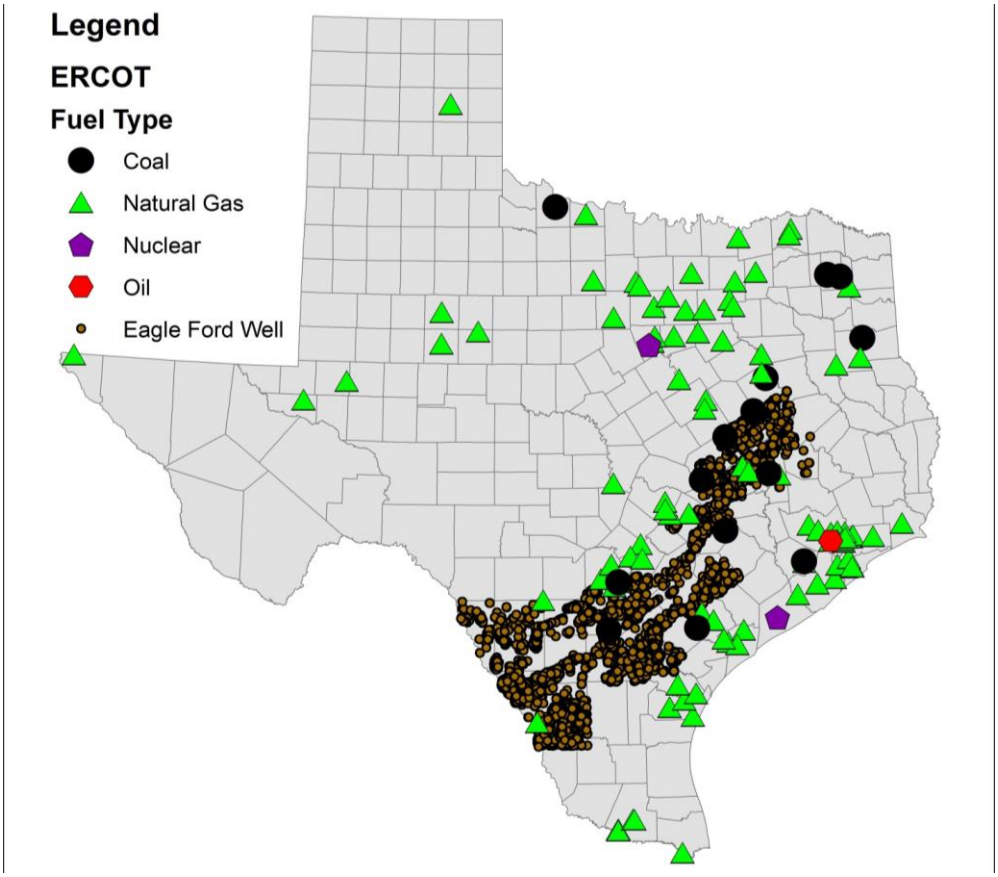

Figure 6-1. Locations of ERCOT power plants and Eagle Ford wells used in this analysis.

The base case emissions scenario for the Eagle Ford Shale ($2.88 per MMBTU natural gas price) was developed to be equivalent to actual production levels in the region in early 2012. Additional oil and gas upstream emission production scenarios were developed to be consistent with the demand for natural gas from the ERCOT. For the additional scenarios, the difference in demand for natural gas between the scenario and the base case was determined, and the Eagle Ford production level was assumed to change based on the difference in natural gas demand for ERCOT. For reference, the average daily production for the Eagle Ford Shale in 2012 was 2.58 billion standard cubic feet (bcf) per day (TXRRC 2014b). For the $1.89 per MMBTU scenario compared to the

base case, the additional demand for natural gas in ERCOT was 1.14 bcf/day. For the $1.89 per MMBTU scenario, overall emissions from Eagle Ford shale oil and gas production activities were multiplied by a factor or 1.44 to account for the increased demand from ERCOT. On the other hand for the $7.74 per MMBTU natural gas price scenario, demand for natural gas from ERCOT was 1.34 bcf/day lower than in the base case, and base case emissions from the Eagle Ford Shale were scaled by a factor of 0.48 in this scenario. The changes in natural gas production levels in the Eagle Ford shale under these scenarios are not intended to estimate the growth or decline in natural gas production at various price points. For example, at $1.89 per MMBTU, it may not be economical for producers to invest in new natural gas wells in the Eagle Ford shale, and thus, the marginal natural gas production needed for ERCOT electricity generation would not necessarily become available from that shale. Determination of these choices would require an economic model that is beyond the scope of this work. Rather, these changes in natural gas production levels (and their associated emissions) are meant to demonstrate the ozone impacts associated with plausible emission levels from the Eagle Ford Shale and from ERCOT. Sensitivity scenarios are undertaken to show the overall ozone impacts of changes to natural gas production emissions versus changes to power sector emissions from ERCOT.

6.4.5 Comparison to Other Eagle Ford Emissions Inventories

The upstream production emissions inventory in this work is based on the assumption that the emissions of NO_x, VOC, and CO per well in the Eagle Ford shale are equivalent to the average upstream natural gas production emissions per well in the Barnett Shale (TCEQ 2011). The overall emissions estimated based on this assumption are compared in Figure 6-2 to an emissions inventory created for the year 2011 and

projected to the year 2012 by the Alamo Area Council of Governments [AACOG] (AACOG 2014), which was concerned about the potential impact of emissions from the Eagle Ford on ozone concentrations in San Antonio. For the upstream oil and gas production sector in the Eagle Ford shale, the overall NO_x emissions for the inventory are 53% higher in the inventory created for this work compared to the AACOG projection for 2012 (Figure 6-2). By contrast, the VOC emissions were 76% lower in the inventory developed for this work compared to the AACOG projection for 2012 (Figure 6-2). From the perspective of regional ozone concentrations, the difference in VOC emissions between the inventories would not be expected to have a substantial impact since the emissions from oil and gas production are largely VOC species with low atmospheric reactivity (Figure 5-2). The lower NO_x emissions in the AACOG inventory for the upstream oil and gas production sector were largely driven by differing emission control regulations assumptions for compressor engines instituted between the development of the Barnett Shale Special Emissions Inventory (TCEQ 2011) for the year 2009 and the development of the AACOG inventory for the Eagle Ford Shale (AACOG 2014) for the year 2011.

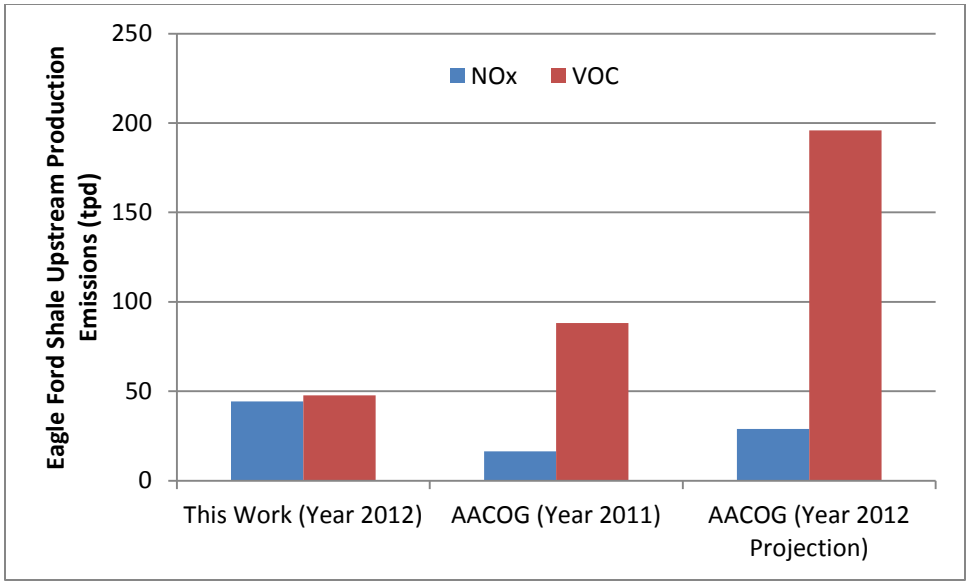

Figure 6-2. Comparison of upstream natural gas production emissions between the emissions inventory developed in this work and the inventory developed by AACOG (AACOG 2014) for the Eagle Ford Shale in 2011 and its projections for 2012 emissions.

It is important to note that the proof of concept inventory developed in this work does not include the emissions from other parts of the oil and gas supply chain that are estimated by the AACOG Inventory (Figure 6-3) and that may be important to assessments of the overall regional ozone impact of emissions from the oil and gas sector. The limitation of oil and gas emissions to only the production emissions would not be expected to have a large impact on VOC emissions from oil and gas operations in the Eagle Ford since 86% of the year 2012 projected VOC emissions from the AACOG Inventory (AACOG 2014) were from the production sector. However, this simplification likely underestimates NO_x emissions since only 26% of the total 2012 projected oil and gas NO_x emissions in the AACOG emissions inventory for the Eagle Ford Shale (AACOG 2014) were from upstream oil and gas production activities.

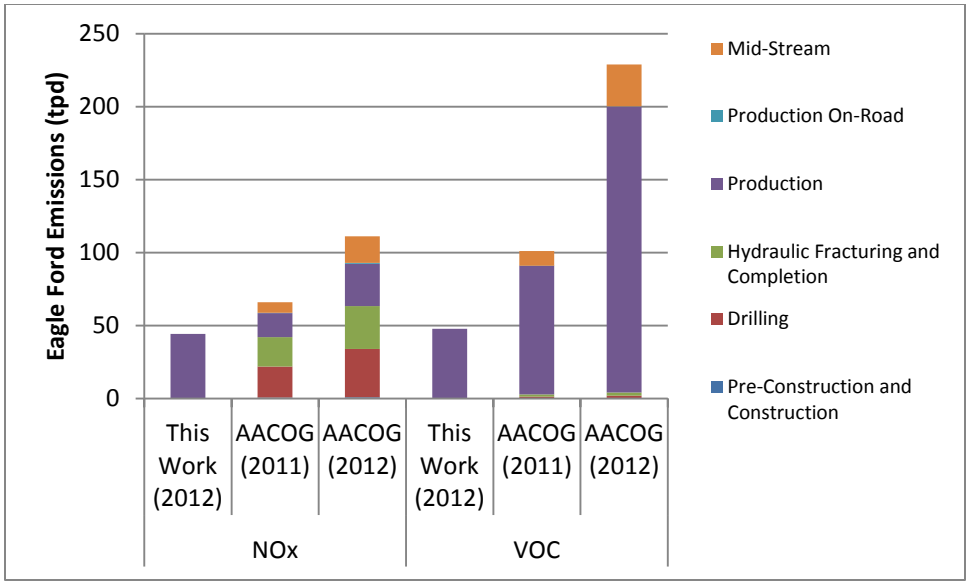

Figure 6-3. Comparison of the emissions inventory developed for this work to the entire Eagle Ford emissions inventory developed by AACOG (AACOG 2014) for 2011 and its projections for 2012.

Upstream production emissions were the focus of this proof of concept study in order to compare results for the Eagle Ford Shale to previously-published results for the Barnett Shale (Pacsi et al. 2013a), which limited oil and gas emissions to this sector. This limitation occurred for several reasons. First, the Barnett Shale Special Emissions Inventory (TCEQ 2011) did not collect emissions information for the pre-construction, construction, drilling, hydraulic fracturing, or well completion stages and did not estimate on-road emissions associated with the production sector. The exclusion of these emission categories in the Barnett Shale inventory for 2012 would not be expected to have a large impact on overall emissions since only 1182 wells were permitted in 2012 (TCEQ 2012a) compared to more than 14,000 over the previous five years. For the Eagle Ford shale, which is a less developed play with more current drilling activity, this same assumption may not be appropriate. For reference, the oil and gas well count in the Eagle Ford shale more than doubled between 2011 and 2012 (AACOG 2014), resulting in a total of 7147

producing wells by the end of 2012. Second, the work in Pacsi et al. (2013a) did not include the midstream emissions estimates from the Barnett Shale Special Emissions Inventory (TCEQ 2011) since the midstream emissions only accounted for 16% of total NO_x emissions (compared to 84% for the upstream production sector) and since the midstream emissions may or may not scale with production in the region, depending on the excess capacity at current midstream facilities. Future work improvements to the proof-of-concept Eagle Ford emissions inventory created for this study will add these and other emission categories from the oil and gas sector.

6.5 RESULTS AND DISCUSSIONS

6.5.1 Overall Emissions

Price-based changes in the dispatch order for ERCOT power plants that affect the relative usage of coal-fired and natural-gas fired power plants have the potential to change ozone precursor emissions rates from the power sector. The estimated average daily emissions for the 33-day study episode of NO_x, CO, and VOC from the power sector at the different natural gas pricing levels examined in this work are presented in Table 6-1. As the price of natural gas decreases, emissions of NO_x and CO from ERCOT decrease. Table 6-1 also outlines the changes in emissions from the Eagle Ford Shale assuming that the change in natural gas demand from ERCOT, compared to the $2.88 per MMBTU base case scenario, is met through increased or decreased production in the Eagle Ford Shale.

Category	$1.89/MMBTU			$2.88/MMBTU			$3.87/MMBTU			$7.74/MMBTU		
	NO_x	CO	VOC	NO_x	CO	VOC	NO_x	CO	VOC	NO_x	CO	VOC
ERCOT EGU Emissions (tpd)	307.0	230.6	16.8	362.5	422.7	15.0	423.2	618.1	14.8	483.5	824.8	15.2
Eagle Ford Upstream Production Emissions (tpd)	63.9	69.9	68.9	44.3	48.5	47.8	31.0	33.9	33.4	21.3	23.4	23.0
Eagle Ford and ERCOT Total Emissions (tpd)	370.9	300.5	85.7	406.8	471.2	62.8	454.2	652.0	48.2	504.8	848.2	38.2
Net Change from Base Case Scenario (tpd)	-35.9	-170.6	23.0	0.0	0.0	0.0	47.4	180.9	-14.5	98.1	377.0	-24.5

Table 6-1. Predicted changes in average daily emissions (tons) from ERCOT and Eagle Ford Shale based on changes in demand in ERCOT

The overall emissions of NO_x and CO are substantially higher from ERCOT than from the Eagle Ford Shale. For the scenario with the highest emissions from the Eagle Ford Shale and the lowest emissions from the power sector ($1.89 per MMBTU), NO_x emissions from ERCOT decrease by 15% (55.5 tpd) from the base case while emissions from the Eagle Ford increase by 44% (19.6 tpd). While combined NO_x emissions from these two sectors decreased by 35.9 tons per day in the $1.89 per MMBTU scenario compared to the base case, the location of the emission changes is not necessarily congruent between the power sector and the Eagle Ford shale. In particular, several coal-fired power plants in northeastern Texas, which were important drivers of maximum regional ozone concentration changes in Pacsi et al. (2013a), are located outside of the Eagle Ford Shale (Figure 6-1).

6.5.2 Impact on Regional Ozone Concentrations

Figure 6-4 shows the combined impact of emission changes (Table 6-1) from ERCOT and the Eagle Ford Shale on the episode average daily maximum 8-hr ozone concentration for each grid cell in the air quality simulation. For the $1.89 per MMBTU case, the episode average daily maximum 8-hr ozone concentration decreased by a maximum of 1.3 ppb. For the $3.87 per MMBTU and $7.74 per MMBTU scenarios, the episode average daily maximum 8-hr ozone concentrations increased by 1.0 ppb and 1.9 ppb, respectively. The spatial locations of the maximum ozone impacts in all scenarios occur in similar spatial locations, which correspond to the locations of coal-fired power plants, predominantly in northeastern Texas (Figure 6-1). The results in Figure 6-4 indicate that the maximum regional changes in the episode average of the daily maximum 8-hr ozone concentration are driven by emission changes at coal-fired power plants, rather than by emission changes in the Eagle Ford Shale production region.

Figure 6-5 is a sensitivity analysis that shows the impact on the episode average of the daily maximum 8-hr ozone concentrations for each scenario considering only the emission changes in the Eagle Ford Shale production region while keeping emissions from ERCOT constant at the base case ($2.88 per MMBTU) level. These sensitivity analyses allow for an estimate of the ozone impacts due only to changes in ozone precursor emissions from the Eagle Ford Shale. When comparing to Figure 6-4, it is important to note the difference in maximum scale for the Figures (±2 ppb in Figure 6-4 versus ±0.5 ppb in Figure 6-5). For the $1.89 per MMBTU case, the episode average of the daily maximum 8-hr ozone concentrations increased by a maximum of 0.4 ppb. For the $3.87 per MMBTU and $7.74 per MMBTU scenarios, the episode average of the daily maximum 8-hr ozone concentrations decreased by 0.4 ppb and 0.5 ppb, respectively. For the oil and gas emission sensitivity scenarios, the largest ozone

concentrations occur in the areas of the Eagle Ford with the highest well density (Figure 6-1) and, thus, apportioned emissions based on study methodology.

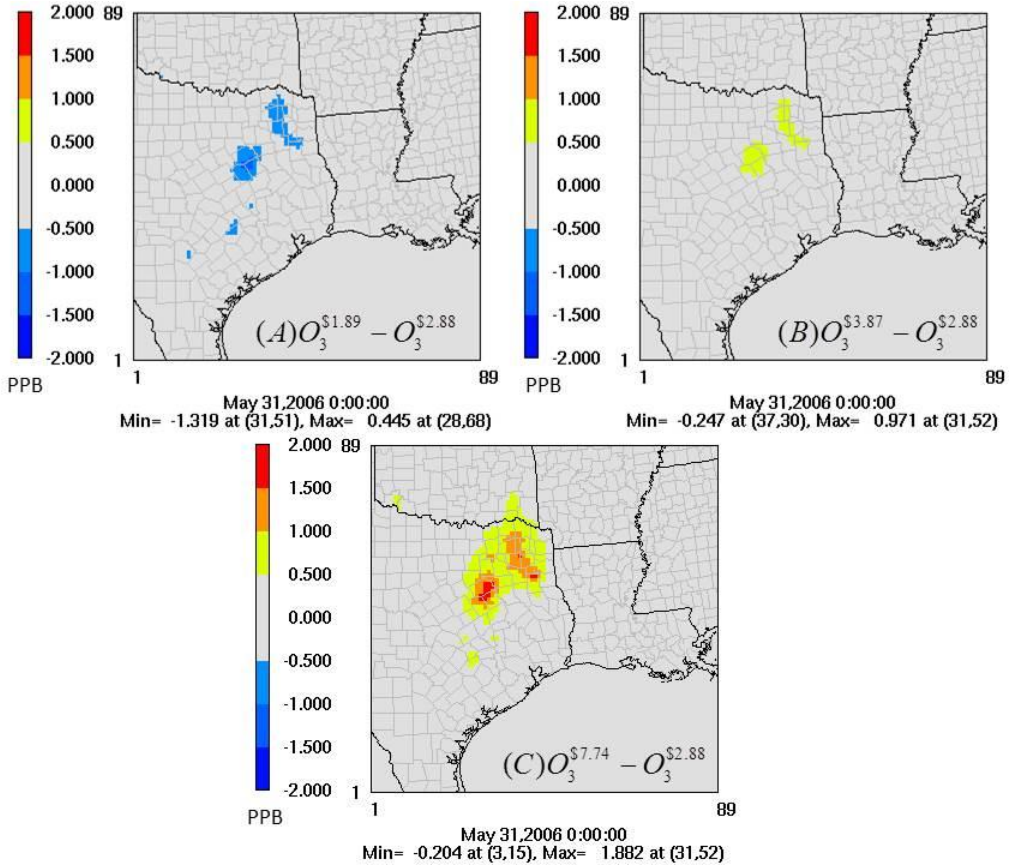

Figure 6-4. Change in average daily maximum 8-hr ozone concentration over the 33-day episode compared to the $2.88 per MMBTU base case. Emissions changes for ERCOT and the Eagle Ford Shale are outlined for each scenario in Table 6-1. Increased ozone concentrations compared to the base case are yellow to red in color. Decreased ozone concentrations compared to the base case are blue in color.

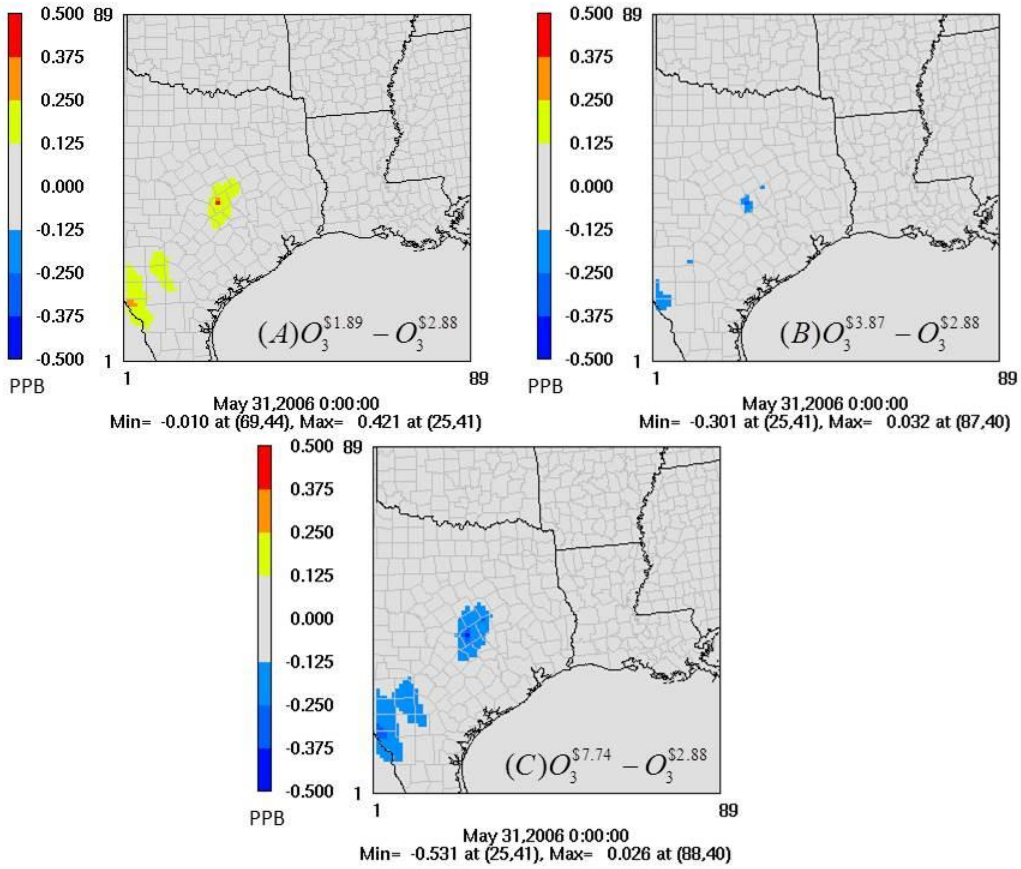

Figure 6-5. Change in average daily maximum 8-hr ozone concentration over the 33-day episode compared to the $2.88 per MMBTU base case considering only changes in oil and gas emissions from the Eagle Ford Shale. For these simulations, the Eagle Ford Shale emissions outlined in Table 6-1 were used for each scenario, but ERCOT emissions were for the $2.88 per MMBTU scenario in all simulations. Increased ozone concentrations compared to the base case are yellow to red in color. Decreased ozone concentrations compared to the base case are blue in color.

Comparing the episode average 8-hr daily maximum ozone results from Figure 6-4 (emission changes in both ERCOT and Eagle Ford Shale) to the results from Figure 6-5 (emission changes only from the Eagle Ford Shale) indicates that an ozone trade-off may exist due to increased natural gas use in the power sector if the additional natural gas production was sourced from the Eagle Ford Shale. Comparing the $1.89 per MMBTU

scenario to the base case, the episode average daily maximum 8-hr ozone concentration decreased 0.5 ppb - 1.8 ppb throughout large sections of northeastern Texas (Figure 6-4a). The sensitivity analysis (Figure 6-5a), which included the 44% increase in emissions from the Eagle Ford Shale but kept emissions from ERCOT constant with base case values, indicated that the episode average daily maximum 8-hr ozone concentration could increase by 0.1 ppb to 0.4 ppb in several high well-density production areas of the Eagle Ford Shale. Detailed analysis (Figure 6-6) of a grid cell in Milam county [(25,41) in the 12-km eastern Texas domain] that showed the highest ozone sensitivity to changes in Eagle Ford Shale emissions (Figure 6-5) could be greater than 2 ppb in that grid cell during morning and evening hours (NG_1.89 and NG_1.89OG in Figure 6-6). Despite a constant emissions profile from the oil and gas sector, the ozone impacts during the mid-day hours for the grid cell were lower in magnitude, indicating either that other emissions sources largely drove ozone formation in the grid cell during mid-day hours or that dilution during the time of day with large mixing heights reduced the impacts of emissions. This is an important result since the periods associated with daily maximum 8-hr ozone concentration typically occurred during daytime hours, when the ozone impact of the Eagle Ford Shale emissions is lower.

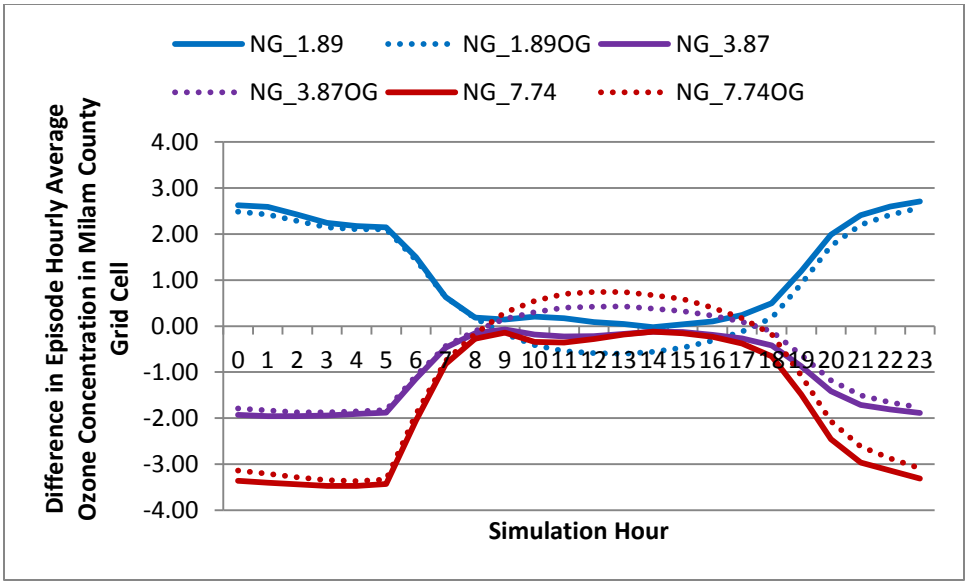

Figure 6-6. Difference in episode average ozone concentration for each hour of the day in ground-level grid cell (25,41), which has the largest ozone sensitivity to oil and gas emissions from the Eagle Ford Shale, compared to the $2.88 per MMBTU base case. OG indicates a sensitivity case in which the Eagle Ford emissions were changed but ERCOT emissions were kept constant at base case levels.

Another important ozone metric to consider when examining the combined impacts of changing emissions in the natural gas production and power sectors is the difference in the episode maximum 8-hr ozone concentration for each grid cell. This metric can be important since Federal ozone standards are based on a three-year average of the 4th highest annual daily maximum 8-hr ozone concentration (EPA 2014c). Thus, reductions to the daily maximum 8-hr ozone concentrations during a photochemical modeling episode would be an important for regulatory consideration if one of those days included one of the top four highest daily maximum 8-hr ozone concentrations for the year.

Figure 6-7 shows the change in episode maximum 8-hr ozone concentration compared to the $2.88 per MMBTU base case and including emission changes from the

electricity generation and the Eagle Ford production sectors. Note that the values represented in the grid cells in Figures 6-7 and 6-8 are not necessarily paired in time with surrounding grid cells. Episode maximum 8-hr average ozone concentration results are similar between the Eagle Ford Shale and northeastern Texas, which is different than the results for the episode average daily maximum 8-hr ozone concentration metric. For example, despite additional upstream production emissions of 19.6 tons per day of NO_x in the $1.89 case (Table 6-1), the episode maximum 8-hr ozone concentration decreased throughout much of the Eagle Ford shale (Figure 6-7a), which were areas with increased episode average daily maximum 8-hr ozone concentrations under the same emissions scenario (Figure 6-5). However, the same increase in production emissions from the Eagle Ford Shale without ERCOT emissions reductions drove an increase in the episode maximum 8-hr average ozone concentration (Figure 6-8a) compared to the base case. Thus, the episode maximum 8-hr average ozone concentration throughout much of the Eagle Ford was more impacted by changes in EGU emissions than local, upstream production emissions.

In addition, several hotspots resulted from changes in the power sector and natural gas emissions when using the episode maximum 8-hr average ozone concentration metric (Figure 6-7). One hotspot occurred on the Texas-Oklahoma border in a pattern consistent with the shape of a plume from a large coal-fired power plant (Figure 6-7a), despite the fact that NO_x emissions decreased from that facility in the $1.89 per MMBTU scenario compared to the base case. The ozone results from this hotspot had two separate drivers. For the dark red dot in the same grid cell as the coal-fired power plant, the decreased NO_x emissions from the coal-fired power plant led to lower titration of ozone in the fresh power plant plume, causing an increased ozone concentration values in the $1.89 per MMBTU case compared to the base case. However, the surrounding yellow color

(Figure 6-7a) also appears in the simulation with only oil and gas emissions (Figure 6-8a), indicating that the ozone increase for the yellow region was driven by increased transport from the Eagle Ford Shale production area. The second hotspot of interest occurred in the Houston area (Figure 6-7a) and was likely driven by increased NO_x emissions from area natural gas EGUs in the $1.89 per MMBTU scenario that increased ozone during the peak hours of the episode. This hotspot was not observed in the cases which considered only emissions from the oil and gas production sector in the Eagle Ford (Figure 6-8a).

6.5.3 Implications of Ozone Results

As the utilization of natural gas power plants in lieu of coal-fired power plants increases based on lower natural gas prices, an ozone trade-off may exist in Texas between areas that are influenced by emissions from coal-fired power plants and those in the Eagle Ford Shale if the additional natural gas production needed in the power sector is sourced from that shale gas production region. These results are based on a proof-of-concept inventory developed for this work that consisted only of upstream production activity emissions. Future work is needed to refine the Eagle Ford emissions inventory to include other emissions categories related to oil and gas development, such as drilling rig engines and midstream compressors, in order to improve the characterization of this potential ozone trade-off. The existence of ozone trade-offs between areas influenced by emissions from the power sector and areas influence by production emissions did not appear in the Pacsi et al. (2013a) analysis for the Barnett Shale in Texas. Thus, analyses of the potential ozone impacts of increased natural gas production and use in the power sector should be examined separately for each region rather than assuming the results from one region are broadly applicable.

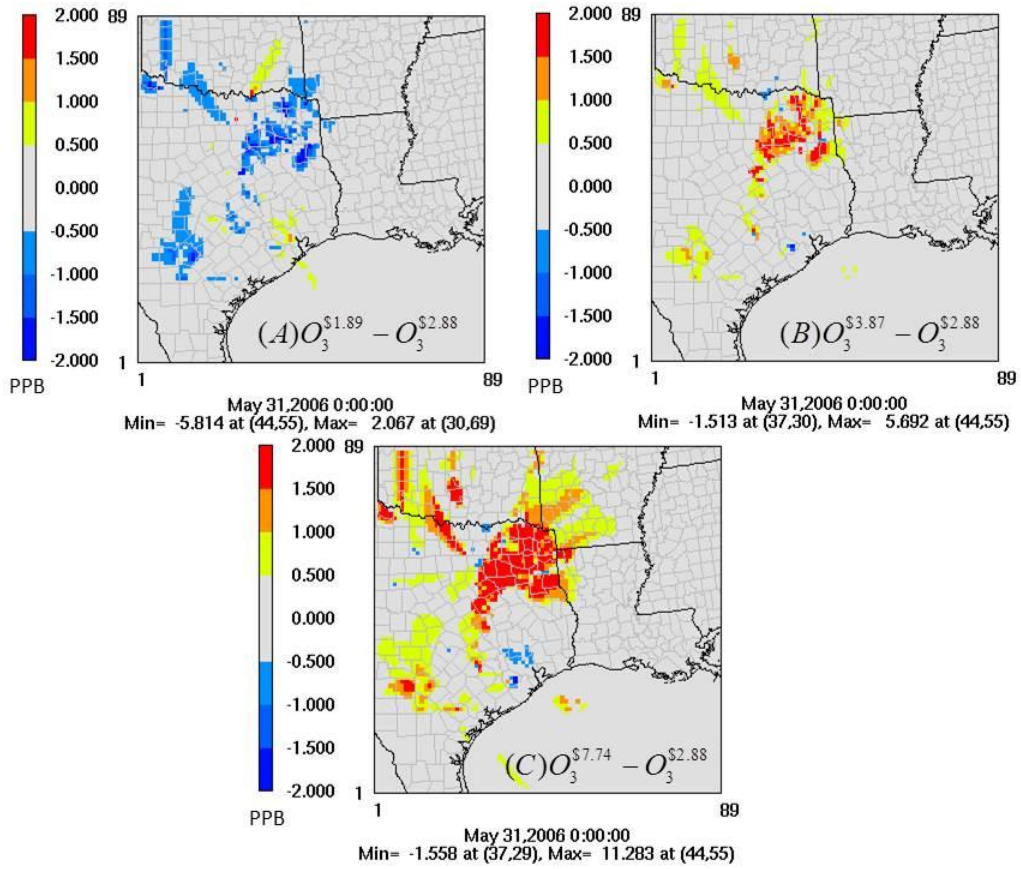

Figure 6-7. Change in maximum 8-hr ozone concentration for the 33-day episode compared to the $2.88 per MMBTU base case. Emissions changes for ERCOT and the Eagle Ford Shale are outlined for each scenario in Table 6-1. Increased ozone concentrations compared to the base case are yellow to red in color. Decreased ozone concentrations compared to the base case are blue in color.

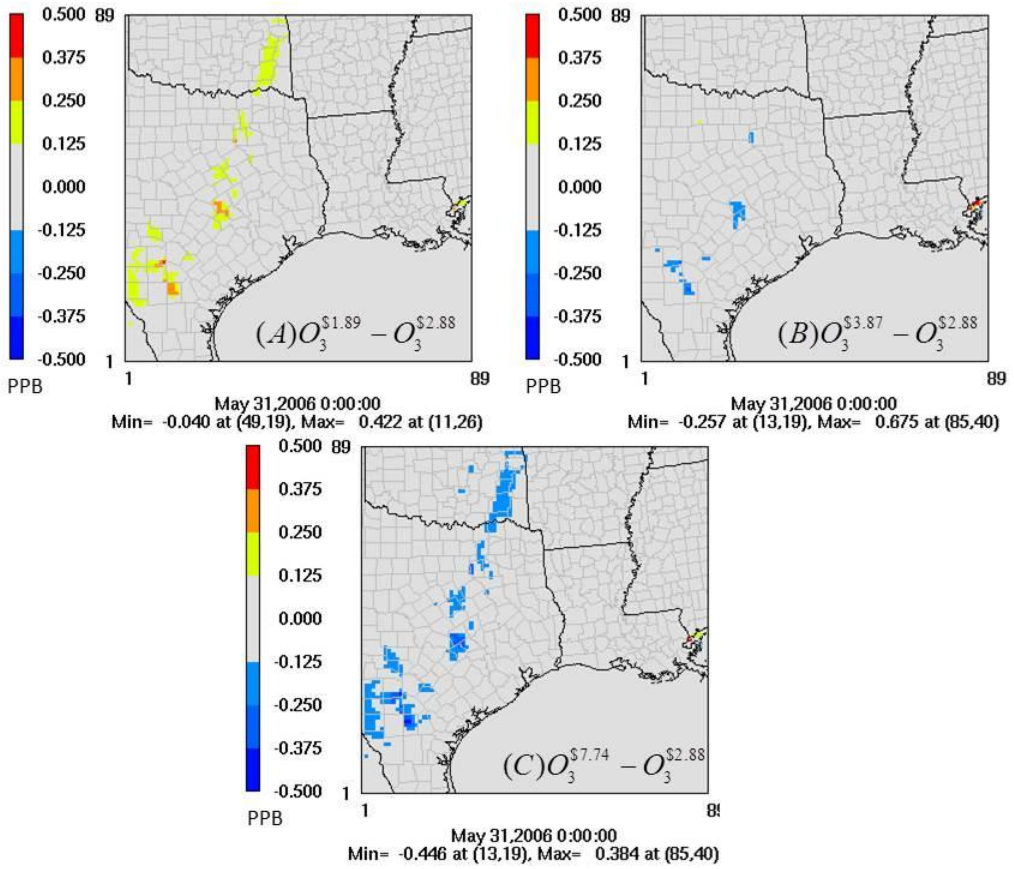

Figure 6-8. Change in episode maximum 8-hr average ozone concentration over the 33-day episode compared to the $2.88 per MMBTU base case considering only changes in oil and gas emissions from the Eagle Ford Shale. For these simulations, the Eagle Ford Shale emissions outlined in Table 6-1 were used for each scenario, but ERCOT emissions were for the $2.88 per MMBTU scenario in all simulations. Increased ozone concentrations compared to the base case are yellow to red in color. Decreased ozone concentrations compared to the base case are blue in color.

Chapter 7: Spatial and temporal impacts on water consumption in Texas from shale gas development and use

Pacsi, A.P.; Sanders, K. T.; Webber, M. E.; Allen, D.T. *ACS Sustainable Chemistry & Engineering*. **2014**, doi: 10.1021/sc500236g

7.1 CONTEXT

Chapter 7 extends the UT/MIT Integrated Model framework to include water use associated with natural gas production (Objective 7) in order to determine the spatially-resolved consumptive water impacts of increased natural gas production and use in Texas.

7.2 ABSTRACT

Despite the water intensity of hydraulic fracturing, recent life cycle analyses have concluded that increased shale gas development will lead to net decreases in water consumption if the increased natural gas production is used at natural gas combined cycle power plants, shifting electricity generation away from coal-fired steam cycle power plants. This work expands on these studies by estimating the spatial and temporal patterns of changes in consumptive water use in Texas river basins during a period of rapid shale gas development and use in electricity generation, from August 2008 through December 2009. While water consumption decreased in Texas overall, some river basins saw increased water consumption and others saw decreased water consumption, depending on the extent of extraction activity in the basin, the mix of power plants using cooling water in that basin, and price-based changes in the power sector. Due to the temporal and spatial heterogeneity in the consumptive water impacts of natural gas development and use in the power sector, local and regional water use impacts must also be considered in addition to the overall supply chain impacts.

7.3 INTRODUCTION

Total natural gas production in the United States is expected to increase by 44% between 2011 and 2040, with shale gas development being the largest source of growth. (EIA 2012) Recently, shale gas extraction has increased due to advances in hydraulic fracturing and horizontal drilling that have enabled economical production of natural gas from shale formations. Shale gas plays in Texas, particularly the Barnett Shale in the Dallas-Fort Worth area, were among the first shale gas resources in the country developed on a large scale (EIA 2012), and the state accounted for 66% of the shale gas production in the United States from 2008 to 2009 (EIA 2014b). Texas is also predominantly served by an electric grid, the Electricity Reliability Council of Texas (ERCOT), which has significant natural gas generation capacity. Thus, Texas is an important early case study for the development and utilization, in electricity generation, of shale gas resources.

The rapid development of shale gas resources in the United States has occurred while research on its environmental impacts -- such as water quantity (Nicot et al. 2012; Rahm et al. 2012; Grubert et al. 2012; Laurenzi et al. 2013; Murray 2013), water quality (Entrekin et al. 2011; Osborn et al. 2011; Rahm 2011; Barbot et al. 2013), air quality (Venkatesh et al. 2012; Litovitz et al. 2013; Pacsi et al. 2013a), and greenhouse gas emissions (Howarth et al. 2011; Jiang et al. 2011; Alvarez et al. 2012) -- is on-going. Previous studies on total water consumption in natural gas production have focused on quantifying the total water used (Nicot et al. 2012; Murray 2013) or available (Rahm et al. 2012) for shale gas production in a particular region, without examining changes to water demand associated with changes in electricity generation. In addition, life-cycle analyses of the consumptive water impacts of shale gas development and use in electricity generation (Grubert et al. 2012; Laurenzi et al. 2013) have generally assumed

that the natural gas is used exclusively to displace coal-fired generation. However, not all marginal natural gas production will necessarily be used to displace coal-fired power generation. In 2011, 48% of the total natural gas consumption in Texas (EIA 2014c), which included natural gas from both new and existing wells, occurred in the power generation sector. Thus, the overall water demands of natural gas production can exceed the demands that would be estimated based just on the use of natural gas in electricity generation.

Prior work on water use in natural gas supply and use chains in Texas found that higher water requirements at the point of natural gas extraction could be offset by water savings due to higher power plant efficiency, cooling system design, and avoided emissions controls at the point of electricity production. These analyses have assumed that conventional coal-fired generation is displaced by natural gas combined cycle units, resulting in net water consumption reductions (Grubert et al. 2012). In practice, the extent to which natural gas from shale production displaces conventional coal-fired generation is controlled by many factors, including operational parameters at the power plant and the relative price of coal and natural gas (Venkatesh et al. 2012; Pacsi et al. 2013a). In addition, shifts in power generation might be located in different regions than shale gas production, resulting in shifts in the spatial distribution of water consumption. Thus, the water savings due to decreased water consumption in coal-fired electricity generation and coal-mining might occur at different locations or times than where and when water is used for natural gas production. Unfortunately, the location and timing of these changes in water consumption are not known, since both a control case without shale gas development and the actual natural gas use due to shale gas development cannot both be known.

To address this knowledge gap, this study will estimate the spatial and temporal characteristics of changes in consumptive water use in Texas during a period of rapid shale gas development that triggered decreased natural gas prices, enabling greater use of natural gas in the electricity generation mix (Rahm 2010). In particular, this study will estimate the extent to which water consumption for hydraulic fracturing in natural gas production regions was offset by reductions in the consumptive water use in electricity generation and lignite (coal) mining in Texas and in specific river basins in the state in order to determine whether local changes differ from state-wide and supply chain impacts.

7.4 Materials and Methods

The analysis in this work quantifies shifts in consumptive water use in Texas that were driven by changes in natural gas production and price in the state during the period from August 2008 through December 2009. During this time, the price of natural gas for electric power producers dropped from $11.09 per million British thermal units (MMBTU) to less than $4 per MMBTU (as shown in Figure 7-1) (EIA 2014d) while total shale gas production in Texas increased by 14% (EIA 2014b). This work compares two cases. Scenario 1 is an actual development scenario which uses historic natural gas price, production, and well completion data. Scenario 2 is a hypothetical alternative development scenario in which hydraulic fracturing of horizontal wells in the Barnett shale and the section of the Haynesville Shale in Texas (the most active areas for new shale gas activities in eastern Texas during this period) is assumed not to have occurred after July 31, 2008. In the alternative scenario, the natural gas price for electricity producers in the state was assumed to remain constant at $11.09 per MMBTU, which was the July 2009 price (EIA 2014d). This price point is used as a plausible scenario to

estimate the behavior of ERCOT at high natural gas prices. However, a full economic analysis (including second-order effects and price inelasticities) of the impact of the forgone production from these horizontal wells, which accounted for 9.2% of total natural gas production in Texas during the period, is beyond the scope of this work.

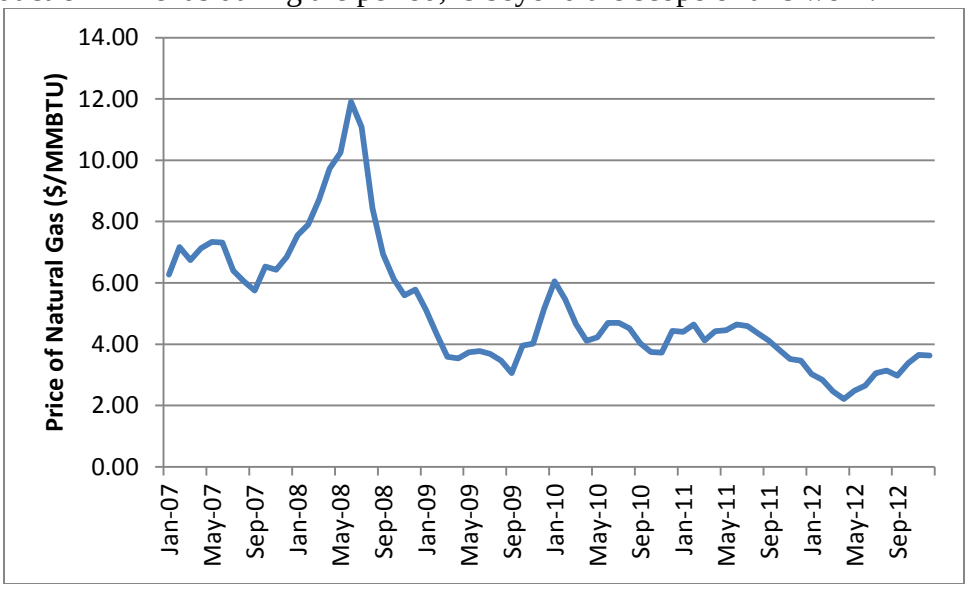

Figure 7-1. Price of natural gas for Texas power producers (EIA 2014d) for 2007 through 2012. The period of interest for the study is August 2008 through December 2009.

For this work, consumption, which is the amount of water taken from a water reservoir but not returned to it (Macknick et al. 2012; Averyt et al. 2013), was chosen as the benchmark water metric rather than withdrawals, which is the total amount of water taken from the source (Macknick et al. 2012; Averyt et al. 2013), so that comparisons could be made to recent studies, (Grubert et al. 2012; Nicot et al. 2012; Laurenzi et al. 2013) which have focused on freshwater consumption. While water withdrawals and consumption can vary by orders of magnitude for power plant cooling, at the point of extraction in the natural gas production sector in Texas, water consumption and withdrawals have historically been similar due to limited re-use of water resources (Nicot

et al. 2012; Nicot et al. 2014). Thus, consumptive water use was determined to be the appropriate metric of comparison of the water impacts in the lignite mining and power generation sectors.

Scenario	*Price of Natural Gas for the Power Sector*	*New Natural Gas Wells in the Barnett Shale and in the Texas Part of the Haynesville Shale*
1	monthly average natural gas price for Texas from August 2008 to December 2009 (Figure 7-1)	actual rate of well completion during study period (IHS 2013)
2	constant price of $11.09 per MMBTU	no new horizontal wells completed after July 31, 2008

Table 7-1. Summary of scenario assumptions for the price of natural gas in the power sector and well completion activity in shale gas production regions in Texas from August 2008 through December 2009.

7.4.1 Spatial Domain

The total change in water consumption from ERCOT, lignite (the type of coal produced in Texas) mining, and natural gas production between the two scenarios was estimated for Texas and for each river basin in the state (TWDB 2014a). These boundaries match the spatial domain used in recent research on Texas water rights modeling (Stillwell et al. 2011a; Stillwell et al. 2013a). Each power plant, horizontal gas well, and lignite mine examined in this study was mapped to a specific water basin in Texas (TWDB 2014a) based on its latitude and longitude using ArcGIS Version 10.1 (ESRI 2012).

7.4.2 Water Consumption in Natural Gas Production

For this study, horizontal natural gas wells that were drilled in Texas in the Haynesville and Barnett shale plays during the study period were identified using the commercially-available IHS database (IHS 2013). This database contained the location (latitude and longitude), completion date, and monthly production of each well in the region. During this period, 2996 horizontal gas wells were completed in the Barnett shale (2664 wells) and the Texas part of the Haynesville shale (332 wells), and these wells accounted for 9.2% of the total natural gas produced in Texas during this period. The spatial location of each well is shown in Figure 7-2. For the actual natural gas production and prices scenario (Scenario 1), the water consumed during hydraulic fracturing at each horizontal well was estimated using a play-median factor of 2.8 million gallons per well for the Barnett Shale and 5.7 million gallons per well in the Haynesville Shale (Nicot et al. 2012). Implications and rationale for the use of the play-median factors rather than individual well water consumption is available in the next section. For the alternative scenario (Scenario 2), the assumption that no horizontal wells were completed after July 31, 2008, was made, and thus, water use in hydraulic fracturing of horizontal wells during the study period was assumed to be negligible. Thus, the difference in water consumed in natural gas production between the two scenarios was assumed to be equal to the amount of water used in hydraulic fracturing of the horizontal wells in the actual development scenario (Scenario 1). While there are other upstream water uses, such as for drilling and for proppant production (Nicot et al. 2012), Laurenzi and Jersey (2013) found that water consumed in these activities was small compared to hydraulic fracturing (which was 89% of upstream natural gas water consumption) and that all upstream water consumption, including hydraulic fracturing, was small compared to the power plant, which accounted for 93% of lifecycle water consumption.

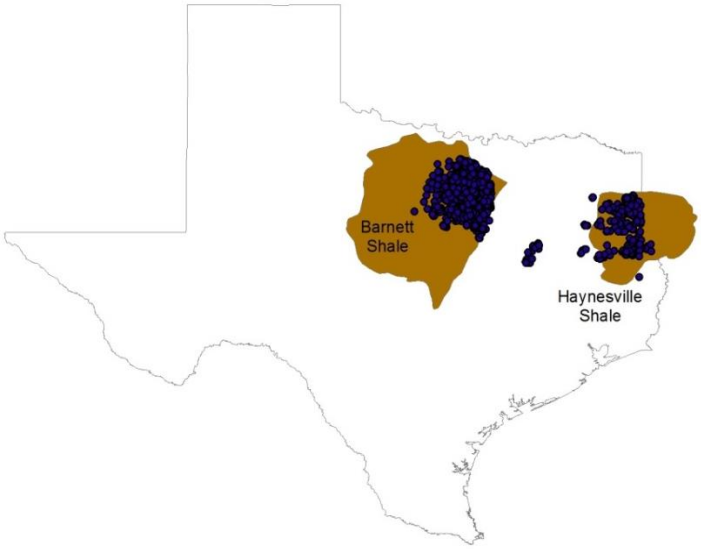

Figure 7-2. Location of horizontal wells completed in the Haynesville and Barnett shale regions during period of interest for this study (August 2008 through December 2009).

Recently, the Eagle Ford shale in south Texas has experienced rapid growth in natural gas production. However, for the period examined in this study, total production from the Eagle Ford Shale was much less than 0.01% of the total natural gas produced in Texas, (TXRRC 2014b) and by the end of 2009, the total number of gas wells in the region was small -- only 67 (TXRRC 2014b) -- compared to more developed natural gas production regions, such as the Barnett Shale, which had more than 10,000 natural gas wells (TXRRC 2014a). Thus, the exclusion of the Eagle Ford shale from the analysis is not expected to have a significant impact on the results of this study. Implications of changes in consumptive water use in the lignite and power production sectors in the river basins in the Eagle Ford Shale, however, are discussed in this work.

7.4.3 Implications of Use of Median Factor for Water Consumed in Hydraulic Fracturing

The IHS database (IHS 2013) that was used in this work for determination of the completion date and spatial coordinates for each well examined in the Haynesville and Barnett shales also contained reported water use for each well. Although the cause was not proven definitively, a detailed analysis (Nicot et al. 2012) of water use entries in the IHS database (IHS 2013) for Texas gas wells revealed that water use reported at some wells was unrealistically high or low compared to wells with similar characteristics. In this work, analysis of the 2996 horizontal gas wells completed in the Haynesville and Barnett shales during the study period revealed similar trends. Of the horizontal gas wells completed during the study period, the IHS database reported zero water use for 350 wells (15.2% of the total) despite indicating that hydraulic fracturing had occurred at those sites and that natural gas was being produced at them. In addition, reported water used in hydraulic fracturing of select wells in each river basin with production activity was more than two orders of magnitude greater than play-median estimates from Nicot and Scanlon (2012). Due to the unrealistic extreme values of water use for some wells in the database, the play-median values for the Haynesville (5.7 million gallons) and Barnett (2.8 million gallons) were used rather than well-specific data from the IHS database.

Table 7-2 compares the net consumptive water use estimate using the play-median water use factor for each well to two alternative cases. The first alternative case is the use of the water consumption data directly from the IHS database. The second alternative case involved replacing the extreme values, which were defined for this purpose as being outside of the 95% confidence interval for water consumed in the hydraulic fracturing of the wells reported by Nicot and Scanlon (2012), with the median value from the play. The 95% confidence intervals were 0.75 to 5.5 million gallons per

well for the Barnett Shale and 0.7 to 7.4 million gallons per well for the Haynesville Shale. The estimate of total water consumption used in hydraulic fracturing during the episode using play-median factors is ~10% higher than using actual data from the IHS database with replacement of extreme values.

River Basin	**Shale Gas Play**	**Cumulative Water Consumption in Hydraulic Fracturing (billion gallons)**		
		Play-Median	*IHS Raw Data* (IHS 2013)	*IHS Data with Extreme Values Replaced with Median Value*
Trinity	Barnett	5.45	5.17	5.37
Brazos	Barnett	2.01	1.77	1.70
Sabine	Haynesville	0.72	0.12	0.55
Cypress	Haynesville	0.28	0.10	0.16
Neches	Haynesville	0.89	0.31	0.70
Total	Barnett & Haynesville	9.35	7.47	8.47

Table 7-2. Comparison of cumulative water consumption used in the hydraulic fracturing in Texas between August 2008 and December 2009 of horizontal gas wells in river basins which included the Haynesville and Barnett shales using three different approaches for estimating water consumed per well.

7.4.4 Water Consumption in Electricity Generation

For each scenario, the hourly generation at each electricity generating unit (EGU) in ERCOT was determined using a PowerWorld (PowerWorld 2012) model that has been used in previous studies (Alhajeri et al. 2011a; Pacsi et al. 2013a; Pacsi et al. 2013b). This model includes constraints on generator minimum and maximum generation levels, total demand in ERCOT, ramp rate, and transmission line capacity, but does not include constraints on facility maximum capacity factor. In the electricity generation model, the price of natural gas was the only variable changed between simulations for Scenario 1, in which the monthly-average natural gas price for Texas power producers was used (as

shown in Figure 7-2) and Scenario 2, in which a constant price of $11.09 per MMBTU was applied across the study period. Hourly electricity generation in ERCOT was equivalent in Scenario 1 and Scenario 2. More information on the PowerWorld model and its performance in estimating the fuel mix for ERCOT, which was equivalent to a similar model in the literature (Venkatesh et al. 2012), is available in the next section.

Water consumption at each power plant in ERCOT was determined by multiplying the generation by an EGU-specific annual-average consumption factor (King et al. 2008b) that were developed for the Texas Water Development Board (TWDB). Using Texas-specific factors for power plant consumptive water use is important since a recent study (Scanlon et al. 2013) found higher consumption rates at natural gas-fired power plants in Texas than national average values (Macknick et al. 2012; Averyt et al. 2013). Compared to using other publicly-available databases which utilize a national average (Averyt et al. 2013) or a Texas average (Scanlon et al. 2013) value for the consumptive water use rate at each power plant based on its cooling system configuration, the use of the power plant-specific database from King et al. (2008b) -- which is the database used in this study -- leads to the smallest estimate of water savings in the power sector from the displacement of coal-fired units with natural gas-fired power plants (see Figure 7-3). For Texas water consumption databases, the King et al. (2008b) database differs from the Scanlon et al. (2013) factors since the King et al. (2008b) database provides specific water consumption estimates for each power plant rather than an average for each power plant cooling system configuration type (for example, recirculating cooling towers for natural gas combined-cycle plants). Thus, the King et al. (2008b) factors account for different power plant cooling requirements based on factors such as local climate and power plant efficiency. In addition, it is important to note that consumption rates would vary with meteorological conditions, but this study does not

estimate meteorological deviations from annual average consumption values for each EGU.

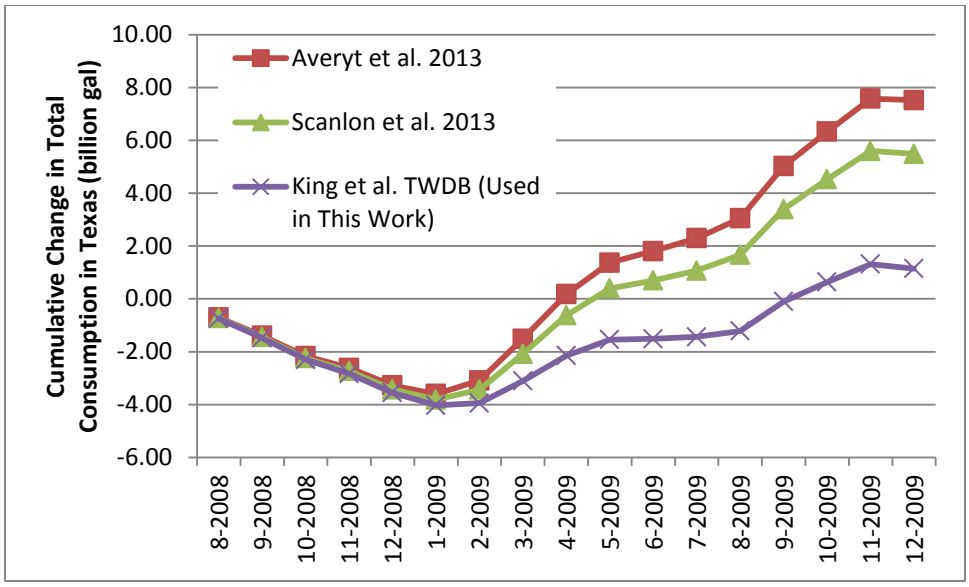

Figure 7-3. Comparison of temporal evolution of total changes in water consumed in Texas throughout the episode using three publicly-available databases for consumptive water use at power plants. Note that positive values indicate a net consumptive water savings in Scenario 1 compared to Scenario 1.

Multiple sectors drive demand for the production of natural gas in Texas, and this study estimates the water consumed in shale gas production regardless of whether the natural gas produced is actually used in electricity generation in ERCOT. Since the amount of additional gas produced in Scenario 1, compared to Scenario 2, is greater than the additional amount of natural gas used in the power sector in Scenario 1, compared to Scenario 2, the excess gas may have been used in power generation or other applications in other parts of the United States. In this circumstance, this work estimates the water used in the production of the natural gas in Texas but not the water savings from the power sector in other states. This distinction might lead to a reduced estimate of total consumptive water savings from the use phase of the natural gas life cycle, since this

study only considers local consumptive water changes in ERCOT's boundaries within the state of Texas. In addition, changes to natural gas use in other sectors (e.g. chemical manufacturing), which might not provide the same level of change in local water consumption in producing regions in Texas as the power generation sector, are not estimated in this study.

7.4.5 Additional Information on the Power World Model and its Performance

This work uses a PowerWorld Simulator Version 16 model (PowerWorld Corporation 2012) for the ERCOT electric grid. The model uses actual hourly demand in ERCOT for the period from August 2008 through December 2009 (ERCOT 2006a), which was a time during which the cost of natural gas for electricity producers in Texas dropped significantly due to increased shale gas production. For each hour, the PowerWorld model solved for the combination of electricity generation at each electricity generating unit (EGU), or power plant, which minimized the total operating cost in ERCOT while including line losses and accounting for constraints on generator minimum and maximum generation levels, total demand in ERCOT, and transmission line capacity. A linear programming (LP) approach was used so that inequality constraints could be included.

In the PowerWorld model, the cost *c* of generation was calculated at each fossil-fuel powered EGU *i*:

$$c_i\,(\$/\text{MWh}) = H_i \times pf_i + OPEX_i$$

where H_i is the heat rate of the specific EGU in MMBTU/MWh (EPA 2012a), pf_i is the fuel cost based on the type of fossil fuel ($/MMBTU), and $OPEX_i$ is the variable operation and maintenance cost ($/MWh) for the unit (EIA 2006). In the actual development scenario, monthly average natural gas prices are used for August 2008

through December 2009 (Figure 7-1). In the alternate development scenario, natural gas prices are assumed to remain at the July 2008 price for natural gas ($11.09/MMBTU) throughout the modeled period. This price is not intended to model the economic outcome of ending new Texas shale gas production from hydraulic fracturing of horizontal wells during the period; rather, the price is used to simulate the behavior of ERCOT during the period if natural gas prices had remained high. A constant coal price of $1.89 per MMBTU was used in both scenarios based on the ERCOT average coal price reported in EIA Form 923 during the period (EIA 2013). This average coal price was a weighted-average of prices for both lignite and sub-bituminous coal. For wind and hydro powered EGUs, the average hourly generation for 2009 for each power plant was used as a constraint for each hour of the simulation (ERCOT 2006a). While wind power in Texas is highly variable, hourly total wind generation is not widely-available for the state before 2010 (ERCOT 2014a). Nuclear power plants were assumed to operate at 90% of their capacity during all hours in the simulation.

Model validation for the period of interest was undertaken by comparing the subset of the actual natural gas prices and production scenario simulation for 2009 to data from the Emissions & Generation Resource Integrated Database (eGRID) (EPA 2012a) for ERCOT in 2009. EGUs in the eGRID database that were primarily used for industrial self-generation were removed from the analysis since these were not modeled in the PowerWorld simulations. The percent generation by fuel type in eGRID and the PowerWorld Model are summarized in Table 7-3, and model performance for this validation is comparable to results from other peer reviewed work (Venkatesh et al. 2012). Based on eGRID data for 2009 (EPA 2012a), ERCOT accounted for 83% of electricity generation in Texas. While the amount of generation at non-ERCOT EGUs in

Texas may also change in response to natural gas prices, estimating these changes is beyond the scope of this study.

	This Study (for year 2009)		Venkatesh et. al [2012] (for year 2010)	
	Industry Data (EPA 2012a)	**PowerWorld Model**	**Industry Data**	**Study Model**
Natural Gas	45%	48%	38%	36%
Coal	35%	32%	40%	45%
Nuclear	13%	14%	13%	13%
Other	6%	6%	9%	6%

Table 7-3. PowerWorld model validation comparing the percent of ERCOT generation by power plant fuel type to actual data from eGRID for 2009. (EPA 2012a) Note that Venkatesh et al. (2012) focused its analysis on the year 2010.

7.4.6 Water Consumption for Lignite (Coal) Production

Fuel for coal-fired power generation in Texas comes from a combination of lignite for mine-mouth power plants and sub-bitumous coal from the Powder River Basin in Wyoming, which is transported to Texas by rail and is more energy dense than lignite. In Texas, some plants burn exclusively lignite or coal, while others utilize a mixture of coal types. For 2009, the fraction of lignite and sub-bitumous coal on a heat basis (MMBTU) was calculated from fuel receipt data (EIA 2013) for each power plant in ERCOT. In 2009, sub-bitumous coal from Wyoming accounted for 68% of the total coal used in ERCOT on a heat basis and 62% on a mass basis.

For this study, upstream water consumption changes were limited to changes in coal production associated with lignite consumption at Texas power plants in ERCOT. Exclusion of the water impacts in Wyoming from changes in the ERCOT demand for sub-bituminous coal is consistent with methodology of other recent studies of the water

impacts of energy production in Texas (Grubert et al. 2012; Nicot et al. 2012), since the water consumption occurs outside of the state boundary. Based on analysis of data from the Energy Information Administration [EIA] (EIA 2013), seven coal-fired power plants in ERCOT used some lignite as a fuel source in 2009, and each power plant was supplied by its associated, nearby lignite mine. For each scenario, the total heat provided by lignite at each of the seven power plants for August 2008 through December 2009 was calculated to determine the total demand for lignite from ERCOT and to establish the upstream production rate of lignite needed for power plant fuel, assuming that the ratio of sub-bitumous coal to lignite coal remained constant at these facilities with changing generation. A recent study (Grubert et al. 2012) found that the production of Powder River Basin coal in Wyoming was 3%-17% as water intensive as lignite production in Texas and established a consumptive water use factor for lignite production in Texas of 16.1 gal per MMBTU, which included mine dewatering per convention by Texas water policymakers. Water consumption for truck transporting of lignite within Texas and for the Texas portion of the rail transport of Powder River Basin coal from Wyoming were considered negligible in this study (Grubert et al. 2012).

7.5 Results and Discussions

7.5.1 Net Impacts on Consumption in Texas

In Texas, between August 2008 and December 2009, total water consumption in the actual natural gas prices and production scenario (Scenario 1) was found to be 1.1 billion gallons less than in Scenario 2 (Table 7-4) including changes in both the electricity generation and the fuel production sectors in the state. These savings are equivalent to 0.4% of the TWDB estimate (TWDB 2014b) for the total water consumed in Texas for mining (which includes natural gas and coal production activities) and power

generation during the period examined in this study. As noted in the Materials and Methods section, this estimate may under-state overall water savings.

Water Consumption Category	**Net Consumption August 2008-December 2009 (billion gallons)**		
	Scenario 1	**Scenario 2**	**Net Change for Scenario 1 compared to Scenario 2**
Hydraulic Fracturing of Horizontal Wells	*9.4*	*0.0*	*+9.4*
Lignite Mining for ERCOT generation	*7.7*	*9.9*	*-2.2*
Net Consumption by ERCOT Power Plants for Electricity Generation			
Coal	68.3	84.1	-15.8
Natural Gas Combined Cycle (NG-CC)	34.3	27.1	+7.2
Natural Gas Steam Turbine (NG-ST)	2.0	1.6	+0.5
Natural Gas Combustion Turbine (NG-GT)	0.6	0.6	-0.0
Other Fuel Types	36.9	37.1	-0.2
ERCOT Total	*142.1*	*150.4*	*-8.3*
Net Total	**159.2**	**160.3**	**-1.1**

Table 7-4. Net changes in consumptive water use by sector in Texas for period from August 2008 through December 2009. Scenario 1 included actual natural gas prices and production in the state. Scenario 2 used an elevated natural gas price and assumed no horizontal well completions via hydraulic fracturing after July 31, 2008. Note that negative values indicate a sector in which Scenario 1 has less water consumption (i.e. a net water savings) compared to Scenario 2.

Much of the potential water savings calculated in this study (Figure 7-4 and Table 7-4) and estimated in other studies (Grubert et al. 2012; Laurenzi et al. 2013) are driven by changes in the fuel mix utilized in the electricity generation sector. Compared to Scenario 2, lower natural gas prices in Scenario 1 caused a shift of 9% of ERCOT total generation from coal-fired to natural gas-fired EGUs (including steam cycle, combined cycle, and combustion turbine plants, see Figure 7-5). Under the actual natural gas prices scenario (Scenario 1), demand for natural gas in ERCOT increased by 0.3 trillion cubic feet (tcf), which was less than the 1.0 tcf of additional natural gas (9.2% of total Texas natural gas production) produced at the horizontal wells completed in the Barnett shale and the portion of the Haynesville shale in Texas during the study period. For reference, total reported natural gas usage in all sectors in Texas (EIA 2014c) during the study period was 4.2 tcf and 2.0 tcf were used in the electric power sector. Total water consumption in ERCOT for power generation was lower in the actual development scenario (Scenario 1), resulting primarily from a 15.8 billion gallon decrease in water consumption at coal-fired power plants that offset a 7.6 billion gallon increase in water consumed at natural-gas EGUs. In Scenario 1, decreased usage of the coal-fired power generation resources in ERCOT led to a 2.2 billion gallon savings in water consumption from lignite mining in Texas compared to Scenario 2. Water consumption from hydraulic fracturing of horizontal gas wells in the Barnett and Texas portion of the Haynesville shale was 9.4 billion gallons during the study period. Water consumption in hydraulic fracturing was only considered in Scenario 1 since Scenario 2 assumed that new well completions in the state ceased after July 31, 2008. Thus, net consumption in the mining sector, which included both natural gas and lignite production, increased by 7.2 billion gallons in Scenario 1 compared to Scenario 2. Thus, the water savings for the actual development scenario (Scenario 1) during the study period from changes in

ERCOT power generation (8.3 billion gallon) were largely offset by increased water consumption in the Texas mining sector (7.2 billion gallons), leading to a net savings of 1.1 billion gallons in Scenario 1.

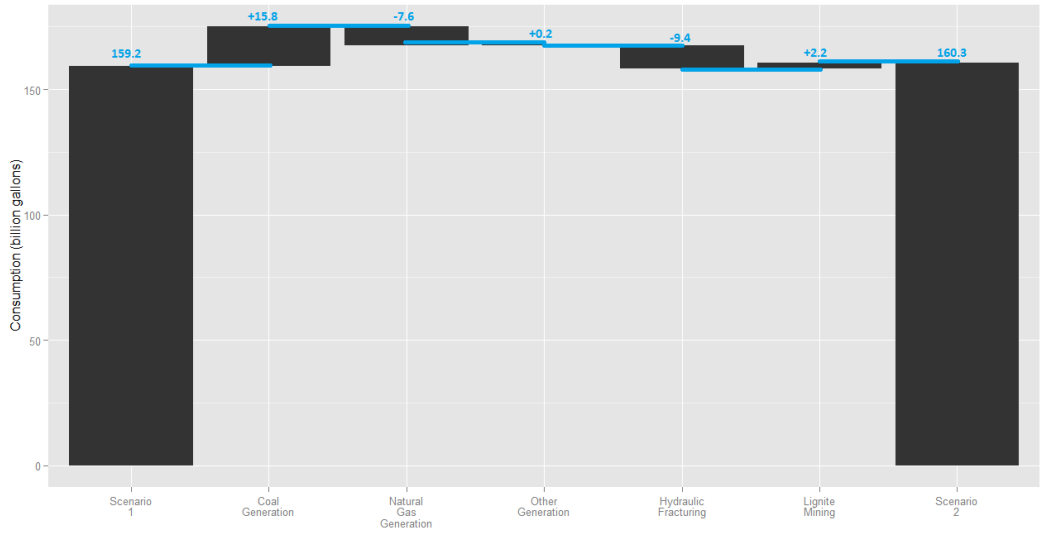

Figure 7-4. For Scenario 1 (actual natural gas prices and production) compared to Scenario 2 (elevated natural gas price and no new horizontal well completions in the Barnett and Texas portion of the Haynesville shale), total water consumption in the power generation and mining sectors decreased by 1.1 billion gallons between August 2008 and December 2009. Water savings from the displacement of coal-fired power generation in ERCOT by natural gas power plants and from decreased lignite mining were largely offset by water consumption for the hydraulic fracturing of horizontal wells completed during the study period.

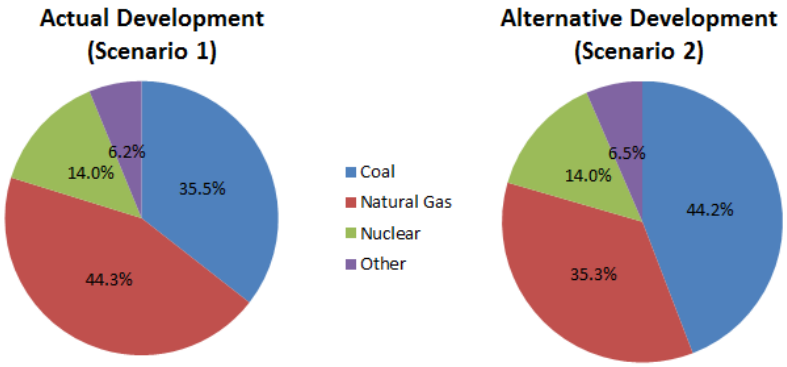

Figure 7-5. Fuel mix used in the modeled ERCOT generation during the August 2008 through September 2009 episode for the actual and alternative development scenarios.

The total consumptive water savings in ERCOT in this study (8.3 billion gallons) from the displacement of 37 TWh of coal-fired power generation by natural gas power plants is less than would be expected using factors from previous work (10.0 billion gallons; Grubert et al. 2012). This difference is due to assumptions in the previous work (Grubert et al. 2012) that all the marginal gas would be used for highly-efficient combined cycle plants and would only displace coal. The analysis presented in this work did not restrict the options to natural gas combined cycle plants; rather it included natural gas boilers -- which consume water at a higher rate than natural gas-combined cycle and coal EGUs (King et al. 2008a; Macknick et al. 2012) in some commonly-used cooling system configurations --, allowed for the possibility that power plants other than coal would be displaced, utilized time-resolved dispatching instead of average displacement assumptions, and only considered localized water consumption changes in electricity generation.

Due to the time delay between the increased water consumption at the point of extraction and subsequent decreased water consumption at the point of combustion, net

consumptive water savings in Texas in Scenario 1 were not realized until a minimum of fourteen months after the start of the study time frame (Figure 7-6). The delay in water consumption changes at the point of combustion was due to the relatively high price of natural gas in late 2008 compared to 2009. Major water savings in the power sector did not begin until February 2009 (Figure 7-6), when the price of natural gas in Texas decreased from $5.12 per MMBTU $4.32 per MMBTU (Figure 7-1). Thus, while there are net life-cycle consumptive water benefits to shale gas production and use in the electricity generation sector in place of coal-fired power plant generation (Grubert et al. 2012; Laurenzi et al. 2013), there is likely a delay between when the water is used in shale gas production and when net water use benefits would be realized.

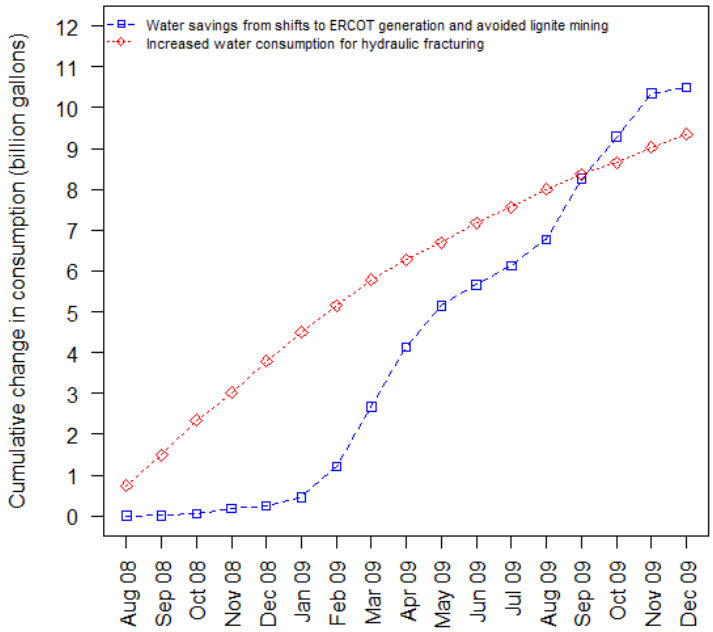

Figure 7-6. Comparison of the change in cumulative water consumption used in hydraulic fracturing of horizontal gas wells in the Barnett shale and the Texas part of the Haynesville shale to cumulative consumptive water savings in the electricity generation and lignite sectors. Note that the point of intersection in September 2009 indicates the month during which the cumulative savings in the power and lignite production sectors surpasses the net water consumed in hydraulic fracturing since the start of the study.

7.5.2 Net Spatial Impacts in Texas River Basins

Figure 7-7 shows the total change in consumptive water use for each river basin in Texas over the entire study timeframe, and Figure 7-8 shows cumulative consumptive water changes at a monthly time resolution for selected water basins with wells completed during the study period in the Barnett shale or the part of the Haynesville shale located in Texas. While overall water consumption decreased in Texas (Figure 7-4 and Table 7-4), water consumption increased in river basins whose boundaries included intense natural gas extraction or natural gas based power generation activities. River basins with increased water consumption in the actual natural gas prices and production scenario (Scenario 1) had several causes: 1) insufficient coal-fired power plant capacity to offset water consumption from natural gas production (Neches river basin), 2) increased use of natural-gas EGUs (Nueces-Rio Grande river basin), or 3) both (Trinity river basin).

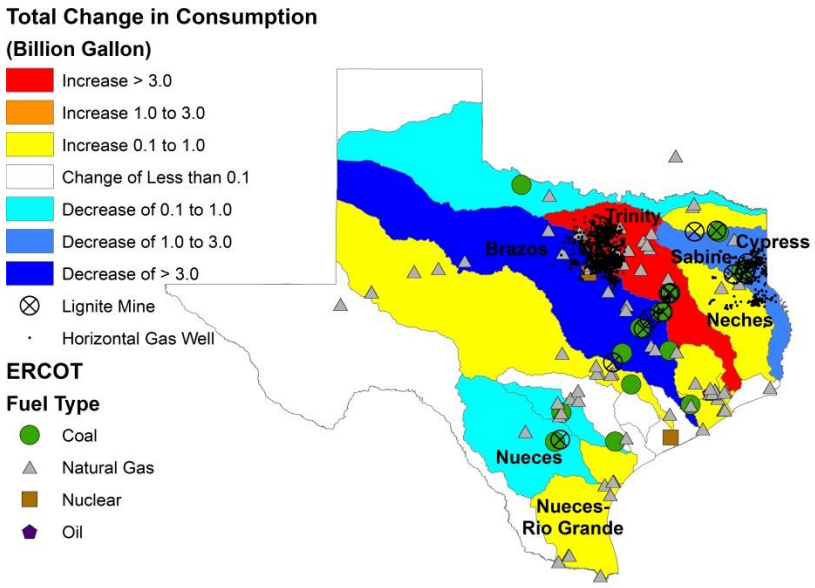

Figure 7-7. Change in total water consumption in Texas river basins during the August 2008 through December 2009 timeframe due to hydraulic fracturing in the Haynesville and Barnett shales and water use changes in the ERCOT and lignite production sectors. Red to yellow areas indicate regions with increased water consumption in the scenario with actual natural gas prices and production (Scenario 1) compared to the case in which natural gas prices in the state remained elevated (Scenario 2).

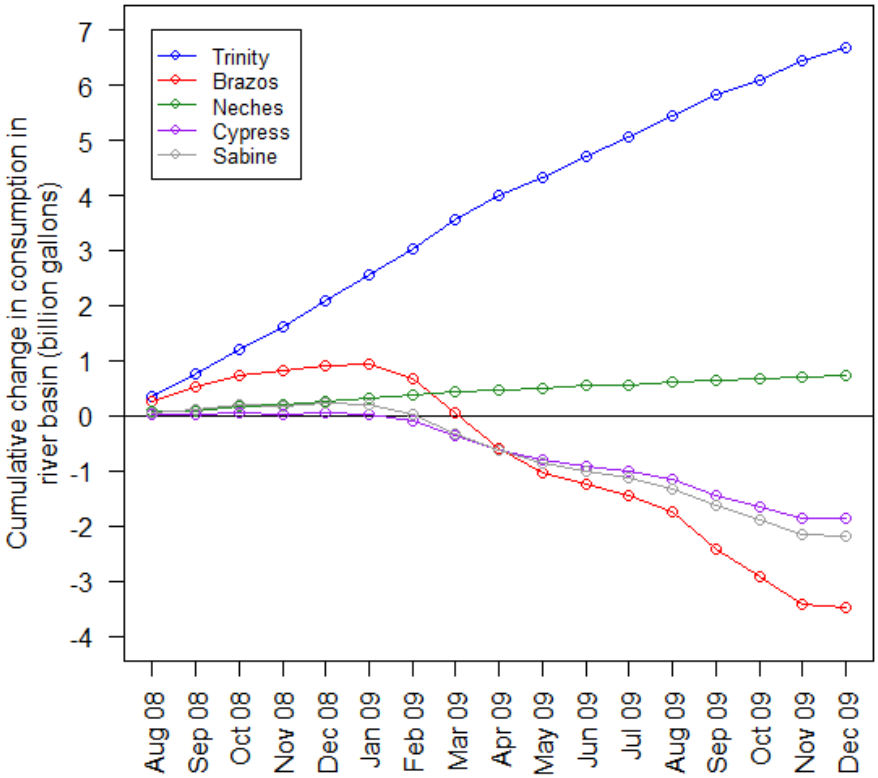

Figure 7-8. Change in cumulative water consumption (billion gallons) in selected river basins from the start of the study period (August 2008), reported monthly. Note that negative values indicate a net reduction in consumption in the river basin since the start of the study in the scenario with actual natural gas prices (Scenario 1) compared to the scenario (Scenario 2) with a constant $11.09 price for natural gas.

Within the Barnett Shale, the Brazos and Trinity river basins, which accounted for 24% and 65% of the wells completed during the study timeframe, had significantly different consumptive water impacts. As shown in Figure 7-8, water consumption in both river basins increased at the beginning of the study period as water was used for hydraulic fracturing. The direction of changes in consumptive water use in the two regions began to diverge as the price of natural gas (as shown in Figure 7-1) decreased. While both areas experienced increased water consumption from natural gas production and use in EGUs (Table 7-5), the Brazos river basin has significantly higher coal-fired

power plant installed capacity (5.5 GW compared to 1.2 GW) and generation (Table 7-5) than the Trinity river basin. When natural gas prices in the actual development scenario decreased, the reduction in water consumption at coal-fired power plants in the Brazos river basin offset increased water consumption from natural gas production and use in electricity generation. In the Trinity river basin, decreased water usage at coal-fired power plants was insufficient to offset increased water usage in the natural gas production sector. Similar patterns were observed in the Haynesville shale with the Sabine and Cypress river basins experiencing net decreases in consumptive water use while the Neches river basin had an increase in net consumptive water use during the study period. Thus, while several life-cycle assessments (Grubert et al. 2012; Laurenzi et al. 2013) have calculated that water use would decrease with shale gas production if it was used in natural-gas fired EGUs as a replacement for coal-fired power plant generation, not all regions have sufficient coal-fired power plant generation for this displacement. Thus, the potential combined consumptive water impacts of new natural gas production and use in the power sector are likely basin-specific.

It should be noted that results from the electricity generation model for ERCOT at the $11.09 per MMBTU natural gas price (Scenario 2) indicated that the capacity factor, which is defined as the fraction of nameplate generation that is utilized during a period, of coal-fired power plants would be 1. In practice, power plants do not usually operate at 100% capacity for the length of the study period examined in this work due to down time for scheduled maintenance and facility constraints. During historic periods with high natural gas prices and consumer demand for electricity, the utilization of coal-fired power generation capacity has been high. During July 2008 when the natural gas price for Texas power producers was at $11.09 per MMBTU, for example, the fleet of coal-fired power plants in ERCOT operated at 90% of its nameplate capacity (EIA 2013). By

comparison, the ERCOT coal-fired power generation was 86% of capacity in July 2009, when the price of natural gas was $3.69 per MMBTU (EIA 2013).

While other electricity generation models (Cohen et al. 2011) have included constraints on maximum capacity factor, that complexity has not been included in the PowerWorld model used in this study and other previously-published research (Alhajeri et al. 2011a; Pacsi et al. 2013a; Pacsi et al. 2013b) that was developed with a focus on characterizing transmission constraints within ERCOT. The model result of 100% utilization of coal generation capacity in Scenario 2 indicated that at the $11.09 per MMBTU price for natural gas, it would be financially feasible to operate any available coal-fired power plant at the maximum available capacity due to the relatively low fuel price compared to natural gas and that ERCOT would utilize such capacity. The development of a maximum capacity factor within the PowerWorld model for ERCOT electricity generation would likely lead to decreased estimates of consumptive water use from the power sector in Scenario 2 (and thus lower potential water savings for Scenario 1) due to increased utilization of natural-gas fired power plants (in particular, NG-CC plants as shown in Table 7-4) and decreased utilization of coal-fired power plants, but the development of such a model is beyond the scope of this work. This simplification might impact the precise magnitude of the outcomes discussed in this work but would not affect the trends or the central conclusions that there are likely spatial and temporal variations in consumptive water patterns occurring as a result of increased natural gas production and use in Texas.

River Basin	Water Consumption for Hydraulic Fracturing (Billion Gallons)		Water Consumption for Lignite Mining (Billion Gallons)		ERCOT Natural Gas EGUs				ERCOT Coal EGUs			
	Scenario 1	Scenario 2	Scenario 1	Scenario 2	Generation (TWh)		Water Consumption (billion gallons)		Generation (TWh)		Water Consumption (billion gallons)	
					Scenario 1	Scenario 2	Scenario 1	Scenario 2	Scenario 1	Scenario 2	Scenario 1	Scenario 2
Brazos	2.01	0.00	2.99	3.74	13.3	10.2	3.1	2.3	55.2	68.4	28.8	35.9
Trinity	5.45	0.00	0.92	1.15	35.6	27.6	6.6	5.1	11.5	14.3	3.3	4.1
Sabine	0.89	0.00	3.19	4.22	5.1	3.9	1.2	0.9	20.1	28.0	7.2	10.0
Cypress	0.28	0.00	0.61	0.79	0.1	0.1	0.0	0.0	18.3	23.4	4.0	5.1
Neches	0.72	0.00	0.00	0.00	0.1	0.0	0.0	0.0	0.0	0.0	0.0	0.0

Table 7-5. Net consumptive water use by category from August 2008 through December 2009 for selected river basins with natural gas production activities.

7.5.3 Implications for Other Production Regions

During a period of rapid shale gas development and use in the electricity generation sector in Texas, net water consumption in the state decreased slightly due to displacement of coal-fired power plant generation by natural gas EGUs, which tend to have less water intensive operation (King et al. 2008a). However, water consumption might increase in some areas where new natural gas production and natural gas based electricity generation is not locally offset by decreases in coal based electricity generation. Thus, there can be spatial and temporal variations in the impacts of shale gas development and use, which are important to consider, in addition to the overall supply chain impacts, when examining the potential impacts of shale gas development on water resources. The methodology outlined in this work could be applied to other regions, which would likely have different spatial distributions and water use intensities for power generation and fuel production.

For this work, the focus of the power sector analysis is on short-term, price-based changes in the dispatch order in ERCOT, before new power plants could be constructed. Over the long term, the retirement of older coal-fired power plants and the construction of new natural gas combined-cycle power plants in Texas, may also be a driver of changes in the spatial location and magnitude of cooling water consumption within the state. The long term driver may cause shifts in consumption at different spatial locations than the shifts observed in this analysis. Estimating the impact of retirements and new construction power plants, however, is beyond the scope of this work.

The conclusion that some river basins may experience increased water consumption, despite overall decreases in water consumption along the natural gas production and electricity generation supply chain has important implications in new natural gas development areas, including the Eagle Ford Shale. The Nueces-Rio Grande

and Nueces river basins in South Texas (see Figure 7-6) each contain parts of this play, and the changes in consumptive water use examined in these river basins were driven entirely by changes in ERCOT since the natural gas production in the area was minimal during the study period. Compared to Scenario 2, the consumptive water use in the actual natural gas prices scenario (Scenario 1) was 0.5 billion gallons less in the Nueces river basin and 0.5 billion gallons higher in the Nueces-Rio Grande basin. In the Nueces river basin, decreased consumption at a coal-fired power plant and its associated lignite mine were sufficient to offset increased consumption at natural gas-fired EGUs within the basin, and the consumptive water savings would be equivalent to the water requirements for the hydraulic fracturing of 104 wells in the area, assuming a play median assumption of 4.3 million gallons per well (Nicot et al. 2012). For the Nueces-Rio Grande river basin, however, net water consumption in the basin increased with lower natural gas prices (Scenario 1) due to increased utilization of natural gas-fired EGUs, and the basin does not have any lignite mines or coal-fired power plants. Thus, it is likely that increased natural gas production and use in the Nueces-Rio Grande basin would lead to increased overall consumption there.

Local water scarcity is an important consideration in determining the impact of changes in consumptive water use patterns in the electricity generation and mining sectors in Texas. It is possible that increasing water consumption for natural gas production in a water scarce region of Texas while saving water in the power generation sector in a water rich area of the state could both lead to water savings overall in the state and exacerbation of local water shortages. In addition, increased recycling of produced (flow-back) water from natural gas wells, which has traditionally been small in the Barnett Shale due to the availability of salt water injection wells (Nicot et al. 2014), could reduce the water footprint of hydraulic fracturing in the state.

Chapter 8: Summary and Recommendations

8.1 CONCLUSIONS

The primary objectives of this dissertation were to expand the UT/MIT Integrated Model framework to include analyses at the month to annual time scales, to include fine PM chemistry, and to add modules for water use and emissions from natural gas production activities. These objectives were accomplished in the context of several case studies for the ERCOT grid in Texas, including seasonal NO_x emissions trading schemes, the impacts of new natural gas development and increased utilization in the power sector, and on the potential for drought-based operation of the grid. The primary conclusions of this dissertation are as follows:

- The implementation of a $20,000 per ton NO_x emissions cost for emissions from ERCOT EGUs only on predicted high ozone days would be more cost effective than a seasonal emissions price of $10,000 per ton NO_x and would lead to larger ozone reductions during periods with high ozone concentrations.
- The potential ozone changes associated with NO_x emission reductions on previous days (the atmospheric memory effect) are much smaller in spatial extent and magnitude than additional NO_x emission reductions on desired days.
- In June 2006, ERCOT had sufficient underutilized capacity in order to shift ~10% of its base case electricity generation from regions with the worst drought conditions (south Texas) to other areas of the grid. The forgone cooling water consumption at these south Texas power plants would have been enough for the water needs of 360,000 Texans in the most drought-stricken areas.
- ERCOT could be used as a virtual water pipeline to shift electricity generation and its associated water use from areas with drought to areas with relatively more water availability. This strategy could be implemented rapidly and could change

based on the spatial location of drought. However, projects such as dry cooling and pipeline construction would be more feasible financially over the long term but would have longer implementation times.

- When the potential emission changes associated with natural gas production in the Barnett Shale in Texas are combined with potential price-based changes in the power sector (increased utilization of natural gas EGUs and decreased utilization of coal EGUs), the emissions changes from the power generation sector (rather than the natural gas production sector) are the primary driver of changes in regional ozone and fine PM sulfate concentrations.
- Modeling of increased emissions in the Barnett Shale with constant power sector emissions indicates that additional emissions (~19% increase) from natural gas production activities there would not have an adverse effect on ozone concentrations in the shale region due to the ozone formation regime present there.
- A similar analysis of the ozone impacts of increased natural gas development coupled with increased utilization in the power sector indicated the potential for trade-offs between ozone decreases in northeastern Texas that are driven by reductions in power sector emissions and ozone increases in the Eagle Ford Shale from production sector emissions.
- The ozone impacts of oil and gas development are likely region-specific, indicating that the air quality impacts of emissions in one region may not be indicative of the ozone effects in a different area.
- The consumptive water impacts of increased natural gas production and use in the power sector can differ between river basins, even within the same shale gas

production region, based on the local mix of power plants and natural gas production activities.

- Some river basins with shale gas production (and its associated water consumption for hydraulic fracturing) may experience increased consumptive water use even considering reductions in cooling water use at coal-fired power plants.

8.2 RECOMMENDATIONS

Recommendations for future work with the UT/MIT Integrated Model includes the following:

- Power plant efficiency as well as associated emission and water use rates can vary as a function of power plant output. The UT/MIT Integrated Model uses a constant heat rate for each EGU based on an annual average value. Future research could include a variable heat rate parameter if sufficient data were to become available.
- Power plants generally must be taken out of service for maintenance and other reasons. The UT/MIT Integrated model could be modified in future work to include constraints on seasonal or annual capacity factors for each power plant type.
- As more data emerges on upstream methane emissions associated with natural gas production, the UT/MIT Integrated model could be used to assess the combined GHG emission impacts of new natural gas development and use in the power sector in a similar manner to the air quality and cooling water analyses undertaken in this work.

- Lower natural gas prices have the potential to impact other sectors besides electricity generation. For example, home heating with oil could potentially be replaced by home heating with natural gas. Future research could examine the potential changes in air quality associated with switches such as this.
- Natural gas production in wet gas plays (such as the Bakken Shale in North Dakota and parts of the Eagle Ford Shale in south Texas) can also produce heavier hydrocarbons, which could be used as feed stocks for chemical processes. The shale condensate-based feedstock could potentially replace more traditional petroleum sources and could potentially even make different chemical processes economical. Changing the chemical processes may have GHG and air quality impacts that could be modeled with a module in the UT/MIT Integrated Model framework.

Appendix A: The Impact of Market-Based Environmental Prices for Power Plant NO_x Emissions on PM Formation in Texas

Pacsi, A.P.; Alhajeri, N. S.; McDonald-Buller, E. C.; Allen, D. T. *2012-A-319-AWMA*

A.1 INTRODUCTION

Electricity Generating Units (EGUs) are major sources of nitrogen oxides (NO_x) and sulfur dioxide (SO_2) emissions. For example, in Texas, electricity generation accounts for 30% of the NO_x emissions and 79% of the SO_2 emissions (EPA 2014b). Because of the role of NO_x and SO_2 in the formation of secondary particulate matter (PM), changes in EGUs emissions can influence PM concentrations. Shifting emissions away from EGUs burning higher sulfur fuels to those burning a lower sulfur fuel source reduces the amount of SO_2 available for oxidation to form particulate sulfate (PSO_4). EGU emissions of NO_x can result in the formation of particulate nitrates and also influence the availability of free radical oxidants, such as the hydroxyl radical, which in turn can influence the formation of particulate sulfate through the oxidation of SO_2, and the formation of secondary organic aerosol (SOA) through oxidation of organic species, such as terpenes. Changing the spatial and temporal pattern of EGU emissions can therefore influence the formation of PSO_4, particulate nitrate, and SOA.

Increasingly, emissions from EGUs are controlled using market based mechanisms. The cap-and-trade system associated with the Acid Rain Program of the US Environmental Protection Agency (EPA) allowed for individual companies to decide whether to meet new emissions requirements by installing new control technologies or by buying permits from facilities that are below their emissions caps (Burtraw et al. 1999). Overall, the Acid Rain Program reduced SO_2 emissions by half since 1980 (EPA 2011).

Most recently, market based approaches are proposed to continue through programs such as the Cross-State Air Pollution Rule (CSAPR). The CSAPR would require that EGUs in 27 states in the Eastern United States reduce overall power plant emissions of SO_2 and NO_x by 73% and 54%, respectively, by 2014 (EPA 2012d). While the CSAPR was still being considered in the courts as this document was being written, emission trading in general can be expected to continue as a method for reducing emissions from EGUs (Nobel et al. 2001). This Appendix will examine the effects of various pricing levels on emission reductions, and subsequent PM formation, in the grid served by the Electricity Reliability Council of Texas (ERCOT). The issues to be considered in this Appendix are, (i) the spatial distribution of changes in PSO_4 and SOA concentrations that would be expected due to switching from high emission EGUs to lower emission EGUs (no additional controls). In addition, the relative contributions of SO_2 emission reductions and decreased conversion of SO_2 to PSO_4 (due to NOx emission reductions) will be reported.

For the ERCOT grid, Alhajeri et al. (2011a) found that a 50% reduction in NO_x emissions could be achieved through NO_x price caps of $0-50,000 per ton, but that NO_x pricing above $25,000 per ton yielded diminishing returns. While Alhajeri et al. (2011a) calculated the overall emission reductions of NO_x, no photochemical modeling was included in the study. Since ozone (Nobel et al. 2001) and secondary PM formation do not vary linearly with NO_x reductions, this study will apply photochemical modeling to the NO_x trading scenarios reported by Alhajeri et al. (2011a). The impact of a $25,000 per ton price for NO_x emissions with a $500 per ton price for SO_2 emissions will be reported, since increases in emission price beyond $25,000 produced relatively little change in emissions for Texas.

A.2 MATERIALS AND METHODS

A.2.1 Modeling Scenario

This work is based on photochemical modeling of the period from May 31-June 15, 2006 that was developed by the Texas Commission on Environmental Quality (TCEQ) for use in determining compliance for 8-hour ozone for the Houston-Galveston-Brazoria (HGB) region of Texas (TCEQ 2012b). The TCEQ developed the base case (without NO_x trading considerations) for use with the CAMx Version 4.53 (ENVIRON 2011), which is the EPA approved regional photochemical model that the state of Texas uses for regulatory compliance. The modeling domain includes the following resolutions: 36-km eastern United States, 12-km eastern Texas, and 4-km HGB area. The CF subroutine for PM chemistry was used with CAMx since it is compatible with Plume-in-Grid (PiG) treatment for large EGU plumes. The dispatching of electricity generation under various NO_x pricing scenarios was modeled using PowerWorld (2012), which uses non-linear optimization algorithms to minimize total cost of electricity generation while accounting for transmission and EGU capacity constraints. The case study used in this work was June 1, 2006, which was an elevated ozone day during the episode.

A.2.2 Low Level Emissions

The TCEQ gas phase inventory for the June 2006 episode (TCEQ 2012b) was used as the base for the low level inventory, which included vehicular emissions. A primary PM and PM precursor (SO_2) inventory (Simon et al. 2008) was added to the gas phase emissions from the TCEQ. For low-level SO_2 emissions, the values from the PM inventory were multiplied by a constant factor of 0.094 to account for reductions in sulfur content of diesel fuel that occurred after the development of the PM inventory. The same low level inventory was used for both the base case and $25,000 per ton NO_x scenarios.

A.2.3 Elevated Point Source Emissions

The gas phase, non-SO_2 point source inventory for the state of Texas was redeveloped to match the base case from the TCEQ. Additional PM (Simon et al. 2008) and SO_2 (TCEQ 2014a) inventories were added to the gas phase emissions developed by the TCEQ for EGUs within Texas. For the $25,000 per ton NO_x scenario on June 1, the gas-phase emissions (NO_x, VOC, CO, and SO_2) at each EGU in the ERCOT grid for each hour were scaled from the base case based on the ratio of electricity generation at that facility in the $25,000 per ton case to the base case.

A.3 Results and Discussions

In order to examine the relative magnitude of the PM effects related to direct emissions reductions versus indirect oxidant reductions, four scenarios were modeled using CAMx, which are described in Table A-1.

Scenario Name	Type of NO_x Emissions	Type of SO_2 Emissions	Daily Tons of NO_x	Daily Tons of SO_2	Percent Reduction of NO_x	Percent Reduction of SO_2
Base case	TCEQ Base case	TCEQ Base case	443.51	1490.42	-	-
25k_Total	$25,000 NO_x price	$25,000 NO_x price	210.24	362.69	52.6%	75.7%
25k_oxidant	TCEQ Base case	$25,000 NO_x price	443.51	362.69	-	75.7%
25k_SO2	$25,000 NO_x price	TCEQ Base case	210.24	1490.42	52.6%	-

Table A-1. CAMx scenario emissions from Texas EGUs for June 1, 2006.

The base case and 25k_total scenarios represent conditions that might exist in the atmosphere, while the 25k_oxidant and 25k_SO2 scenarios are model constructs designed to examine the relative roles of SO_2 emission reductions and changes in the oxidation of secondary PM precursors on PM formation.

A.3.1 Particulate Sulfate Formation

The maximum decrease in PM sulfate formation (indicated by positive values in Figure A-1) occurred between 3PM and 4PM in each of the scenarios described in Table A-1. The 25k_Total scenario (upper left) shows that PSO4 decreases on the order of 1-3 µg/m³ across the regions where most of the coal fired power plants in the state are located. Highly localized maximum decreases on the order of 8 µg/m³ are also shown. The reductions can be driven both by decreases in available oxidants (lower right) and decreased emissions of SO_2 from EGUs (lower left). However, changes caused by oxidant availability are lower in magnitude and encompass smaller regions than changes in SO_2 concentrations. Finally, the magnitude of the changes in the 25k_Total case (upper left) is smaller than combined magnitude of the 25k_oxidant and 25k_SO2 cases (upper right).

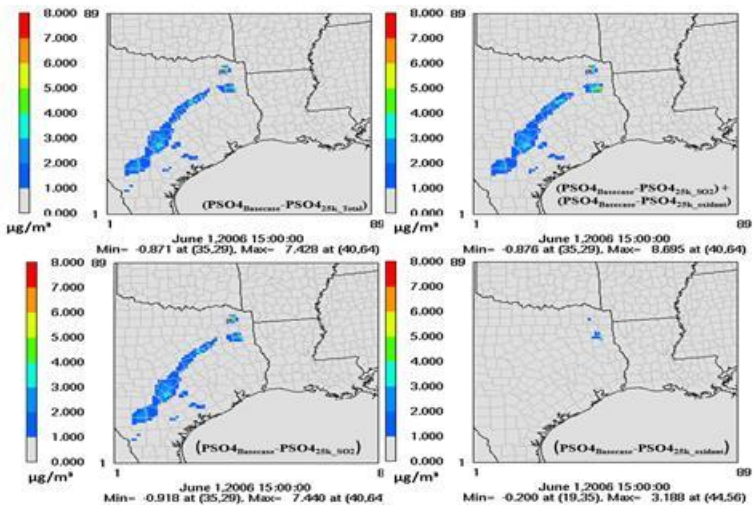

Figure A-1. PSO_4 Decreases from Base Case for June 1, 2006 at 15:00.

A.3.2 Secondary Organic Aerosol Formation

SOA formation exhibits highly localized increases (negative numbers in Figure A-2) and decreases (positive numbers in Figure A-2) with a magnitude of less than ± 1

µg/m³ (right box) in the 25k_Total Case from the base case. The changes tend to occur in the forested region of northeastern Texas. The region exhibiting increased SOA formation has higher concentrations of NO_x and SO_2 and lower concentrations of terpenes compared to the area exhibiting a decrease in SOA during the same hour.

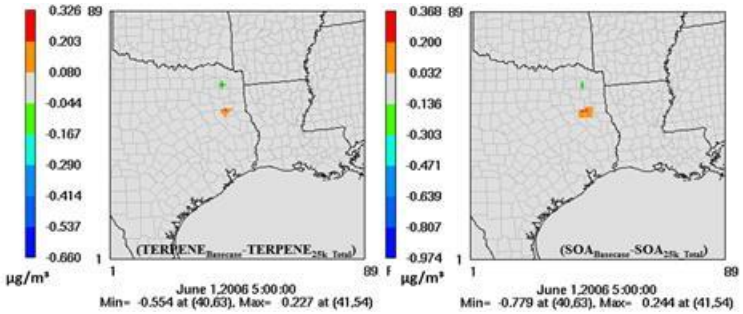

Figure A-2. SOA reductions from base case for June 1, 2006, at 5:00AM.

A.4 SUMMARY

Changing EGU emissions can have an impact on the formation of SOA and secondary PSO_4 in Texas. Previous research indicated that changes in sulfate aerosol formation could be driven both by changes in available oxidant levels (from changes in NO_x emissions) and from changes in SO_2 emissions from EGUs. While both these changes can have effects on the regional PSO_4 concentrations, the 1-3 µg/m³ regional reductions in particulate sulfate concentrations associated with a $25,000 per ton NO_x and $500 per ton SO_2 scenario were dominated by reductions in SO_2 emissions. As with previous research, the effects on SOA formation were both lower in magnitude (less than 1 µg/m³), more localized than the effects on sulfate aerosol, and dominated by terpene chemistry.

References

Alamo Area Council of Governments (AACOG). *Oil and Gas Emissions Inventory, Eagle Ford Shale, Technical Report* [Online]. **2014**, http://www.aacog.com/DocumentCenter/View/19069 (Accessed June 28, 2014).

Alhajeri, N. S.; Donohoo, P.; Stillwell, A. S.; King, C. W.; Webster, M. D.; Webber, M. E.; Allen, D. T. Using market-based dispatching with environmental price signals to reduce emissions and water use at power plants in the Texas grid. *Environmental Research Letters*. **2011a**, *6*, doi: 10.1088/1748-9326/6/4/044018.

Alhajeri, N. S.; McDonald-Buller, E. C.; Allen, D. T. Comparison of air quality impacts of fleet electrification and increased use of biofuels. *Environmental Research Letters*. **2011b**, *6*, doi: 10.1088/1748-9326/6/2/024011.

Alhajeri, N. S. Sustainable energy systems: the environmental footprints of electricity generation systems – mechanisms for managing electricity, water resources, and air quality. Ph.D. Dissertation, University of Texas at Austin, 2012.

Allen, D.T.; Torres, V. M.; Thomas, J.; Sullivan, D. W.; Harrison, M.; Hendler, A.; Herndon, S. C.; Kolb, C.E.; Fraser, M. P.; Hill, A. D.; Lamb, B. K.; Miskimins, J.; Sawyer, R. F.; Seinfeld, J. H. Measurements of methane emissions at natural gas production sites in the United States. *Proceedings of the National Academy of Sciences of the United States of America*, **2013**, doi: 10.1073/pnas.1304880110.

Alvarez, R. A.; Pacala, S. W.; Winebrake, J. J.; Chameides, W. L.; Hamburg, S. P. Greater focus on needed methane leakage from natural gas infrastructure. *Proceedings of the National Academy of Sciences of the United States of America*, **2012**, *109* (17), 6435-6440.

Andreadis K. M.; Clark E. A.; Wood A. W.; Hamlet A. F.; Lettenmaier D. P. Twentieth-century drought in the conterminous United States. *Journal of Hydrometeorology*. **2005**, *6*, 985-1001.

Anenberg, S. C.; Horowitz, L. W.; Tong, D. Q.; West, J. J. An estimate of the global burden of anthropogenic ozone and fine particulate matter on premature human mortality using atmospheric modeling. *Environmental Health Perspectives*. **2010**, *118* (9), 1189-1195.

Averyt, K.; Macknick, J.; Rogers, J.; Madden, N.; Fisher, J.; Meldrum, J.; Newmark, R. Water use in electricity in the United States: an analysis of reported and calculated water use information for 2008. *Environmental Research Letters*. **2013**, *8*, doi:10.1088/1748-9326/8/1/015001.

Barbot, E.; Vidic, N. S.; Gregory, K. B.; Vidic, R. D. Spatial and temporal correlation of water quality parameters of produced waters from Devonian-Age shale following hydraulic fracturing. *Environmental Science and Technology*. **2013**, *47*, 2562-2569.

Bell, M. I.; McDermett, A.; Zeger, S. I.; Samet, J. M.; Dominici, F. Ozone and short-term mortality in 95 urban communities, 1987-2000. *Journal of the American Medical Association*. **2004**, *292*, 2372-2378.

Bell, M. L.; Peng, R. D.; Dominici, F. The exposure curve for ozone and risk of mortality and the adequacy of current ozone regulations. *Environmental Health Perspectives*. **2006**, *114* (4), 532-536.

Bergin, M. S.; Shih, J. S.; Krupnick, A. J.; Boylan, J. W.; Wilkinson, J. G.; Odman, M. T.; Russell, A. G. Regional air quality: local and interstate impacts of NO_x and SO_2 emissions on ozone and fine particulate matter in the eastern United States. *Environmental Science and Technology*. **2007**, *41*, 4677-4689.

Brandt, A. R.; Heath, G. A.; Kort, E. A.; O'Sullivan, F.; Petron, G.; Jordaan, S. M.; Tans, P.; Wilcox, J.; Gopstein, A. M.; Arent, D.; Wofsy, S.; Brown, N. J.; Bradley, R.; Stucky, G. D.; Eardley, D.; Hariss, R. Methane leaks from North American natural gas systems. *Science*, **2014**, *343*, 733-735.

Brock, C. A.; Wshenfelder, R. A.; Trainer, M.; Ryerson, T. B.; Wilson, J. C.; Reeves, J. M.; Huey, L. G.; Holloway, J. S.; Parrish, D. D.; Hubler, G.; Fehsenfeld, F. C. Particle growth in the plumes of coal-fired power plants. *Journal of Geophysical Research*. **2002**, *107*, doi:10.1029/2011JD001062.

Burnett R. T.; Steib D.; Brook, J. R.; Cakmak, S.; Dales, R.; Raizenne, M.; Vincent, R.; Dann, T. Associations between short-term changes in nitrogen dioxide and mortality in Canadian cities. *Archives of Environmental Health*. **2004**, *59*, 228-236.

Burtraw, D.; Mansur, E.; Environmental effects of SO_2 trading and banking. *Environmental Science and Technology.* **1999**, *33*, 3489-3494.

Burtraw, D.; Palmer, K.; Bharvirkar, R.; Paul, A. Cost-effective reduction of NO_x emissions from electricity generation. *Journal of the Air & Waste Management Association*. **2001**, *51* (10), 1478-1489.

Burtraw, D.; Evans, D. A.; Krupnick, A.; Palmer, K.; Toth, R. *Economics of pollution trading for SO_2 and NO_x* [Online]. Resources for the Future: Washington, DC, 2005. http://www.rff.org/documents/rff-dp-05-05.pdf (Accessed June 18, 2014).

Butler, T. J.; Vermeylen, F. M.; Rury, M.; Likens, G. E.; Lee, B.; Bowker, G. E.; McCluney, L. Response of ozone and nitrate to stationary source NO_x emission reductions in the eastern USA. *Atmospheric Environment*. **2011**, *45*, 1084-1094.

Carter, W. P. L.; Seinfeld, J. H. Winter ozone formation and VOC incremental reactivities in the Upper Green River Basin of Wyoming. *Atmospheric Environment*, **2012**, *50*, 255-266.

Cass, G. R. Sulfate air quality control strategy design. *Atmospheric Environment*. **1980**, *15(7)*, 1227-1249.

Chen, Y.; Hobbs, B. F. An oligopolistic power market model with tradable NO_x permits. *IEEE Transactions on Power Systems.* **2005**, *20* (1), 119-120.

Chestnut, L. G.; Mills, D. M. A fresh look at the benefits and costs of the US acid rain program. *Journal of Environmental Management.* **2005**, *77*, 252-266.

Chiyangwa, D. K. Strategic investment in power generation under uncertainty Electricity Reliability Council of Texas. Master's Thesis, Massachusetts Institute of Technology, 2010.

Clean Air Science Advisory Committee (CASAC). Response to charge questions on the reconsideration of the 2008 National Ambient Air Quality Standards. 2012.

Clean Air Science Advisory Committee (CASAC). Integrated science assessment for particulate matter. 2009.

Cohen, S. M.; Chalmers H. L.; Webber, M. E. Comparing post-combustion CO_2 capture operation at retrofitted coal plants in the Texas and Great Britain electric grids. *Environmental Research Letters*. **2011**, *6*, doi:10.1088/1748-9326/6/2/024001.

Cook E. R.; Seager R.; Cane M. A.; and Stahle D. W. North American drought: Reconstructions, causes, and consequences *Earth-Science Reviews.* **2007**, *81*, 93-134.

Dai, A.; Trenberth, K. E.; Qian, T. A global dataset of Palmer Drought Severity Index for 1870-2002: Relationship with soil moisture and effects on surface warming. *Journal of Hydrometeorology.* **2004**, *5*, 1117-1130.

Daneshi, H.; Srivastava, A. K. ERCOT electricity market: Transition from zonal to nodal market operation. *Power and Energy Society General Meeting 2011*. **2011**, 1-7.

Daum, P. H.; Kleinman, L. I.; Springston, S. R.; Nunnermacker, L. J.; Lee, Y. N.; Weinstein-Lloyd, J.; Zheng, J; Berkowitz, C. M. A comparison study of O_3 formation in the Houston urban and industrial plumes during the 2000 Texas Air Quality Study. *Journal of Geophysical Research,* **2003**, *108*, doi:10.1029 /2003JD003552.

DeGouw, J. A.; Parrish, D. D.; Frost, G. J.; Trainer, M. Reduced emissions of CO_2, NO_x, and SO_2 from U.S. power plants owing to switch from coal to natural gas with combined cycle technology. *Earth's Future*. **2014**, *2*, doi: 10.1002/ 2013EF000196.

Devlin, R.B.; Raub, J. A.; Folinsbee L. J. Health effects of ozone. *Science & Medicine.* **1997,** *4*, 8-17.

Dockery, D. W.; Pope, C. A. Acute respiratory effects of particulate air pollution. *Annual Review of Public Health*. **1994**, *15*, 107-132.

Edwards, P. M.; Young, C. J.; Aikin, K.; deGouw, J.; Dube, W.P.; Geiger, F.; Gilman, J.; Helmig, D.; Holloway, J. S.; Kercher, J.; Lerner, B.; Martin, R.; McLaren, R.;

Parish, D. D.; Peischl, J.; Roberts, J. M.; Ryerson, T. B.; Thorton, J.; Warnecke, C.; Williams, E. J.; Brown, S. S. Ozone photochemistry in an oil and natural gas extraction region during winter: simulations of a snow-free season in the Uintah Basin, Utah. *Atmospheric Chemistry and Physics*, **2013**, *13*, 8955-8971.

Electricity Reliability Council of Texas (ERCOT). *Balancing energy services daily report archive* [Online]. 2006a. http://www.ercot.com/gridinfo/zonal_archives (Accessed June 3, 2014).

Electricity Reliability Council of Texas (ERCOT). *Report of existing and potential electric system constraints and needs* [Online]. 2006b. http://www.ercot.com /content/news/presentations/2006/2006_ERCOT_Reports_Transmission_Constrai nts_and_Needs.pdf (Accessed June 3, 2014).

Electricity Reliability Council of Texas (ERCOT). *2006 Annual Report* [Online]. 2007. http://www.ercot.com/content/news/presentations/2007/2006_Annual_Report.pdf (Accessed June 18, 2014).

Electricity Reliability Council of Texas (ERCOT). *NERC Interconnections* [Online]. 2009. http://www.ercot.com/news/mediakit/maps/index (Accessed June 3, 2014).

Electricity Reliability Council of Texas (ERCOT). *ERCOT Quick Facts* [Online]. 2012. http://www.ercot.com/content/news/presentations/2012/ERCOT_Quick_Facts_Jul y_%202012.pdf (Accessed June 3, 2014).

Electricity Reliability Council of Texas (ERCOT). *Wind Integration* [Online]. 2014a. http://www.ercot.com/gridinfo/generation/windintegration (Accessed June 3, 2014).

Electricity Reliability Council of Texas (ERCOT). *Quick Facts* [Online]. 2014b. http://www.ercot.com/content/news/presentations/2014/ERCOT_Quick_Facts_05 2014.pdf (Accessed June 19, 2014).

Entrekin, S.; Evans-White, M.; Johnson, B.; Hagenbuch, E. Rapid expansion of natural gas development poses a threat to surface waters. *Frontiers in Ecology and the Environment*. **2011**, *9* (9), 503-511.

ENVIRON International Corporation. *Comprehensive Air Quality Model with Extensions (CAMx)*. Version 4.53; Environ International Corporation: Novato, California, 2011.

ESRI. *ArcGIS*. Version 10.1; ESRI: Redlands, California, 2012.

Farrell, A.; Carter, R.; Raufer, R. The NO_x budget: market-based control of troposperic ozone in the northeastern United States. *Resource and Energy Economics*. **1999**, *21*, 103-124.

Feely, T. J.; Skone, T. J.; Stiegel, G. J.; McNemar, A.; Nemeth, M.; Schimmoller, B.; Murphy, J. T.; Manfredo, L. Water: A critical resource in the thermoelectric power industry. *Energy*. **2008**, *33*, 1-11.

Fowlie, M. Emissions trading, electricity restructuring, and investment in pollution abatement. *American Economic Review*, **2010**, *100*, 837-869.

Frost, G. J.; McKeen, S. A.; Trainer, M.; Ryerson, T. B.; Neuman, J. A.; Roberts, J.M.; Swanson, A.; Holloway, J.S.; Sueper, D. T.; Fortin, T.; et al. Effects of changing power plant NO_x emissions on ozone in the eastern United States: Proof of concept. *Journal of Geophysical Research.* **2006**, *111*, D12306.

Gégo, E.; Gilliland, A.; Godowitch, J.; Rao, S. T.; Porter, P. S.; Hogrefe, C. Modeling analyses of the effects of changes in nitrogen oxides emissions from the electric power sector on ozone levels in the eastern United States. *Journal of the Air & Waste Management Association.* **2008**, *58*, 580-588.

Godowitch, J. M.; Gilliland, A. B.; Draxler, R. R.; Rao, S. T. Modeling assessment of point source NO_x emissions reductions on ozone air quality in the eastern United States. *Atmospheric Environment.* **2008**, *42*, 87-100.

Grubert, E. A.; Beach, F. C.; Webber, M. E. Can switching fuel save water? A life cycle quantification of freshwater consumption for Texas coal and natural gas-fired electricity. *Environmental Research Letters*. **2012**, *7*, doi:10.1088/1748-9326/7/4/045801.

Gryparis, A.; Forsberg, B.; Katsouyanni K.; Analitis, A.; Touloumi, G.; Schwartz, J.; Samolt, E.; Medina, S.; Anderson, H. R.; Niclu, E. M.; Wichmann, H. E.; Kriz, B.; Kosnik, M.; Skorkovsky, J.; Vonk, J. M.; Dortbudak, Z. Acute effects of ozone on mortality from the "Air Pollution and Health: A European Approach" project. *American Journal of Respiratory and Critical Care Medicine*. **2004**, *170*, 1080-1087.

Hightower, M.; Pierce, S. A. The energy challenge. *Nature*. **2008**, *452* (20), 285-286.

Howarth, R. W.; Santoro, R.; Ingraffea, A. Methane and the greenhouse-gas footprint of natural gas from shale formations. *Climate Change*. **2011**, *106*, 679-690.

Huston, S. S.; Barber, N. L.; Kenny, J. F.; Linsey, K. S.; Luima, D. S.; Maupin, M. A. *Estimated use of water in the United States in 2000* [Online]; U. S. Geological Survey: Reston, VA, 2004. http://pubs.usgs.gov/circ/2004/circ1268/ (Accessed June 3, 2014).

IHS. *US Well Data*; IHS: Englewood, Colorado, 2013.

Ito K.; De Leon, S. F.; Lippmann, M. Associations between ozone and daily mortality. *Epidemiology*. **2005**, *16*, 446-457.

Jackson, R. B.; Down, A.; Phillips, N. G.; Ackley, R. C.; Cook, C. W.; Plata, D. L.; Zhao, K. Natural gas pipeline leaks across Washington, DC. *Environmental Science and Technology*, **2014**, *48* (3), 2051-2058.

Jaramillo, P.; Griffin, W. P.; Matthews, H. S. Comparative life-cycle air emissions of coal, domestic natural gas, LNG, and SNG for electricity generation. *Environmental Science and Technology*. **2007**, *41*, 6290-6296.

Jiang, M.; Griffin, W. P.; Hendrickson, C.; Jaramillo, P., Van Briesen, J.; Venkatesh, A.; Life cycle greenhouse gas emissions of Marcellus shale gas. *Environment Research Letters*. **2011**, *6*, 034014.

Kargbo, D. M.; Wilhelm, R. G.; Campbell, D. J. Natural gas plays in the Marcellus Shale: challenges and potential opportunities. *Environmental Science and Technology.* **2010**, *44*, 5679-5694.

Kemball-Cook, S.; Bar-Ilan, A.; Grant, J.; Parker, L.; Jung, J.; Santamaria, W.; Mathews, J.; Yarwood, G. Ozone impacts of natural gas development in the Haynesville shale. *Environmental Science and Technology*, **2010**, *44* (24), 9357-9363.

Kenny, J. F.; Barber, N. L.; Hutson, S. S.; Linsey, K. S.; Lovelace, J. K.; Maupin, M. A. *Estimated use of water in the United States in 2005* [Online]; U.S. Geological Survey Circular: Reston, Virginia, 2009. http://pubs.usgs.gov/circ/1344/pdf/c1344.pdf (accessed June 3, 2014).

King, C. W.; Holman, A. S.; Webber, M. E. Thirst for energy. *Nature Geoscience*. **2008a**, *1*, 283-286.

King, C. W.; Duncan, I.; Webber, M. E. *Water demand projections for power generation in Texas* [Online]; Bureau of Economic Geology: Austin, Texas, 2008b. https://www.twdb.texas.gov/publications/reports/contracted_reports/doc/0704830756ThermoelectricWaterProjection.pdf (accessed June 3, 2014).

King, C. W.; Webber, M. E. Water intensity of transportation. *Environmental Science and Technology*. **2008c,** *42* (21), 7866-7872.

Laurenzi, I. J.; Jersey, G. R. Life cycle greenhouse gas emissions and freshwater consumption of Marcellus shale gas. *Environmental Science and Technology*. **2013**, *47* (9), 4896-4903.

Lin S.; Liu X.; Le L. H.; Hwang, S. A.; Chronic exposure to ambient ozone and asthma hospital admissions among children. *Environmental Health Perspectives*. **2008**, *116*, 1725-1730.

Litovitz, A.; Curtright, A.; Abramzon, S.; Burger, N.; Samaras, C. Estimation of regional air-quality damages from Marcellus Shale natural gas extraction in Pennsylvania. *Environmental Research Letters*. **2013**, *8*, doi:10.1088/1748-9326/8/1/014017.

Macknick, J.; Newmark, R.; Heath, G.; Hallett, K. C. Operational water consumption and withdrawal factors for electricity generating technologies: a review of existing literature. *Environmental Research Letters*. **2012**, *7*, doi:10.1088/1748-9326/7/4/045802.

Manuel, J. Drought in the Southeast: Lessons for water management. *Environmental Health Perspectives*. **2008**, *116* (4), A168-A171.

Mauzerall, D. L.; Sultan, B.; Kim, N.; Bradford, D. F. NO_x emissions from large point sources: variability in ozone production, resulting health damages, and economic costs. *Atmospheric Environment*. **2005**, *39*, 2851-2866.

Mesbah, S. M.; Hakami, A.; Schott, S. Improving NO_x cap-and-trade system with adjoint-based emission exchange rates. *Environmental Science & Technology*. **2012**, *46*, 11905-11912.

Mesbah, S. M.; Hakami, A.; Schott, S. Optimal ozone reduction policy design using adjoint-based NO_x marginal damage information. *Environmental Science & Technology.* **2013**, *47*, 13528-13535.

Mueller, S. F.; Bailey, E. M.; Kelsoe, J. J. Geographic sensitivity of fine particle mass to emissions of SO_2 and NO_x. *Environmental Science and Technology*. **2004**, *38*, 570-580.

Muller, N. Z.; Mendelsohn, R. Efficient pollution regulation: getting the prices right. *American Economic Review.* **2009**, *99* (5), 1714-1739.

Murray, K. E. State-scale perspective on water use and production associate with oil and gas operations, Oklahoma, U.S. *Environmental Science and Technology*, **2013**, *47* (9), 4918-4925.

Nam, J.; Kimura, Y.; Vizuette, W.; Murphy, C.; Allen, D. T. Modeling the impacts of emissions events on ozone formation in Houston, Texas. *Atmospheric Environment*. **2006**, *40* (28), 5329-5341.

National Climatic Data Center (NCDC). *U.S. Palmer Drought Indices*. http://www.ncdc .noaa.gov/oa/climate/research/prelim/drought/palmer.html (Accessed June 3, 2014).

National Renewable Energy Laboratory (NREL). *U.S. Lifecycle Inventory Database* [Online]. Version 1.5.4; NREL: Golden, Colorado, 2013.

Newcomer, A.; Blumsack, S. A.; Apt, J.; Lave, L. B.; Morgan, M. G. Short run effects of a price on carbon dioxide emissions from U.S. electric generators. *Environmental Science and Technology*. **2008**, *42* (9), 3139-3144.

Newell, R. G.; Stavins, R. N. Cost heterogeneity and the potential savings from market-based policies. *Journal of Regulatory Economics.* **2003**, *23* (1), 43-59.

Nicot, J. P.; Scanlon, B. R. Water use for shale gas production in Texas, U.S. *Environmental Science and Technology*. **2012**, 7, 3580-3586.

Nicot, J. P.; Scanlon, B. R.; Ready, R. C.; Costley, R. A. Source and fate of hydraulic fracturing water in the Barnett Shale: A historic perspective. *Environmental Science and Technology.* **2014**, *48* (4), 2464-2471.

Nielsen-Gammon, J. W. The 2011 Texas drought. *Texas Water Journal*. **2012**, *3*, 59-95.

Nobel, C. E.; McDonald-Buller, E. C.; Kimura, Y.; Allen, D. T. Accounting for spatial variability in ozone productivity in NO_x emissions trading. *Environmental Science and Technology*. **2001**, *35*, 4397-4407.

Nobel, C. E.; McDonald-Buller, E. C.; Kimura, Y.; Lumbley, K. E.; Allen, D. T. Influence of population density and temporal variation in emissions on the air quality benefits of NO_x emissions trading. *Environmental Science & Technology*. **2002**, *36*, 3465-3473.

Osborn, S. G.; Vengosh, A.; Warner, N. R.; Jackson, R. B. Methane contamination of drinking water accompanying gas-well drilling and hydraulic fracturing. *Proceedings of the National Academy of Sciences*. **2011**, *108 (20)*, 8172-8176.

Pacsi, A. P.; Alhajeri, N. S.; Webster, M. D.; McDonald-Buller, E. C.; Allen, D. T. The impact of market-based environmental prices for power plant NO_x emissions on PM formation in Texas. In *Proceedings of the Air & Waste Management Association's (A&WMA) 105th Annual Conference & Exhibition*, San Antonio, TX, United States, June 19-22, 2012; 2012-A-319-AWMA.

Pacsi, A. P.; Alhajeri, N. S.; Zavala-Araiza, D.; Webster, M. D.; Allen, D. T. Regional air quality impacts of increased natural gas production and use in Texas. *Environmental Science and Technology*. **2013a**, *47*, 3521-3527.

Pacsi, A. P.; Alhajeri, N. S.; Webster, M. D.; Webber, M. E.; Allen, D. T. Changing the spatial location of electricity generation to increase water availability in areas with drought: a feasibility study and quantification of air quality impacts in Texas. *Environmental Research Letters*. **2013**, *8*, doi:10.1088/1748-9326/8/3/035029.

Peterson, J. R.; Rochelle, G. T.; Aqueous reaction of fly ash and $Ca(OH)_2$ to produce calcium silicate absorbent for flue gas desulfurization. *Environmental Science and Technology*. **1988**, *22* (11), 1299-1304.

Pope, C. A.; Burnett, R. T.; Thun, M. J.; Calle, E. E.; Krewski, D.; Ito, K.; Thurston, G. D. Lung cancer, cardiopulmonary mortality, and long-term exposure to fine particulate air pollution. *Journal of the American Medical Association*. **2002**, *287* (9), 1132-1141.

PowerWorld Corporation. *PowerWorld Simulator*. Version 16.1; PowerWorld Corporation: Champaign, IL, 2012.

Rahm, B. G.; Riha, S. J. Towards strategic management of shale gas development: Regional, collective impacts on water resources. *Environmental Science & Policy*. **2012**, *17*, 12-23.

Rahm, D. Regulating hydraulic fracturing in shale gas plays: The case of Texas. *Energy Policy*. **2011**, *39*, 2974-2981.

Rieder, H. E.; Fiore, A. M.; Polvani, L. M.; Lamarque, J. F.; Fang, Y. Changes in the frequency and return level of high ozone pollution events over the eastern United States following emissions controls. *Environmental Research Letters*. **2013**, *8*, doi:10.1088/1748-9326/8/1/014012.

Ruiz-Alsop, R.; Rochelle, G. Coprecipitation of organic acids with calcium sulfite solids. *Industrial & Engineering Chemistry Research*. **1988**, *27*, 2123-2126.

Russell, M.; Allen, D. T.; Collins, D. R.; Fraser, M. P. Daily, seasonal, and spatial trends in $PM_{2.5}$ mass and composition in southeast Texas. *Aerosol Science and Technology*. **2004**, *38* (1), 14-26.

Scanlon, B. R.; Reedy, R. C.; Duncan, I. J.; Mullican, W. F.; Young, M. Controls on water use for thermoelectric generation: case study Texas, U.S. *Environ. Sci. Technol.* **2013**, *47* (19), 11326-11334.

Schnell, R. C.; Oltmans, S. J.; Neely, R. R.; Endres, M. S.; Molenar, J. V.; White, A. B. Rapid photochemical production of ozone at high concentrations in a rural site during winter. *Nature Geoscience*, **2009**, *2*, 120-122.

Schnelle, K. B.; Brown, C. A. *Air Pollution Control Technology Handbook*. CRC Press: Boca Raton, Florida, 2002.

Schnoor, J. L. The U.S. drought of 2012. *Environmental Science and Technology*. **2012**, *46*, 10480.

Seinfeld, J. H.; Pandis, J. H.; *Atmospheric Chemistry and Physics: From Air Pollution to Climate Change*, 2nd ed; Wiley: New Jersey, 2006.

Sillman, S. The relationship between ozone, NO_x, and hydrocarbons in urban and polluted rural environments. *Atmospheric Environment*. **1999**, *33*, 1821-1845.

Simon, S.; Allen, D. T.; Wittig, A. E. Fine particulate matter emissions inventories: comparisons of emissions estimates with observations from recent field programs. *Journal of the Air & Waste Management Association*. **2008**, *58* (2), 320-343.

Smith, S.; Swierzbinski, J.; Assessing the performance of the UK Emissions Trading Scheme. *Environmental and Resource Economics.* **2007**, *37*, 131-158.

Solomon, S.; Qin, D.; Manning, M.; Chen, Z.; Marquis, M., Averyt, K. B.; Tignor, M.; Miller, H. L. *Contribution of working group I to the fourth assessment report of the Intergovernmental Panel on Climate Change*; **2007**; Cambridge University Press, Cambridge, U.K.

Sovacool, B. K.; Sovacool, K. E. Identifying future electricity-water trade-offs in the United States. *Energy Policy*. **2009**, *37*, 2763-2773.

Srivastava, R. K.; Jozewicz, W. Flue gas desulfurization: the state of the art. *Journal of the Air & Waste Management Association*, **2001**, *51*, 1676-1688.

Stillwell, A. S.; Clayton, M. E.; Webber, M. E. Technical analysis of a river basin-based model of advanced power plant cooling technologies for mitigating water management challenges. *Environmental Research Letters*. **2011a**, *6*, doi:10.1088/1748-9326/6/3/034015.

Stillwell, A. S.; King, C. W.; Webber, M. E.; Duncan, I. J.; Hardberger, A. The energy-water nexus in Texas. *Ecology and Society*. **2011b**, *16* (1), 2.

Stillwell, A. S.; Webber, M. E. Novel methodology for evaluating economic feasibility of low-water cooling technology retrofits at power plants. *Water Policy*. **2013a**, *15*, 292-308.

Stillwell A. S.; Webber, M. E. Evaluation of power generation operations in response to changes in surface water reservoir storage. *Environmental Research Letters*. **2013b**, *8*, doi:10.1088/1748-9326/8/2/025014.

Strzepek K.; Yohe G.; Neumann J.; Boehlert, B. Characterizing changes in drought risk for the United States from climate change. *Environmental Research Letters.* **2010**, *5*, doi:10.1088/1748-9326/5/4/044012.

Sun, L.; Webster, M. D.; McGaughey, G.; McDonald-Buller, E. C.; Thompson, T.; Prinn, R.; Ellerman, A. D.; Allen, D. T. Flexible NO_x abatement from power plants in the eastern United States. *Environmental Science and Technology*. **2012**, *46*, 5607-5615.

Texas Commission on Environmental Quality (TCEQ). *Dallas-Fort Worth attainment demonstration state implementation plan revision for the 1997 eight-hour ozone standard* [Online]. TCEQ: Austin, Texas, 2010. http://www.tceq.texas.gov /airquality/sip/dfw_revisions.html (Accessed June 3, 2014).

Texas Commission on Environmental Quality (TCEQ). *Barnett Shale special emissions inventory Phase 1*. TCEQ: Austin, Texas, 2011. https://www.tceq.texas.gov/ airquality/point-source-ei/psei.html#barnett (Accessed June 3, 2014).

Texas Commission on Environmental Quality (TCEQ). *DFW8H2 CAMx Modeling Directory* [Online]. TCEQ: Austin, Texas, 2012a. ftp://amdaftp.tceq.texas.gov /pub/DFW8H2/camx/ (Accessed June 3, 2014).

Texas Commission on Environmental Quality (TCEQ). *Houston-Galveston-Brazoria 8-hour ozone SIP modeling* [Online]. TCEQ: Austin, Texas, 2012b. http://www.tceq.state.tx.us/airquality/airmod/data/hgb8h2/hgb8h2.html (Accessed Feb. 4, 2012).

Texas Commission on Environmental Quality (TCEQ). *Texas state and local air quality planning program: modeling files and information* [Online]. TCEQ: Austin, Texas, 2014a. https://www.tceq.texas.gov/airquality/airmod/rider8/rider8Modeling (Accessed June 3, 2014).

Texas Commission on Environmental Quality (TCEQ). *Today's Texas air quality forecast* [Online]. TCEQ: Austin, TX, 2014b. https://www.tceq.texas.gov /airquality/monops/forecast_today.html (Accessed June 18, 2014).

Texas Railroad Commission (TXRRC). *Barnett Shale Information* [Online]. TXRRC: Austin, Texas, 2014a. http://www.rrc.state.tx.us/barnettshale/index.php (Accessed June 3, 2014).

Texas Railroad Commission (TXRRC). *Eagle Ford Information* [Online]. TXRRC: Austin, Texas, 2014b. http://www.rrc.state.tx.us/eagleford/ (Accessed June 3, 2014).

Texas Railroad Commission (TXRRC). *Oil and Gas Production Data Query* [Online]. TXRRC: Austin, Texas, 2014c. http://webapps.rrc.state.tx.us/PDQ/general ReportAction.do (Accessed June 3, 2014).

Texas Water Development Board (TWDB). *2012 Water for Texas* [Online]. TWDB: Austin, Texas, 2012. http://www.twdb.state.tx.us/publications/state_water_plan /2012/2012_SWP.pdf (Accessed June 3, 2014).

Texas Water Development Board (TWDB). *Major River Basins* [Online]. TWDB: Austin, Texas, 2014a. http://www.twdb.state.tx.us/mapping/gisdata.asp (Accessed June 3, 2014).

Texas Water Development Board (TWDB). *Historical Water Use Estimates Major River Basin*. TWDB: Austin, Texas, 2014b. https://www.twdb.state.tx.us/waterpla nning/waterusesurvey/estimates/index.asp (Accessed June 3, 2014).

Tong, D. Q.; Muller, N. Z.; Mauzerall, D. L.; Mendelsohn, R. O. Integrated assessment of the spatial variability of ozone impacts from emissions of nitrogen oxides. *Environmental Science & Technology*. **2006**, *40* (5), 1395-1400.

Thompson, T. M.; King, C. W.; Allen, D. T.; Webber, M. K. Air quality impacts of plug-in hybrid electric vehicles in Texas: evaluating three battery charging scenarios. *Environmental Research Letters*. **2011**, *6*, doi:10.1088/1748-9326/6/2/024004.

United States Department of Energy (DOE). *Estimating freshwater needs to meet future thermoelectric generation requirements 2008 update* [Online]. DOE: Washington, DC, 2008. http://www.netl.doe.gov/research/energy-analysis/publications/details? pub=5b4bcd05-45fc-4f53-ac7a-eb2d6eaedce7 (Accessed June 3, 2014).

United States Drought Monitor (USDM). *U.S. Drought Monitor* [Online]. 2014. droughtmonitor.unl.edu (Accessed June 3, 2014).

United States Energy Information Administration (EIA). *Electricity Power Monthly*. EIA: Washington, DC, 2006. http://www.eia.gov/electricity/monthly/backissues.html (Accessed June 3, 2014).

United States Energy Information Administration (EIA). *Review of emerging resources: U.S. shale gas and shale oil plays* [Online]. EIA: Washington, DC, 2011. http://

www.eia.gov/analysis/studies/usshalegas/pdf/usshaleplays.pdf (Accessed June 3, 2014).

United States Energy Information Administration (EIA). *Annual energy outlook with projections to 2035* [Online]. EIA: Washington, D.C., 2012. http://www.eia.gov/forecasts /aeo/pdf/0383(2012).pdf (Accessed June 3, 2014).

United States Energy Information Administration (EIA). *Form EIA-923 detailed data* [Online]. 2013. http://www.eia.gov/electricity/data/eia923/ (Accessed June 3, 2014).

United States Energy Information Administration (EIA). *Natural gas annual supply & disposition by state* [Online]. 2014a. http://www.eia.gov/dnav/ng /ng_sum_snd_a_EPG0_FPD_Mmcf_a.htm (Accessed June 3, 2014).

United States Energy Information Administration (EIA). *Shale gas production* [Online]. 2014b. http://www.eia.gov/dnav/ng/ng_prod_shalegas_s1_a.htm (Accessed June 3, 2014).

United States Energy Information Administration (EIA). *Natural gas consumption* [Online]. 2014c. http://www.eia.gov/naturalgas/data.cfm#consumption (Accessed June 3, 2014).

United States Energy Information Administration (EIA). *Natural gas prices* [Online]. 2014d. http://www.eia.gov/dnav/ng/ng_pri_sum_dcu_nus_m.htm (Accessed June 3, 2014).

United States Energy Information Administration (EIA). *Short-term energy outlook* [Online]. 2014e. http://www.eia.gov/forecasts/steo/ (Accessed June 3, 2014).

United States Energy Information Administration (EIA). *Annual Energy Outlook 2014* [Online]. 2014f. http://www.eia.gov/forecasts/aeo/ (Accessed June 27, 2014).

United States Environmental Protection Agency (EPA). *Clean Air Interstate Rule, Acid Rain Program and former NO_x Budget Trading Program 2010 Progress Report* [Online]. 2011. http://www.epa.gov/airmarkt/progress/ARPCAIR10.html (Accessed June 18, 2014).

United States Environmental Protection Agency (EPA). *2007 Emissions & Generation Resource Integrated Database* [Online]. 2012a. http://www.epa.gov/cleanenergy /energy-resources/egrid/ (Accessed June 3, 2014).

United States Environmental Protection Agency (EPA). *Human health and environmental effects of emissions from power generation* [Online]. 2012b. http://www.epa.gov/capandtrade/documents/power.pdf (Accessed June 3, 2014).

United States Environmental Protection Agency (EPA). *Particulate Matter (PM) regulatory actions* [Online]. 2012c. http://www.epa.gov/pm/actions.html#jun12 (Accessed June 3, 2014).

United States Environmental Protection Agency (EPA). *Cross-state air pollution rule* [Online]. 2012d. http://epa.gov/airtransport (Accessed Feb. 3, 2012).

United States Environmental Protection Agency (EPA). *2008 ground-level ozone standards – Region 6 final designations, April 2012* [Online]. 2013. http://www.epa.gov/airquality/ozonepollution/designations/2008standards/final/region6f.htm (Accessed June 3, 2014).

United States Environmental Protection Agency (EPA). *Inventory of U.S. greenhouse gas emissions and sinks: 1990-2012* [Online]. EPA: Washington, DC, 2014a. http://www.epa.gov/climatechange/ghgemissions/usinventoryreport.html (Accessed June 3, 2014).

United States Environmental Protection Agency (EPA). *Where you live: state and county emissions summaries* [Online]. EPA: Washington, DC, 2014b. http://www.epa.gov/air/emissions/where.htm (Accessed June 18, 2014).

United States Environmental Protection Agency (EPA). *National ambient air quality standards (NAAQS)* [Online]. EPA: Washington, DC, 2014c. http://www.epa.gov/air/criteria.html (Accessed June 18, 2014).

Venkatesh, A.; Jaramillo, P.; Griffin, W. M.; Matthews, H. S. Implications of changing natural gas prices in the United States electricity sector for SO_2, NO_x, and life cycle GHG emissions. *Environmental Research Letters*. **2012**, *7*, doi:10.1088/1748-9326/7/3/034018.

Wang L.; Thompson, T.; McDonald-Buller, E. C.; Webb, A.; Allen, D. T. Photochemical modeling of emissions trading of highly reactive volatile organic compounds in Houston, Texas. 1. Reactivity based trading and potential for ozone hotspot formation. *Environmental Science & Technology*. **2005**, *41(7)*, 2095-2102.

Webber, M.E. *The looming natural gas transition in the United States* [Online]. Center for Climate and Energy Solutions: Austin, TX, 2012. http://www.c2es.org/docUploads/natural-gas-transition-us.pdf (Accessed 7.2.14).

Xiao, X.; Cohen, D. S.; Byun, D. W.; Ngan, F. Highly non-linear ozone formation in the Houston region and implications for emissions controls. *Journal of Geophysical Research*. **2010**, *115*, D23309, doi: 10.1029/2010JD014435.

Zavala-Araiza, D.; Sullivan, D.; Allen, D. T. Analysis of atmospheric hydrocarbon concentrations in a shale gas production region. In *Air & Waste Management Association 105th Conference and Exposition*: San Antonio, Texas, 2012.

Zhai, H.; Rubin, E. S. Performance and cost of wet and dry cooling systems for pulverized coal powerplants with and without carbon capture and storage. *Energy Policy*. **2010**, *38*, 5653-5660.

Vita

Adam Philip Pacsi grew up in Nashville, Tennessee. After completing his studies at Pope John Paul II High School, he attended Tulane University. He received a Bachelor of Science in Engineering in Chemical Engineering with Honors from Tulane University in May 2010. Adam started the Ph.D. program in Chemical Engineering at the University of Texas at Austin in the Fall of 2010.

Permanent email: adam.pacsi@gmail.com

This dissertation was typed by the author.